# Blue Bird final report





#### **Contributions:**

G. Aranda Almansa (ECN)

A. Bos (ECN)

L.E. Fryda (ECN)

I. van Zandvoort (Avantium)

J.K. van der Waal (Avantium)

G. van Klink (Avantium)

J. van Doorn (Kodok)

C.M. Lok (Catalok)

#### Disclaimer

Although the information contained in this document is derived from reliable sources and reasonable care has been taken in the compiling of this document, ECN cannot be held responsible by the user for any errors, inaccuracies and/or omissions contained therein, regardless of the cause, nor can ECN be held responsible for any damages that may result therefrom. Any use that is made of the information contained in this document and decisions made by the user on the basis of this information are for the account and risk of the user. In no event shall ECN, its managers, directors and/or employees have any liability for indirect, nonmaterial or consequential damages, including loss of profit or revenue and loss of contracts or orders.

In co-operation with









Page 2 of 79 ECN-E--18-027

# Acknowledgement

The Dutch Ministry of Economic Affairs is gratefully acknowledged for the funding of this TKI project (reference TEBE 115001).

ECN-E--18-027 Page 3 of 79

## **Abstract**

'Blue Bird - Concomitant generation of energy and chemicals from biomass waste streams' (5.4111) is a 2-year TKI innovation project financed by RVO (reference TEBE 115001) in which a number of technologies have been developed for the recovery of valuable compounds (BTX, ethylene) from gasification product gas in co-production schemes. The implementation of co-production allows the reduction of the production cost of bio-SNG by harvesting valuable compounds. Moreover, the production cost can be further reduced if low-cost biomass residues are used as feedstock (as the humins considered in this project). The co-production technologies studied include liquid absorption for bio-BTX harvesting, adsorption for the capture of bio-ethylene, and catalytic conversion of ethylene to aromatics (reactive separation). Moreover, the thermochemical valorization of humins (a by-product from Avantium's YXY biorefinery process for sugar conversion into chemicals) has also been assessed in this project. The research and development work was complemented with a market analysis and environmental impact assessment (LCA). This report summarizes the main achievements of the project.

Project reference number	TEBE115001		
Drainet title	Blue Bird - Concomitant generation of energy and chemicals from		
Project title	biomass waste streams		
Project partners ECN (coordinator), Avantium, Catalok, Kodok			
Project duration	01/01/2016 - 31/12/2017		

Page 4 of 79 ECN-E--18-027

## Table of contents

Sur	nmary			/
1.	Intro	duction		10
	1.1	Project	objective	10
	1.2	Project	overview	11
	1.3	Structur	re of the report	11
2.	Valor	isation of	humins	13
	2.1	Introduc	ction	13
	2.2	Product	ion of humins at Avantium	15
	2.3	Feeding	tests	15
	2.4	Gasifica	tion/combustion tests of humins	17
3.	BTX s	crubbing:	AWOS condensation unit	23
	3.1	The AW	OS unit - description	24
	3.2	Develop	oment of the AWOS unit	28
	3.3	Final pro	oof-of-concept of AWOS unit	29
4.	Ethyl	ene separa	ation via adsorption	32
	4.1	Develop	oment of ethylene sorbents	32
		4.1.1	Overview of studied sorbents	32
		4.1.2	Experimental setup	33
		4.1.3	Results of screening tests	35
		4.1.4	Long term testing	41
		4.1.5	Conclusions	42
	4.2	Final tes	sts of selected sorbents	42
		4.2.1	Experimental setup	42
		4.2.2	Results of tests with [Mn]A sorbent	44
		4.2.3	Results of tests with [Mn]Y zeolite sorbent	47
		4.2.4	Conclusions of sorbent testing	50
5.	Catal	ytic aroma	atization of ethylene	51
	5.1	Why rea	active separation?	51
	5.2	State-of	52	
	5.3	Experim	nents for ethylene aromatization	52
	5.4	Results		54
		5.4.1	Effect of reaction temperature	54

**Page** 5 of 79

9.	Dissemination, exploitation and project deliverables			76
8.	Concl	usions an	d outlook	73
	7.2	Life Cyc	le Analysis (LCA) of co-production schemes	69
	7.1	Selected	d pathways and preliminary economic evaluation of co-production	67
7.	LCA a	nalysis of	co-production schemes	67
	6.2	Summa	ry	66
		6.1.2	Bio-ethylene production	66
		6.1.1	Bio-BTX production	62
	6.1	Existing	processes for bio-BTX and bio-ethylene production	62
6.	Mark	et analysi:	s of bio-BTX and bio-ethylene	62
		5.4.4	Effect of catalyst preparation – impregnation vs. ion-exchange	60
		5.4.3	Proposed reaction mechanism	59
		5.4.2	Effect of Ga loading	57

**Page** 6 of 79

## Summary

'Blue Bird - Concomitant generation of energy and chemicals from biomass waste streams' (TEBE 115001) is a 2-year TKI innovation project financed by RVOWithin the Blue Bird project, a number of technologies have been developed for the recovery of valuable compounds (BTX, ethylene) from gasification product gas in co-production schemes. The implementation of co-production allows the reduction of the production cost of bio-SNG (or other biofuels). Moreover, the SNG production cost can be further reduced if low-cost biomass residues are used as feedstock. Within Blue Bird, thermochemical valorization of humins (a by-product from Avantium's YXY biorefinery process for sugar conversion into chemicals) via fluidized-bed gasification and combustion has been evaluated. The co-production technologies studied in the project include liquid absorption for bio-BTX capture, solid adsorption for the separation of bio-ethylene, and catalytic conversion of ethylene to aromatics (reactive separation).

In 2016, Avantium completed the production of 1000 kg humins from the XYX process at the Geleen pilot plant. Humins from different sugar sources and containing different concentrations of 5-hydroxymethyl furfural were produced. Part of this batch of humins was delivered to ECN for gasification/combustion tests. Preliminary spraying tests confirmed that the tested humins presented reasonable properties to be mixed with water and then to be fed by spraying. The tested humins showed to be very challenging materials for thermochemical conversion. Due to its low reactivity, accumulation of humins-char in the bed is expected to create operational problems under gasification conditions. Combustion seems to be more appropriate for humins valorization under the fluidized-bed conditions tested due to higher conversion rates. Stable combustion operating conditions were achieved with complete fuel conversion and no emissions. However, bed temperatures higher than 950°C should be used, which is not compatible with most FB existing systems. Humins in-bed injection proved to be a good option for the feeding of this problematic fuel, but a more efficient probe cooling system must be considered to avoid pyrolysis of the humins before injection (which will clog the feeding line). The sample of humins tested in this project showed to be not problematic considering bed ash agglomeration, slagging and fouling issues. Thus, the optimization of the Avantium's process increases the chances of the valorization of the resulting humins.

Within WP3 of the project, ECN has worked on the improvement of the BTX scrubbing unit for the harvesting of bio-BTX from biomass gasification gas. In particular, ECN has designed, constructed and tested a unit for the automated separation of water and aromatics. The new AWOS unit (Aromaat-Water Opvang en Scheiding) enables continuous, automated operation of BTX harvesting from gasification product gas. Along the design process, a number of experiments were

ECN-E--18-027 Page 7 of 79

performed to test some of the critical phenomena: the formation of turbulence in the condensing unit, the conductivity of the water and aromatics entering the AWOS unit, and spillover of washing liquid. All these issues were properly handled before the final commissioning test. The whole BTX scrubbing unit including the new AWOS unit was successfully tested for almost 12 hours with product gas coming from the MILENA gasifier and the OLGA tar removal. The main goal was to test whether the level sensors and the water pump operated within specifications, switching between the sensors (essential for continuous operation). It was demonstrated that the automation of the condensing unit worked very well, and proper separation of water and aromatics was achieved. The benzene removal efficiency of the BTX scrubber was approximately 98.6%, whereas 100% toluene removal was achieved.

Reactive separation of ethylene from producer gas via catalytic conversion to aromatics has successfully been proven as a promising and feasible option for the implementation of coproduction schemes. An extensive experimental plan using bifunctional Ga-loaded ZSM-5 zeolites as catalysts was carried out at ECN. The results showed that 80-97% ethylene can be converted depending on the operating conditions (Ga loading and operating temperature). In all cases, acetylene conversion was complete. The carbon contained in ethylene and acetylene is mainly converted to benzene, toluene, ethane and methane (the two latter being by-products of the reaction). Ethane and methane by-products end up in turn as part of the bio-SNG product, which is favorable in view of the application in bio-SNG processes. The addition of Ga to the zeolite significantly improved both the ethylene conversion (90-97%) and the carbon selectivity to benzene. On the contrary, the unloaded zeolite exhibited the highest values of carbon selectivity to toluene (~ 45%). The 0.5 wt.% Ga catalyst achieved the highest total carbon selectivity to aromatics (73%). The reaction temperature dramatically influences the distribution of carbon selectivity towards aromatics. Lower temperatures favor the production of ethylbenzene and xylenes, whereas benzene, naphthalene and naphthalene derivatives are promoted at higher temperatures. Based on the results, it is proposed that the formation of benzene and toluene need different active sites to promote their reaction.

Avantium has worked on the development of solid sorbents for the selective removal of ethylene from gasification product gas. An extensive screening campaign of different types of sorbents was performed. The preliminary sorbent screening revealed that amorphous metal oxides are not suitable as ethylene sorbents due to the lack of porosity. A- and X zeolites have potential as ethylene sorbent. Despite ion exchange and functionalization of zeolites, high affinity towards  $CO_2$  and water could not be overcome. MOFs have potential in gas adsorption and separation. However, the MOF small crystals lead high pressure drop over the sorbent bed and should therefore be shaped into larger particles (which in turn leads to a decrease in adsorption capacity). Specific adsorption of ethylene in active carbons could be obtained by impregnation with material with an ethylene specific interaction.

The 2 best Avantium candidates from the screening tests ([Mn]A and [Mn]Y zeolites) were delivered to ECN for testing under relevant gasification conditions. Both sorbents were tested in a number of adsorption/desorption cycles. Both sorbents showed a temperature increase upon start of adsorption, whereas the desorption process resulted in a drop in the temperature bed. The [Mn]Y sorbent exhibits a more modest temperature increase as well as a different temperature profile compared to the [Mn]A sorbent. Both sorbents were shown to be able to capture a large fraction of ethylene from the gas, but they also co-adsorb CO<sub>2</sub>, ethane and acetylene (as well as other C3-C5 hydrocarbons and organic sulphur compounds). In both sorbents, rapid breakthrough of CO<sub>2</sub> took place within 10 minutes after start of operation. The ethylene adsorption capacity of the [Mn]A sorbent was determined as 66-87 g ethylene/kg sorbent, whereas the [Mn]Y sorbent has a capacity of ~76.6 g ethylene/kg sorbent. During the tests with [Mn]Y sorbent, it was

Page 8 of 79 ECN-E--18-027

observed that although the ethylene capture is reduced from ~90% to 72% when decreasing the operating pressure from 5.7 bar to 1.6 bar, the ethylene adsorption selectivity considerably improved, since C<sub>2</sub>H<sub>6</sub> and CO<sub>2</sub> are not adsorbed by the [Mn]Y material anymore. Still, the sorbent co-adsorbs acetylene. Based on the results, its seems that operation at low pressures and high gas flows, together with the use of materials with improved sorption capacity such as the [Mn]Y sorbent, could lead to a good trade-off between capture efficiency and sorption selectivity. However, further work is required to get a window of suitable operating conditions of the sorbent and explore new strategies of regeneration.

In parallel to the technology development work, Blue Bird has included a market analysis of bio-BTX and bio-ethylene, and a cradle to grave environmental impact assessment of the production and use of bio-SNG from gasification of residual wood and the effect of the implementation of coproduction schemes for the combined production and use of bio-SNG + bio-BTX. The market analysis has shown that the production of bio-BTX via gasification and/or pyrolysis in the short term can contribute to the overall production of BTX to a limited extent (in the order of a few %) due to the very large production volumes of these aromatics. Different processes for BTX production predominantly based on pyrolysis and gasification are being developed. Most of these processes are in lab- or pilot scale phase. At first it is recommended to focus on niche applications of BTX in order to be competitive. A number of BTX producing and consuming companies have also been identified in the study. On the other hand, the results of the LCA analysis have revealed that substituting natural with bio-SNG is environmentally beneficial concerning global warming and fossil fuel depletion. Co-production of bio-SNG + bio-BTX performs environmentally better than the base case of production of only bio-SNG. Due to avoiding any fossil base auxiliary heat and power consumption, the combined bio-SNG and bio-BTX leads to an overall reduced impact even at production stage. Therefore, the results from the LCA analysis reveal that co-production of bio-SNG and BTX is not only a promising option to improve the business case of bio-SNG production, but also environmentally performs better.

All in all, the extensive work performed within the Blue Bird project has resulted in a number of successful results which contribute to the development and demonstration of co-production technologies, the implementation of which will lead to lower production cost of bio-SNG and biofuels.

ECN-E--18-027 Page 9 of 79

## 1. Introduction

#### 1.1 Project objective

The TKI Blue Bird project (TEBE115001) aims at the development of technologies for the implementation of co-production schemes in bioenergy processes (particularly from biomass gasification). Co-production consists of the recovery of valuable compounds present in the product gas, such as BTX (benzene, toluene, xylenes) and ethylene. These compounds not only have a high value, but they have to be removed anyway from the gas (through costly upgrading), since they can otherwise deactivate downstream catalysts, e.g. nickel catalysts in a bio-SNG process. Therefore, the recovery of these valuable compounds improves the economic feasibility of bio-SNG and other biofuels projects.

On the other hand, the cost of the biomass feedstock is an important part of the overall production cost of biofuels. The use of low-cost biomass feedstock (e.g. waste biomass) can significantly contribute to the (further) reduction of production cost of biofuels. Thus, Blue Bird also considers the valorization of humins, a by-product of the YXY biorefinery process owned by Synvina (joint venture of Avantium and BASF) in gasification/combustion.

Page 10 of 79 ECN-E--18-027

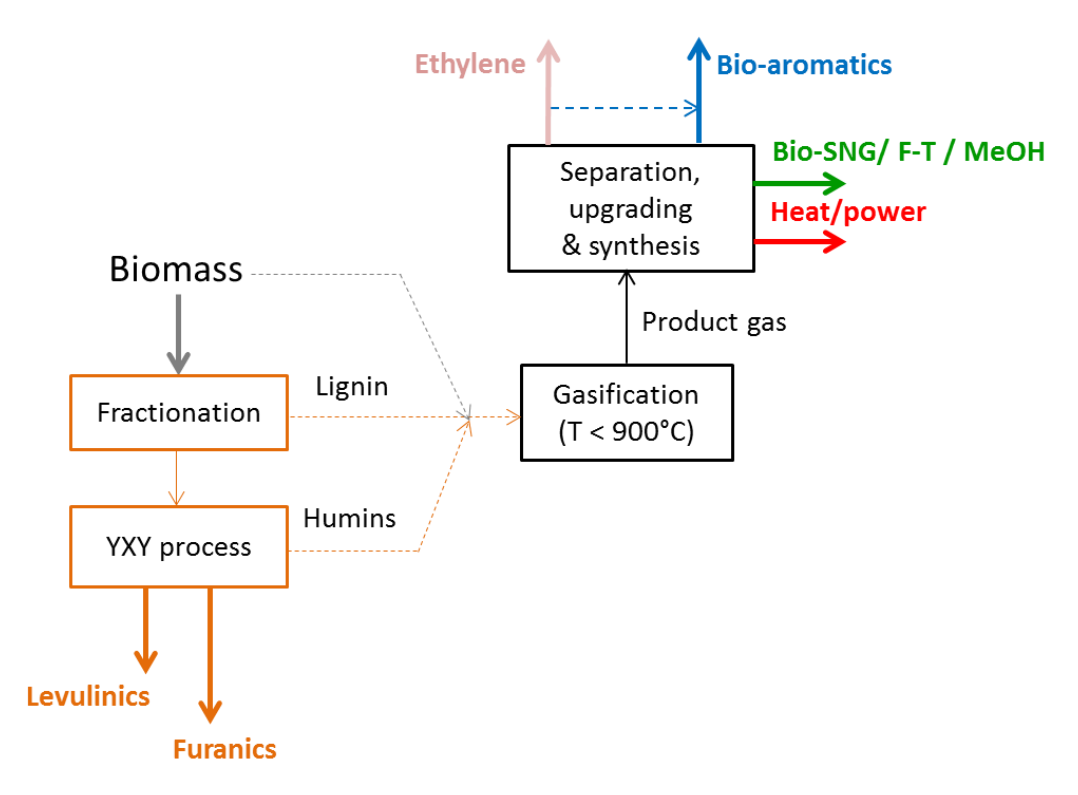


Figure 1. Overview of the Blue Bird concept.

Figure 1 schematically shows the overall concept of the Blue Bird project. The process starts with the use of biomass feedstock, preferably low-cost biomass residues (in this project, valorization of humins from the YXY biorefinery process is evaluated). The biomass is gasified at low temperature (750-850°C), and as part of the gas cleaning and upgrading section, technologies for the recovery of valuable compounds (bio-BTX and bio-ethylene) are implemented. The clean gas is then used for the production of heat/power or for the synthesis of biofuels. Within Blue Bird, we focus on bio-SNG production.

#### 1.2 Project overview

Project reference number TEBE115001	
Project title	Blue Bird - Concomitant generation of energy and chemicals from
Project title	biomass waste streams
Project partners	ECN (coordinator), Avantium, Catalok, Kodok
Project duration 01/01/2016 – 31/12/2017	

The project consortium is formed by ECN (coordinator, development of bio-BTX scrubbing unit, ethylene aromatization and testing of humins and sorbents), Avantium (production of humins and development of ethylene sorbents), Kodok (market analysis) and Catalok (consultant in catalytic processes).

#### 1.3 Structure of the report

This final project report is structured as follows: after the description of the project background, chapters 2-6 contain the scientific results obtained within the project (*inhoudelijk eindrapport*). Section 2 describes the production and valorization of humins as feedstock for thermochemical conversion. Section 3 contains the results of upgrading of the BTX scrubbing unit for the capture of

ECN-E--18-027 Page 11 of 79

bio-aromatics from product gas; the results of the development of sorbents for the adsorption of bio-ethylene are shown in Section 4. Section 5 summarizes the findings of the catalytic conversion of ethylene to aromatics. Sections 6 and 7 describe the transversal activities of the project, namely market analysis (Section 6), life cycle analysis and a preliminary economic assessment of co-production schemes applied to bio-SNG production (Section 7). Section 8 summarizes the conclusions and outlook of the project. Finally, Section 9 lists the dissemination and exploitation items that have resulted from the research work performed.

Page 12 of 79 ECN-E--18-027

## 2. Valorisation of humins

#### 2.1 Introduction

Humins is a carbonaceous, heterogeneous, syrup-like by-product from the YXY biorefinery process (currently owned by Synvina, joint venture of Avantium and BASF). The YXY process (schematically shown in Figure 2) produces furfurals from sugars. In the process, humins (a carbonaceous, heterogeneous, syrup-like material, plotted in Figure 3) are a byproduct of the sugar dehydration and purification step. Thermochemical conversion of humins for the production of heat, power or fuels/chemicals is an attractive option for the valorization of this residue. During previous work (Green Birds project) it was already seen that this feedstock poses a big challenge in terms of feeding heating up behavior and conversion due to its high viscosity, its tendency to foaming and its very low reactivity. Therefore, new strategies for the proper feeding and conversion were necessary. This was part of the scope of the Blue Bird project. Meanwhile, process improvements in the YXY process led to the production of humins with a different composition, which needed to be tested.

ECN-E--18-027 Page 13 of 79

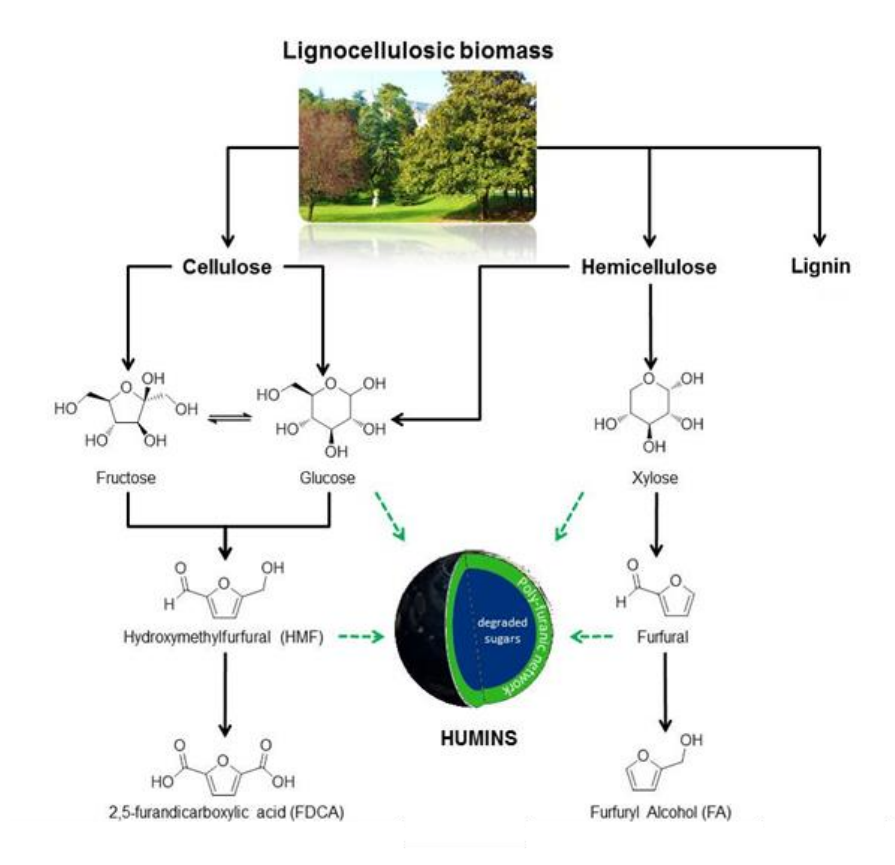


Figure 2. Overview of Avantium/BASF YXY process, with indication of where humins are formed.



Figure 3. Humins produced in YXY process.

During WP2, a batch of humins resulting from improvements in the YXY process was produced at Avantium's Geleen pilot plant. Within WP3, a sample of the new batch (30 kg) was supplied to ECN for fluidized-bed gasification/combustion tests using a new feeding strategy to explore the feasibility of the thermochemical conversion of humins. The results of this work are shown below in this section.

**Page** 14 of 79

#### 2.2 Production of humins at Avantium

In the 4th quarter of 2016, Avantium completed the production of 1000 kg humins from the XYX process at the Geleen pilot plant. Humins from different sugar sources and containing different concentrations of 5-hydroxymethyl furfural were produced.

From this batch, Avantium delivered to ECN ca. 30 kg of humins (Figure 4). The sub-sample used for the tests at ECN was from batch 117 produced on the 20th December 2016 at the Avantium plant.



Figure 4. Batch of humins supplied to ECN.

#### 2.3 Feeding tests

In previous work (Green Birds project), where preliminary gasification tests were performed using humins as feedstock, it was observed that carbon foaming was formed in the fuel feeding screw. The foam resulted in clogging of the fuel inlet, and thus in failure of operation. The combination of high viscosity, and tendency to foaming made humins a challenging feedstock<sup>1</sup>.

Within Blue Bird, a new strategy for feeding based on spraying of the feedstock for in-bed injection was explored. For this, a feeding system for high-viscosity liquids was designed and implemented at ECN (Figure 5 left). The feeding system was tested before coupling it to the fluidized bed reactor. For that, the humin sample was heated in an electrical heated stove to 65 °C, temperature at which the humins became able to flow, and about 3 kg were mixed with distilled water to make a blend composed of 80 wt.% humins and 20 wt.% of water. The mixture was then stirred to become homogeneous and until no more viscous lumps were observed. This mixture was then fed to the fuel buffer tank of the feeding system, which is equipped with a continuous stirring device. All the feeding system components were heated to 60-65 °C.

ECN-E--18-027 Page 15 of 79

\_

<sup>&</sup>lt;sup>1</sup> In practice, the combination of these properties poses a challenge in the feeding system, since a narrow temperature range is required during feeding (temperature high enough to ensure proper viscosity, but low enough as to prevent foaming). The sodium content poses challenges in the reactor and downstream in the cooling section.





Figure 5.The ECN feeding system developed for high viscous liquids and the injection point located in the centre of the WOBs distributor plate (right).

Figure 6 displays the results of the spraying tests of the humins for liquid feeding. During the tests it was confirmed that the tested humins presented reasonable properties to be mixed with water and then to be fed by spraying. After the functional tests of the feeding system, this was connected to the fluidized-bed reactor. The humins feeding point was located in the centre of the distributor plate, as can be seen in Figure 5 right.

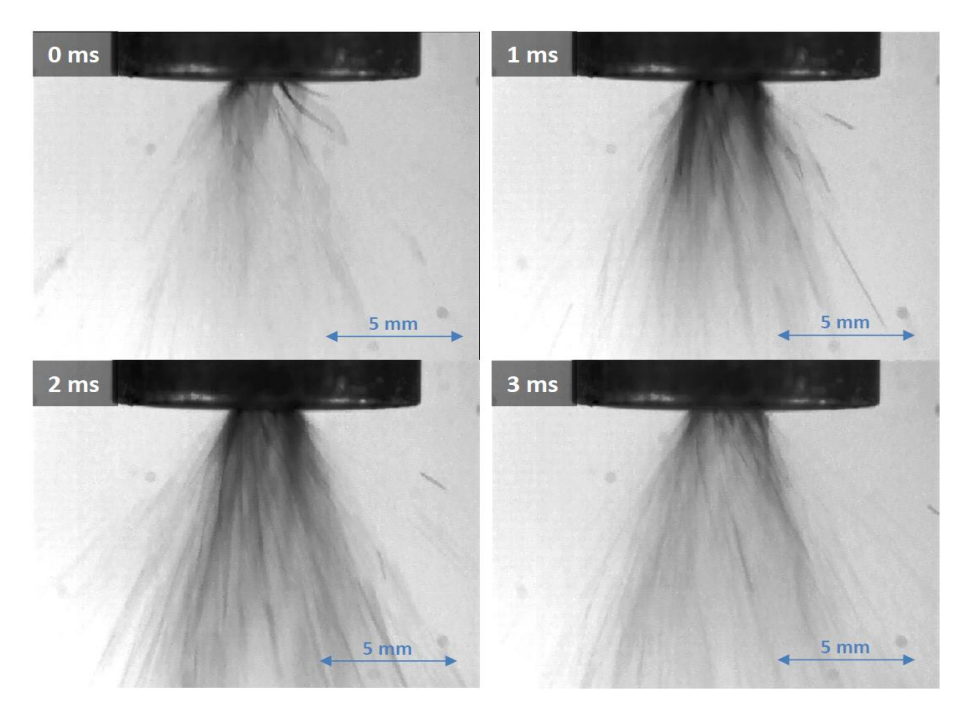


Figure 6. Spraying tests with humins.

**Page** 16 of 79

#### 2.4 Gasification/combustion tests of humins

After the spraying tests for feeding optimization, gasification/combustion tests with the new batch of Avantium humins were carried out at the BFB gasifier setup located at ECN laboratories. The objective of the experimental plan was to determine the effect of the temperature and the gasifying agent (air, steam,  $CO_2$ ) on the composition of the resulting producer gas. Moreover, a final combustion test was also performed. Table 1 summarizes the test plan designed for conversion in the bubbling fluidized bed reactor. The fuel was a mixture of 80 wt.% humins and 20 wt.% water, fed by a pump. In all cases ca. 0.3 kg/h of this fuel mixture was fed to the gasifier (pump frequency was calibrated prior to the test). The air flow in the reactor was adjusted to get an equivalent ratio (ER) of approximately 0.3 (typical value in gasification processes). The bed material used in the reactor was olivine and 25 L/min of gas was used to assist the spraying of the humins through the probe. The bed was fluidized with 10 L/min of  $N_2$  (15 L/min of air during combustion), fed through the distributor plate.

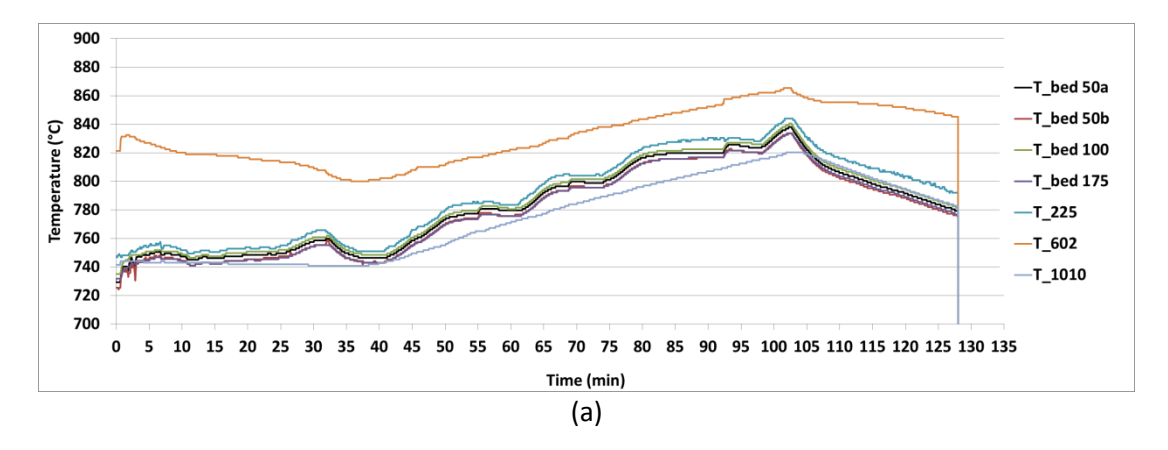
Table 1.Experimental plan of gasification/combustion of humins.

Test #	T (°C)	mf (kg/h)	m steam (kg/h)	V CO₂ (NL/min)	V air (NL/min)	V N₂ (NL/min) probe	V N <sub>2</sub> (NL/min) distributor
1	750	0.3	0	0	7	18 <sup>(1)</sup>	10
2	800	0.3	0	0	7	18	10
3	850	0.3	0	0	7	18	10
4	850	0.3	0.34	0	0	18	10
5	850	0.3	0	7	0	18	10
6	850	0.3	0	0	25	0	15 (air)

<sup>(1)</sup> Balance in the probe: 25 NL/min.

The first test was performed under air gasification conditions (ER 0.3). The bed temperature was set at 750°C and the humins were fed at 0.3 kg/h. The spraying feeding was assisted by injecting simultaneously a gas mixture of air and  $N_2$ . The temperature profile during this test is presented in Figure 7. During the first 25 minutes performed at 750 °C as starting temperature, it was observed an increase in the windbox pressure and also significant pressure fluctuations. The pressure of the humins feeding system increased from about 200 mbar to 6 bar and the system safety alarm pressure was reached and therefore, the system was automatically shut down. The pressure in the wind box decreased from a peak of 220 mbar to about 100 mbar and the feeding system was able to be restarted, although the pressure was still indicating about 1 bar in the feeding system, meaning that there was some sort of obstruction to the humins spraying. Based on previous tests it was known that the humins conversion is relatively slow and that the unconverted (partial liquid) material could be accumulating in the bed. For this reason it was decided to gradually increase the bed temperature to 850°C to see if the humins could be fed with an increased rate of conversion avoiding the unstable pressure fluctuations.

ECN-E--18-027 Page 17 of 79



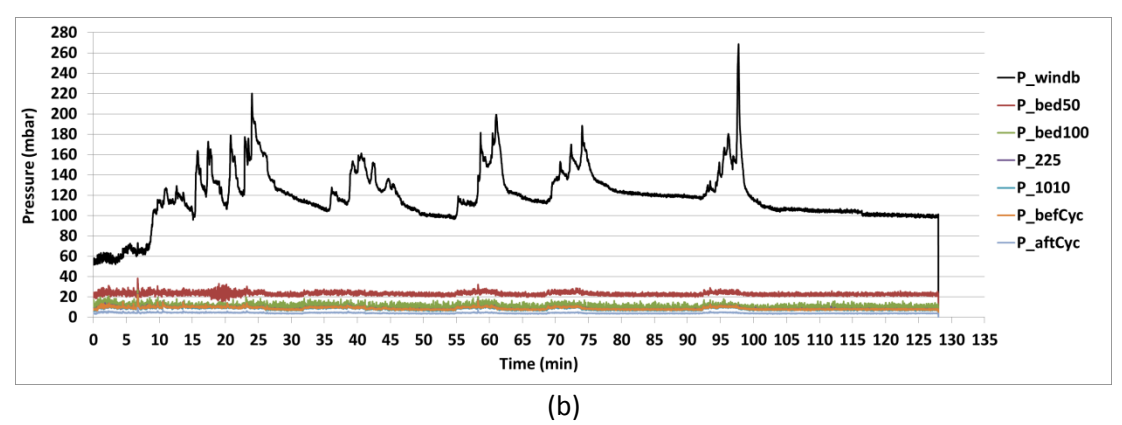


Figure 7. Temperature profile (a) and pressure profile (b) during the humins gasification tests. Start bed temperature of 750°C. End bed temperature of 850°C.

In Figure 7 it can be seen that further attempts to feed the humins resulted in an increase in the windbox pressure and in the feeding system, until the pressure alarm was again reached and the feeding stopped. After 100 min of testing it was decided to stop and the reactor was let to cool under inert atmosphere to be opened in the following day for internal inspection. Figure 8 shows the results of the internal inspection of the reactor after the gasification tests. There was no signs of slagging neither in the internal walls of the reactor or on the thermocouple surfaces. However, an agglomerate of unconverted humins-char mixed with bed particles, which was on the top of the distributor/feeding probe was taken out the reactor. This in-bed humins-char accumulation process, due to insufficient conversion rates, gave origin to the windbox pressure increase and significant pressure fluctuations and it seems that even a temperature of 850 °C is not enough to ensure sufficient conversion rates of the humins under fluidized bed air gasification conditions. This agglomerate build-up blocked the humins probe injection orifice, which caused the injection pressure to increase and the alarm safety stoppages of the feeding system.

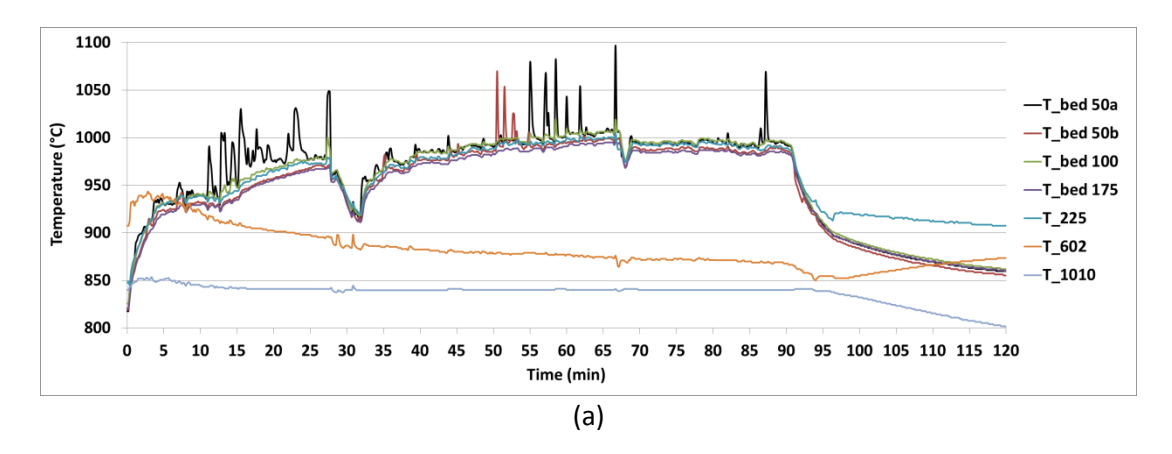
Page 18 of 79 ECN-E--18-027



Figure 8. Internal view of the reactor and the unconverted humins-char agglomerate obtained during the humins gasification tests. Start bed temperature of 750°C.

Due to the accumulation of humins-char under air gasification conditions (more reactive atmosphere for gasification compared with steam or  $CO_2$  gasification) during the first experiments, it was decided to perform the following tests under air combustion conditions. Additional measures were also applied (shift in position of the feeding probe to immerse the tip inside the bed, more vigorous fluidization conditions, start at 850°C) to promote a faster conversion and more reliable operating conditions. About 25 L/min air was injected through the probe to spray the humins and additional 15 L/min air was injected through the distributor plate to maintain the bed more vigorously fluidized. It was also decided to start the combustion test at 850°C to promote a faster conversion. The temperature profile obtained in the combustion test is displayed in Figure 9, where it can be observed that the bed temperature further increased to about 975°C as soon as the humins were fed and, from there on, no electric induced heat was necessary so the electric furnace of the reactor was turned off. After about 27 minutes of operation, the bed higher alarm temperature (1050°C) was reached which caused a safety shutdown of the system and the humins feeding was also stopped.

ECN-E--18-027 Page 19 of 79



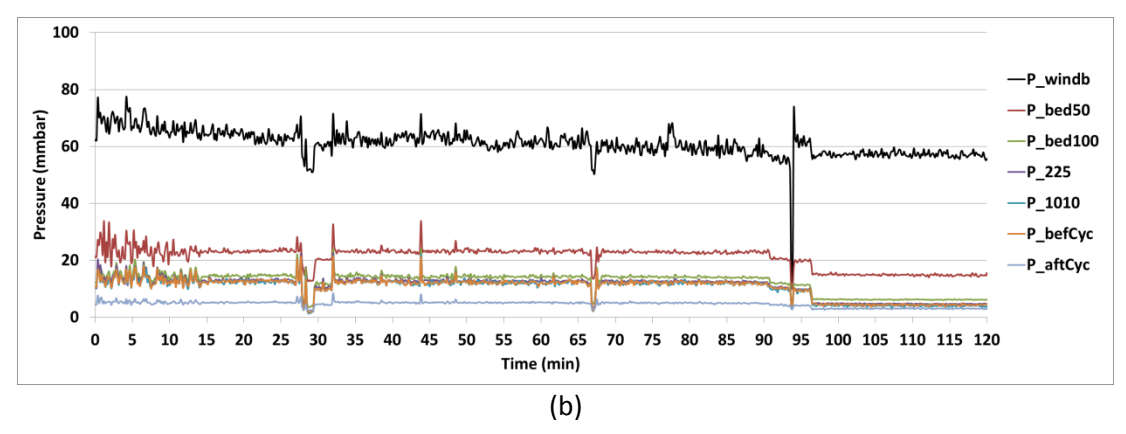


Figure 9. Temperature profile (a) and pressure profile (b) during the humins combustion tests. Starting bed temperature of 850 °C.

The humins feed was started again and the temperatures were able to recover. A period of stable conditions was attained until about 50 min of operation, when both bed thermocouples, placed at 50 mm of the distributor, started to show again significant high temperature peaks, around minute 67, causing again the alarm temperature to be reached and another shutdown was observed. After 2 min the system could be restarted and the operation proceeded again with stable conditions of temperature and pressure. These high temperature peaks must be related to the combustion of small lumps of humins-char that are formed in the bottom of the reactor close to the injection point. However, as the conversion rate was increased compared to gasification conditions, these lumps seem to burn completely, without accumulation, although giving rise to hot spots locally in the bed. During the following period of operation the pressure in the feeding system was observed to be increasing and at around minute 90 the maximum pressure of 6 bar was reached and it was decided to stop with the experiment. The system was let to cool under inert conditions (N<sub>2</sub>) to be opened in the following day. The flue gas composition is shown in Figure 10, where, it can be seen that during the first 28 minutes it was possible to obtain a relative constant operation to allow an almost complete fuel conversion and with very low pollutant emissions. The average bed temperature was then about 971°C.

Page 20 of 79 ECN-E--18-027

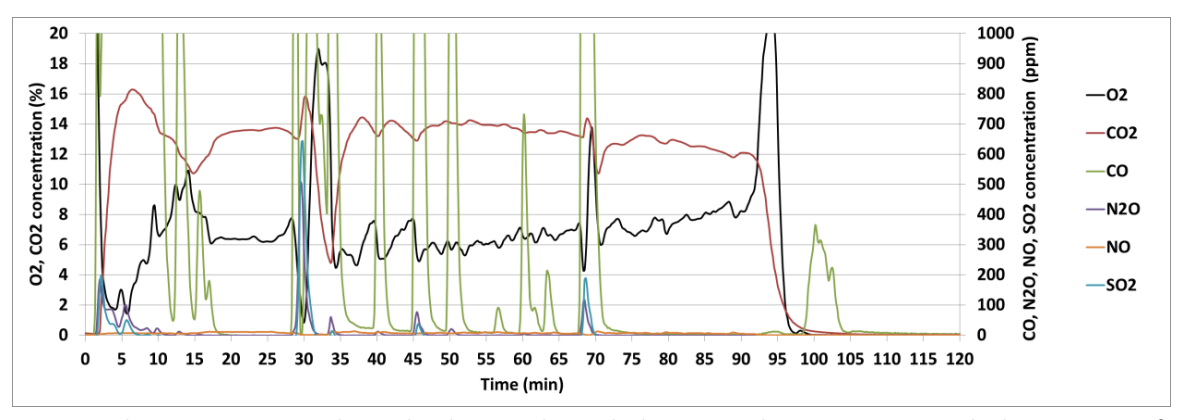


Figure 10. Flue gas composition obtained in the WOB during the humins combustion test. Starting bed temperature of 850°C.

After the system reset due to high temperature alarm, it followed a second period of relative stable operation (35-67 min), also with low emissions interrupted sometimes with high CO peaks well above 1000 ppm (Figure 10), probably related to fuel feed rate perturbations as can be verified by the  $O_2$  variation around minutes 40 and 45. During this period the average bed temperature was 996°C. In the third period (starting around 72 min.) about of 20 minutes of stable operation was again achieved almost with no CO emissions, which indicates a good fuel conversion. During this period the average bed temperature was 991°C. However, during this period it is possible to observe that the  $O_2$  concentration slowly raised showing that the fuel feed rate probably was decreasing due to the slow obstruction build-up in the probe tip. This is also consistent with the slow increase observed in the feeding system pressure, which at the end dictated the conclusion of the test. The use of neon as tracer gas allowed calculating the total volumetric flow of combustion gases. Based on the balance calculations, the conversion of the fuel carbon to  $CO_2$  (plus CO) was roughly 100 %. This is further supported by the absence of visible carbon, both on the bed material as well as in the cyclone dust.

After opening the reactor (Figure 11), no signs of char agglomeration were observed and the bed material was also free of agglomerated particles. Also no slagging was verified on the inner walls. However, the inspection of the humins probe tip shown evident signs of blockage of the inner tube hole, by partial pyrolysed humin material. It seems that the air and the humins flow through the probe was not enough to maintain the probe tip temperature within a level to prevent slow pyrolysis of the material. A temperature measurement with the probe immersed 10 mm in the bed, showed a value of 337°C at 1 mm distance of the injection hole (at 11 mm height from the distributor). Thus, in an industrial system the injection probe should be further cooled.

ECN-E--18-027 Page 21 of 79





Figure 11. View of the bed material and the humins injection probe tip after the combustion test with humins.

All in all, the tested humins showed to be a very challenging material for thermochemical conversion. The humins exhibited lower rates of conversion than desirable at air gasification conditions using fluidized bed technology and therefore, accumulation of humins-char in the bed is expected to create operational problems under gasification conditions (at least up to 850°C). Combustion seems to be more appropriate for humins valorisation under the fluidized-bed conditions tested due to higher conversion rates. Stable combustion operating conditions were achieved with complete fuel conversion and almost no gaseous pollutant emissions. However, bed temperatures higher than 950°C should be used, which is not compatible with most FB existing systems. Humins in-bed injection proved to be a good option for the feeding of this problematic fuel, but a more efficient probe cooling system must be considered to avoid pyrolysis of the humins before injection (which will clog the feeding line). The sample of humins tested in this project did not show operational problems in terms of bed agglomeration, slagging and fouling issues. Thus, the optimization of the Avantium's process increases the chances of the valorisation of the resulting humins.

**Page** 22 of 79

# 3. BTX scrubbing: AWOS condensation unit

Within WP3 of the project, ECN has worked on the improvement of the BTX scrubbing unit for the harvesting of bio-BTX from biomass gasification gas (Figure 12). In particular, within Blue Bird, ECN has designed, constructed and tested a unit for the automated separation of water and aromatics. The new AWOS unit (Aromaat-Water Opvang en Scheiding, i.e. Capture and Separation of Aromatics-Water) enables continuous, automated operation of BTX harvesting from gasification product gas. This chapter contains the main highlights of the design, HAZOP, assembly, commissioning and functional testing work performed <sup>2</sup>.



 $\label{thm:continuity} \textit{Figure 12. Upgraded BTX scrubbing unit, including new AWOS setup. } \\$ 

ECN-E--18-027 Page 23 of 79

-

<sup>&</sup>lt;sup>2</sup> Please refer to Deliverables ECN-BEE-2018-004 for more details about this topic.

#### 3.1 The AWOS unit - description

Figure 13 displays the AWOS unit, indicating its elements – the condenser, the central vessel, a second cooler for the final removal of the remaining slipping BTX, and 2 weighing units for aromatic product and water, with their corresponding collecting vessels. The connection between the AWOS unit and the BTX stripper is schematically depicted in Figure 14. Figure 15 is a close up of the central vessel, core of the AWOS unit. The vessel is composed of 2 compartments, one at the left and one at the right. The condensed stripping products (water + aromatics) enter the vessel on the right side. This usually results in turbulent entrance which makes it impossible to control the product layer with level control sensors. So the second compartment is separated by a dampening wall with just a few small openings to even out the liquid products and gas phase between both sides. The sensors to control the height of the product layer are mounted on the right compartment. The dampening wall works in such a way that the liquid water and product layers are completely free from turbulence in this second compartment. This enables the level control sensors, mounted in this section, to function without interruption.



Figure 13. Upgraded BTX scrubbing system including the new AWOS unit (outlined in red). The existing elements are outlined in green.

Page 24 of 79 ECN-E--18-027

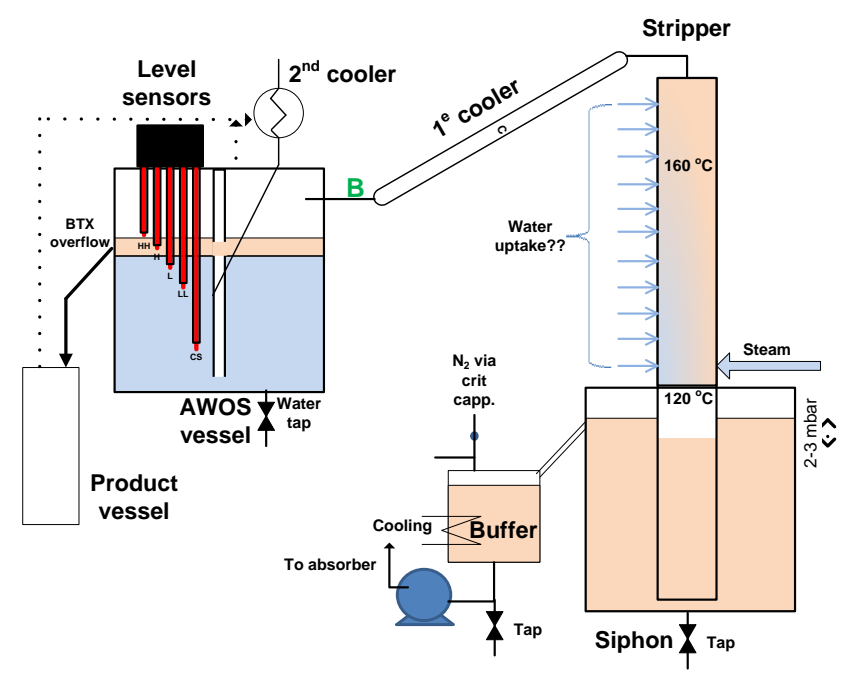


Figure 14. Schematic configuration of the connection between the BTX stripper, the condenser and the AWOS unit.

Figure 16 is a close up of the sensors and the aromatic product outlet located at the left side of the central AWOS vessel. The level control sensor is a conductive point level detection liquid point. The central electrode can conductively connect with all the alarm electrodes (LL, L, H and HH). If one of those alarm electrodes is connected, by electrical conductivity, with the central electrode, a signal will be given to and processed by the PLC (Programmable Logic Computer). As soon as the water reaches the H alarm sensor the PLC signals the water pump to operate at 40% of its capacity. This will lower the water level. This will continue until the L alarm is released. At that moment the PLC signals the water pump to operate at 25% of its capacity resulting in an increase of the water level in the AWOS vessel until the H alarm sensor is reached. This process repeats itself when in operation. Meanwhile, the growing BTX product layer will remain on top of the water because of its lower overall density and will periodically be discharged through the outlet pipe. The products are captured in special product vessels (Figure 17). The pump settings can be changed on line and can also be overruled by manual operation. Water must never reach the aromatic outlet (HH alarm) or run too low (LL alarm). In both cases the BTX system goes in shutdown mode.

ECN-E--18-027 Page 25 of 79

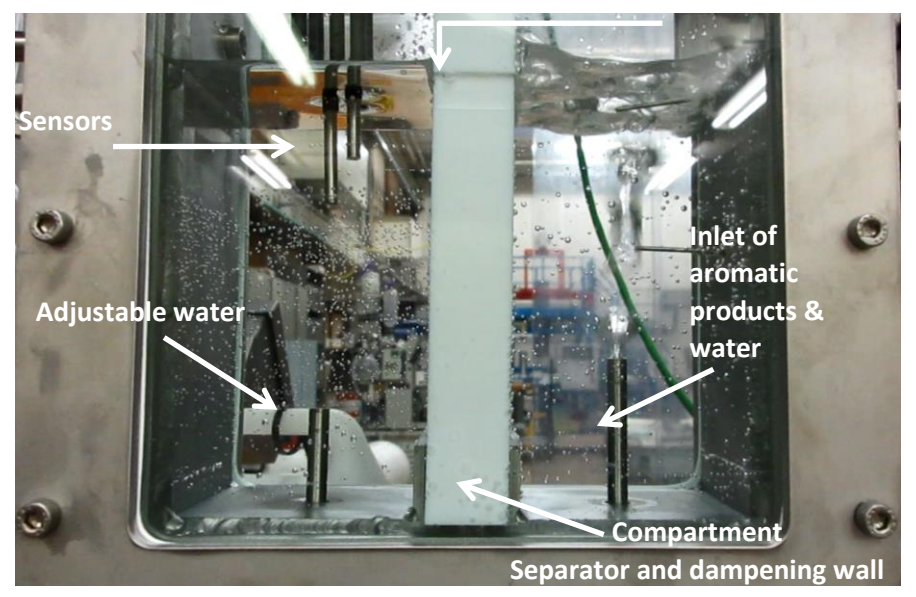


Figure 15. Close-up of central AWOS vessel.

Directly above the central AWOS vessel, a prototype second cooler vessel is mounted (Figure 14). This subunit, which is still in glass to be able to observe processes of capturing products at 5°C, enables to maximize the aromatic product yield at relatively low energy cost because most of the water and aromatics are already captured at room temperature in the central AWOS vessel. The metal collecting vessels are connected to ground preventing electrostatic discharge. Figure 18 shows a print screen of the main computer operating screen of the upgraded bio-BTX unit.

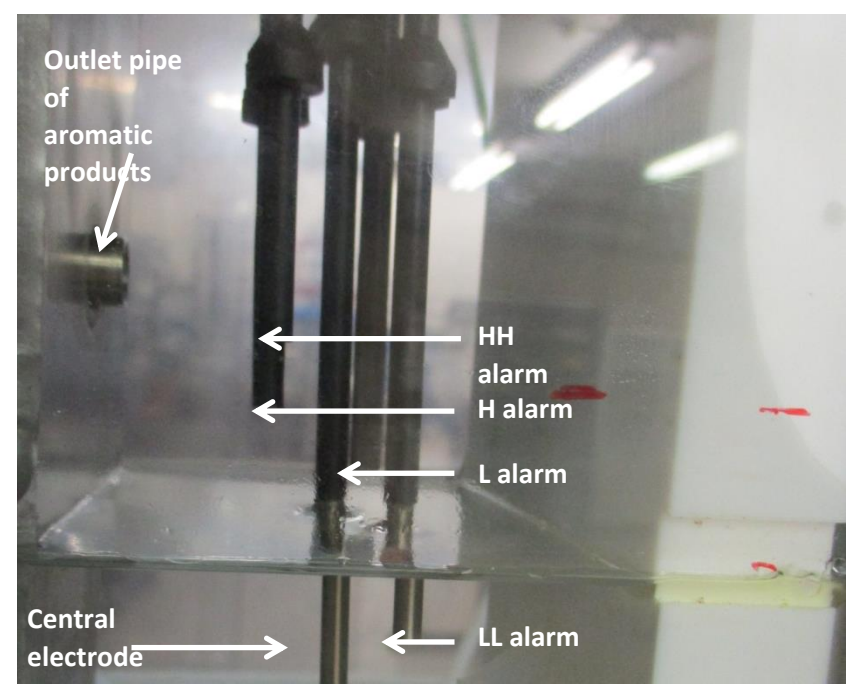


Figure 16. Close-up of the sensors and aromatic product outlet of the AWOS unit.

Page 26 of 79 ECN-E--18-027

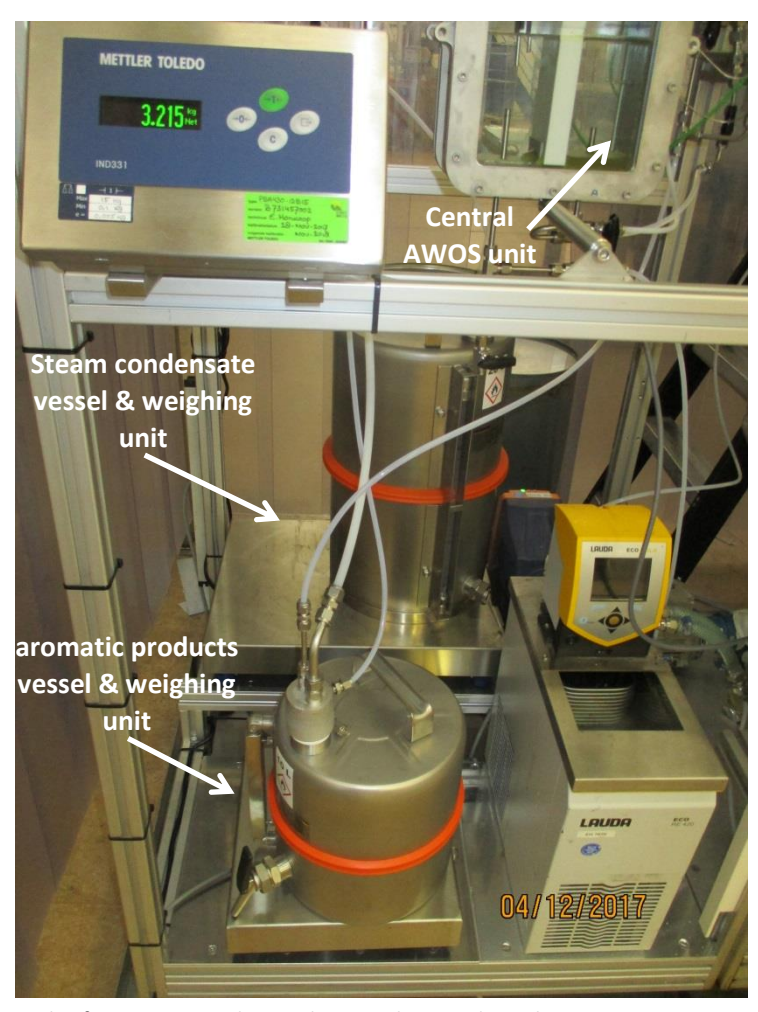


Figure 17. Collecting vessels of aromatics product and water phase and weighing units.



 $\label{thm:computer} \textbf{Figure 18. Computer controlled and automated system of bio-BTX scrubbing system.}$ 

ECN-E--18-027 Page 27 of 79

#### 3.2 Development of the AWOS unit

The first experiment performed to gather data for the design of the AWOS unit was performed in 2016. In this test, joint condensation from the OLGA absorber and the BTX absorber was applied<sup>3</sup>. This configuration was intended to set the most stringent conditions that the condenser could encounter (conservative case), that is, to assess whether proper condensation of the combined streams from OLGA tar removal and the BTX absorber could be achieved, and how the product streams would be collected. Based on this experiment, the process design of AWOS could be initiated. The considerations for the design of AWOS were discussed in an internal note<sup>4</sup>.

Based on the first design, a glass prototype mimicking the concept was built in order to prove that the fundamentals of the unit worked properly, and if not, to bring further improvements to the design. Different tests performed with this glass prototype derived in further adjustments in the design of the AWOS unit, until reaching the final version based on which the unit was constructed.

The new AWOS unit was mounted and integrated in the BTX scrubbing unit, and after a HAZOP analysis, functional tests were performed to test some of the critical phenomena that could jeopardize the performance of the unit before the final commissioning of the unit. The formation of turbulences in the condensing unit was one of the most important phenomena governing the operation of the unit. The creation of turbulences could lead to unstable, disturbed operation of the unit, thus it was critical to ensure that the sensors located in the left side of the AWOS vessel were not affected by turbulences created by the feeding of condensed products in the right side. This issue was also checked after the assembly of the unit in functional tests, during which  $N_2$  gas was fed to the right side of the AWOS unit creating a turbulent surface. The functional tests showed that the surface of the left section was not moving at all, thus indicating undisturbed operation of the sensors.

Another issue that was addressed during the functional tests was the conductivity of the water and aromatics entering the AWOS unit. The sensors of the AWOS unit respond to electric conductivity, and thus proper electrical conductivity of water is crucial to ensure good operation of the sensors and the pumps of water and aromatic product. With this purpose, the conductivity of real process stripping water was checked with an electric conductivity measuring device and that water had enough conductivity to activate the sensors. The aromatic layer was tested the same way and as expected there is no electric conductivity present in that layer. Therefore the product controlling sensors are expected to work as specified and undisturbed by turbulences. An additional issue investigated during the functional tests was related to the spillover of washing liquid (used to capture aromatics from the gas in the scrubbing unit).

Finally, some additional small adjustments of the unit were applied, which included PLC programming, rewiring electrical circuits, repositioning of thermocouples, updating technical documents, adjustments derived from the HAZOP analysis, etc. All these issues were properly handled before the final test.

Page 28 of 79 ECN-E--18-027

-

<sup>&</sup>lt;sup>3</sup> See ECN-BEE-2016-077 for more details about this experiment.

<sup>&</sup>lt;sup>4</sup> See ECN-BEE-2016-081

#### 3.3 Final proof-of-concept of AWOS unit

After the first functional tests described in Section 3.2, the whole BTX scrubbing unit including the new AWOS unit was commissioned for a final duration test. On the  $20^{th}$  and  $21^{st}$  December 2017, the automated AWOS unit was tested for 11.6 hours in daytime with product gas coming from the MILENA gasifier and the OLGA tar removal<sup>5</sup>. The main goal was to test whether the level sensors and the PLC connected, water pump operated within specifications, switching between the H and L sensor. This is the essential basic system that will enable continuous operation. It was demonstrated that automation worked very well. The BTX stripper was operated with the standard washing liquid and  $160^{\circ}$ C steam (A-steam unit). The condensates were collected at ~25  $^{\circ}$ C in the AWOS unit.

The benzene concentration in the inlet product gas was measured as 6000 ppmv, whereas the outlet gas contained 86 ppmv benzene. This implies a benzene removal efficiency of approximately 98%, whereas 100% toluene removal was achieved, as observed in Figure 21. The BTX removal efficiency depends on several factors, including the system pressure, the absorber temperature and the stripper temperature. Both conditions depend in turn on factors such as the surface area of the internals, the distribution of the washing liquid over the internals, the inlet gas flow/washing liquid flow ratio, the length of the columns and the equilibrium constants for absorption and stripping.

The benzene product harvested during the final duration test can be seen in Figure 19 (b). The benzene balance was almost completely accounted for (98.88%), whereas the water balance can be almost completely closed.

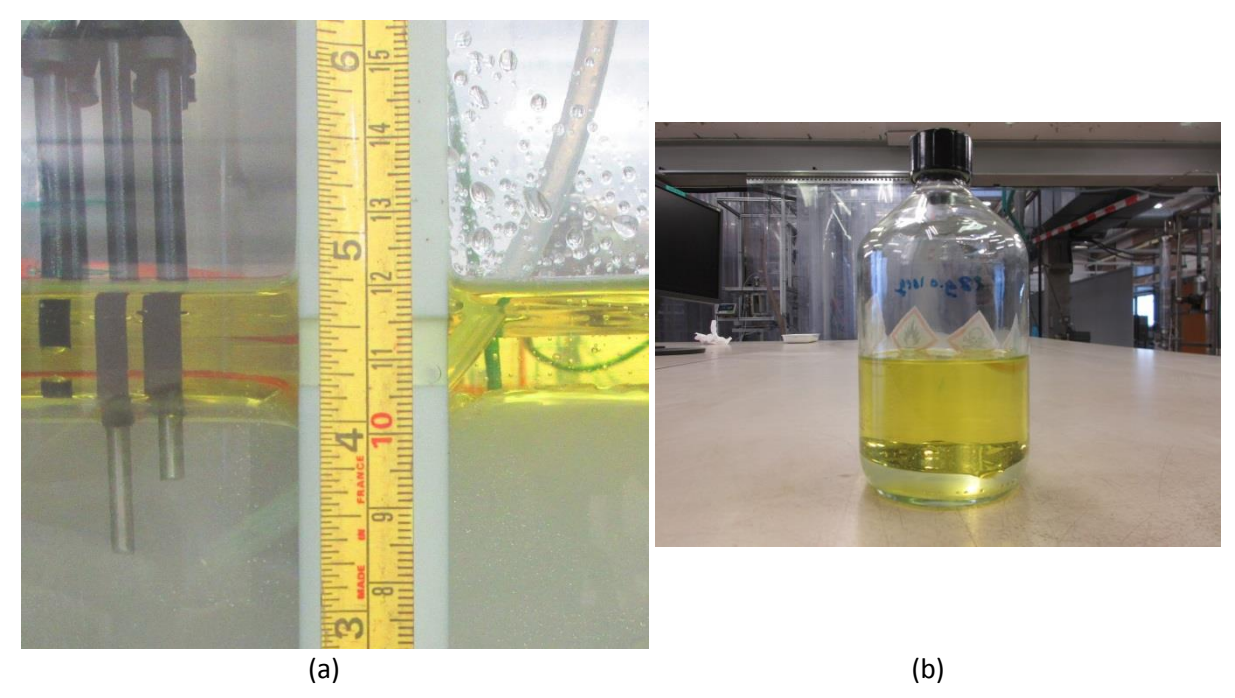


Figure 19. Final AWOS duration test: (a) close-up on benzene layer in AWOS vessel; (b) bio-BTX product harvested from the gas during the test.

ECN-E--18-027 Page 29 of 79

-

<sup>&</sup>lt;sup>5</sup> The duration test was about 11:40 hours (split in 2 periods, one of 7 hours on the 20<sup>th</sup> December 2017, and a second period of 4.7 hours on the 21<sup>st</sup> December 2017).



Figure 20. Final AWOS duration test: AWOS vessel at the beginning of the test, with only water in it; (b) creation of benzene layer in AWOS vessel during final duration test.

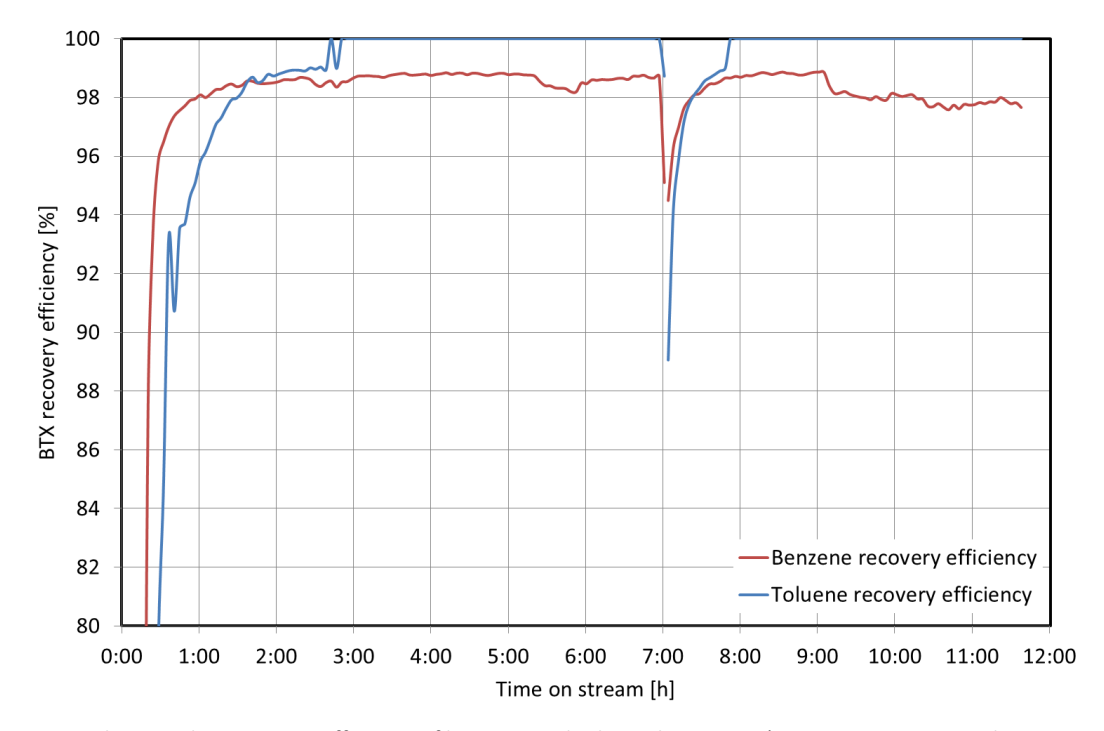


Figure 21. Final AWOS duration test: efficiency of benzene and toluene harvesting (cut in X-axis at 7:00 indicating system stop overnight between 2 parts of the test).

After some time operation, when the level sensors were in contact with (or exposed to) the BTX phase the outer insulation layer started to expand a little. This created a hollow pocket around the metal sensor tip. The return flow, of the BTX 2<sup>nd</sup> (5°C) cooler, also produced some gas bubbles. Once a gas bubble got stuck in the sensor pocket, it blocked contact with the water phase and left it functionless. This was easily overcome by removing some of the insulation material after finishing this test, manually operated.

Initially the washing liquid heater could not be operated properly connected to the PLC and driven by a solid state relay (instability). The momentary heat injections were too severe and caused local boiling, resulting in washing liquid spillover. For this test we decided to operate this heater manually with a variac (AC-AC adjustable transformer). This reduced the unwanted spillover to a minimum. There will be a re design of this washing liquid heating section in an attempt to achieve minimal, preferably zero spillover. In this test still a little water transport from the stripper gas

Page 30 of 79 ECN-E--18-027

(steam), via washing liquid water uptake, to release in the absorber fuel gas outlet. This is also an unwanted side effect which will be studied further in order to reduce this to a minimum, also preferably to zero. The water balance could be completely accounted for and the benzene balance was 98.88%.

Therefore, the commissioning test showed the successful performance of the integrated BTX scrubber unit, with automated separation of the BTX product, and good aromatics recovery efficiency.

ECN-E--18-027 Page 31 of 79

# 4. Ethylene separation via adsorption

Avantium has worked within WP4 of the project on the development of sorbents that allow the selective adsorption of ethylene from gasification product gas. After the synthesis and screening tests of sorbents at Avantium, a batch of the selected candidates was sent to ECN for testing under relevant gasification conditions. This section describes the results obtained during the development work.

#### 4.1 Development of ethylene sorbents <sup>6</sup>

#### 4.1.1 Overview of studied sorbents

Within Blue Bird, the library of sorbents is extended to find stable and selective sorption materials for ethylene, especially in the presence of water and CO<sub>2</sub>. These molecules are difficult to separate from ethylene by adsorption due to their polarity and small kinetic diameter. The selected materials include amorphous metal oxides, clay, active carbon, and metal-organic frameworks (MOFs).

- Zeolites: In the previous project Green Birds<sup>7</sup>, mainly zeolites were tested as adsorbents for ethylene. In literature, zeolites are reported to be good adsorbents and their adsorption properties vary depending on pore size, silica to alumina ratio (SAR) and ion exchangeable groups. In general, zeolites with a low SAR, such as zeolite A and X, have good potential as ethylene sorbent. The effect of ion exchange on the properties of zeolites is a well-studied subject. It was reported in literature that [Ag]A functions as an absolute molecular sieve and selectively adsorbs ethylene from a mixture of ethane and ethylene. In the Green Birds project, [Ag]A turned out to be selective for ethylene, even in the presence of water, but was not stable as sorption selectivity and capacity decreased over repeated cycles at 40 °C and 5 bar. [Ca]A was selected as best candidate with good ethylene sorption capacities and fair selectivity. The biggest downside of the [Ca]A based sorbents is its high affinity to water.
- Metal-organic frameworks are built up from transition-metal cations, which are linked via coordinating multidentate organic groups. The structure of MOFs is characterized by an open framework that can be porous, which makes them suitable for application as a sorbent. Only a few MOFs are easily available on a commercial scale. These materials were studied in this project and

Page 32 of 79 ECN-E--18-027

-

<sup>&</sup>lt;sup>6</sup> From I. van Zandvoort, J.K. van der Waal, G.van Klink, E. de Jong. Selective adsorption of ethylene. Confidential report (2017)

Please refer for more details to the final report of Green Birds (ECN-E—17-046): <a href="https://www.ecn.nl/publications/ECN-E--17-046">https://www.ecn.nl/publications/ECN-E--17-046</a>

listed in Table 3, pore sizes are not mentioned as some MOFs are reported to have a flexible framework.

In the first stage of the project, commercial materials were screened for their ethylene adsorption behaviour. Selected materials were subsequently functionalized, e.g. by ion exchange or organic modification, in order to tune their selectivity for ethylene, which was tested by feeding a mixture containing ethylene, methane and ethane. The complexity of the feed was increased by mixing CO,  $CO_2$ ,  $H_2O$  and  $H_2$ .

Table 2. Properties of different zeolites tested in Blue Bird.

Framework	Cationic form	Window	Effective channel diameter Å
	Na	8-ring	3.8
Α	Ca	8-ring	4.4
	K	8 ring	2.9
	Na	12-ring	8.4
X	Ca	12-ring	8.0
Υ	Na	12-ring	8.0
Mordenite	Н	12-ring	7.0
ZSM-5	Na	10-ring	6.0
Ferrierite		10-ring	5.3

Table 3. Overview of commercially available MOFs tested in Blue Bird.

MOF	Cation	Linker	Commercial name	
ZIF-8	Zn <sup>2+</sup>	2-imidazole	Basolite Z1200	
MIL-53	Al <sup>3+</sup>	Terephthalate	Basolite A100	
HKUST-1/	Cu <sup>2+</sup>	Benzene-1,3,5-	Decelite C200	
Cu-BTC	Cu	tricarboxylate	Basolite C300	
Fo DTC	Fe <sup>3+</sup>	1,3,5-	Decelite F200	
Fe-BTC	re	tricarboxylate	Basolite F300	

Commercial zeolites, MOFs, carbon materials and metal oxides were obtained from Sigma Aldrich, Zeolyst, Norit, Cabot, Acros, Sasol, NorPro, Evonik, Grace Davison, PICA, Alfa Aesar, Sachtleben, Zeochem, TOSOH Corporation, and Sued Chemie (now Clariant). Further details about the preparations of the materials can be found in Avantium's report.

#### 4.1.2 Experimental setup

In order to study the adsorption of ethylene the in-house Avantium adsorption technology, which is based on patented Flowrence technology, was further improved. The Avantium Flowrence setup is schematically shown in Figure 22. The feed selector valve selects one reactor that is fed with the adsorption gas mixture. All other reactors are filled with nitrogen (the desorption gas). Different gas mixtures are available for testing and CO, CO<sub>2</sub>, H<sub>2</sub> can be mixed with the gas feed via separate mass flow controllers.

Water is led to the reactors by a separate feed section using a Jasco HPLC pump. The total flow of 0.01 mL/min is split in to 16 lines of which 15 are recycled and one is giving a net flow of 0.6  $\mu$ L/min, which is fed one reactor using a selector valve. At the top of the reactor water is vaporized and mixed with the gas feed. As water is added via a separate selector valve it can be added during the adsorption or desorption step.

ECN-E--18-027 Page 33 of 79

The Flowrence has four heated reactor blocks (40-300 °C), each containing four reactors of 560 mm height, 6 mm OD and 4 mm ID. The isothermal zone was determined to be 200 mm. During a run, one blank and 15 sorbent materials can be tested. At the bottom of the reactor a diluent gas  $(N_2)$  can be mixed with the effluent, which be used to dilute the gas flow before analysis, increase the flow rate and prevent back mixing under the reactor.

A selector valve in the effluent is used to lead the effluent gas from the selected reactor to the mass spectrometer (Hiden Analytical). The selected reactor is fed with the mixed gas feed and continuously monitored by the MS and GC to record breakthrough curves. A second selector valve in the effluent section leads the effluent from one of the desorbing reactors to the other channels of the GC to monitor desorption of CO<sub>2</sub>, ethylene and ethane.

Analytics are optimized by combining an MS and GC. The GC allows monitoring CO adsorption every minute. Adding a second sample line, which is connected to the GC, allowed for monitoring desorption curves while the next reactor is desorbing. This way, a step towards parallelization of the unit is made.

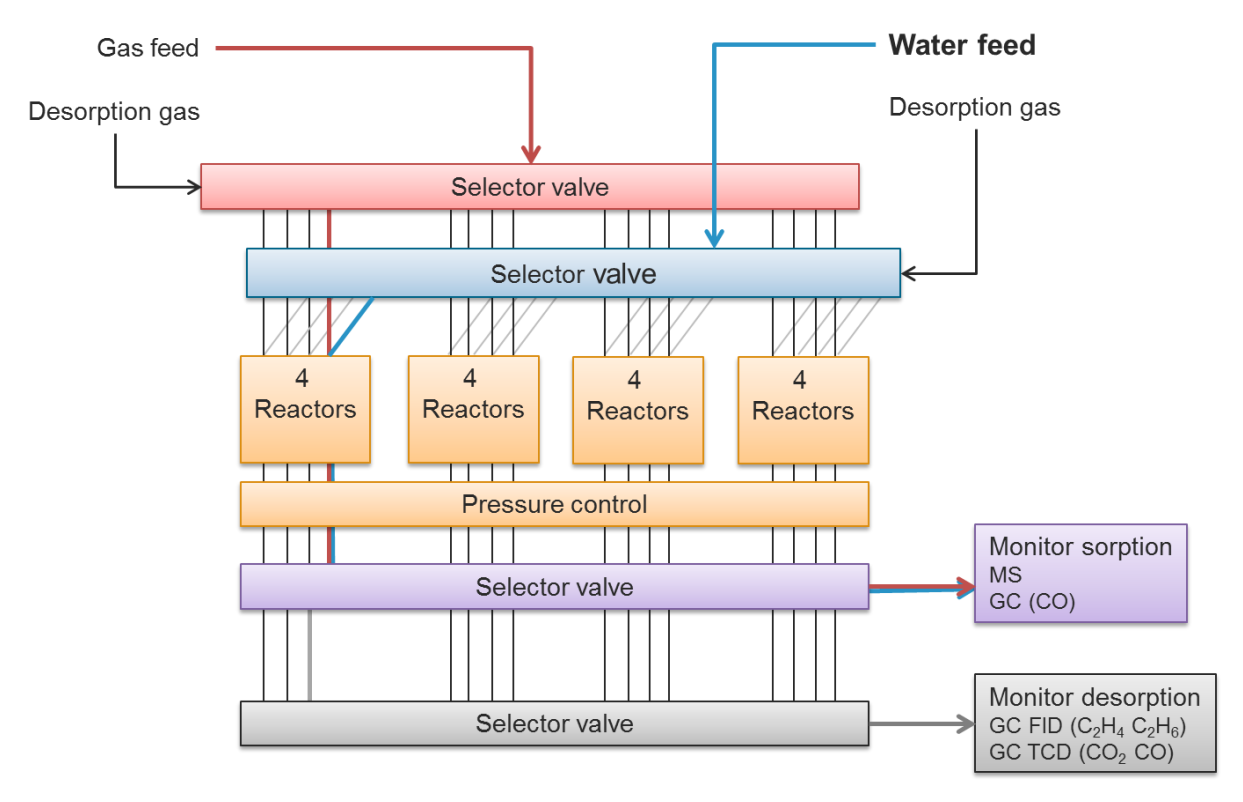


Figure 22. Schematic overview of the Avantium's Flowrence setup used for the adsorption experiments.

Page 34 of 79 ECN-E--18-027

#### 4.1.3 Results of screening tests

#### a) Zeolites

Zeolites are well-known sorbents and can have good sorption capacity for ethylene. However previous research has shown that their selectivity should be further improved, especially in the presence of  $CO_2$  and/or water. Zeolite A was extensively studied during the Green Birds project<sup>8</sup>, and therefore used as a reference to test the adsorption unit. The obtained breakthrough profiles were similar as observed in previous experiments. [K]A did not show adsorption of ethylene. On [Na]A sorption of ethylene was kinetically limited as the breakthrough curve was relatively flat. The adsorption on [Ca]A was unhindered and resulted in a sharp, steep breakthrough curve. One difference was found in the effect of temperature as sorption capacity of [Na]A decreased with increasing temperature, which could be related to the use of a different brand of molecular sieves with slightly different properties or pore sizes. These standard forms of zeolite A are known to have a very high affinity to  $CO_2$  and water. [Na]A and [Ca]A co-adsorb some ethane. In order to improve the selectivity of these materials, the effect of ion exchange and organic surface groups of these zeolites was further investigated.

Ion exchange of [Na]A with Li<sup>+</sup> decreased the sorption capacity decreased due to the large diameter of the Li<sup>+</sup> ion. Ion exchange with silver ions did increase the sorption capacity but, as shown in the Green Birds project, the use of easily reducible ions such as Ag<sup>+</sup> is unwanted. Ion exchange with Mg<sup>2+</sup>, Mn<sup>2+</sup> or Sr<sup>2+</sup> also led to an increase in ethylene sorption capacity (Figure 23). The shape of the ethylene breakthrough curve on [Sr]A indicated a kinetically limited process. The selectivity of the zeolites [Mn]A and [Sr]A was determined. Based on these curves [Mn]A seems to have the highest selectivity towards ethylene with a reasonable sorption capacity (Figure 24). Ion exchange of [K]A with Ca<sup>2+</sup> or Mn<sup>2+</sup> did not improve the ethylene sorption adsorption, as the metal ions are not able to enter the 3Å pores, limiting the extent of ion exchange.

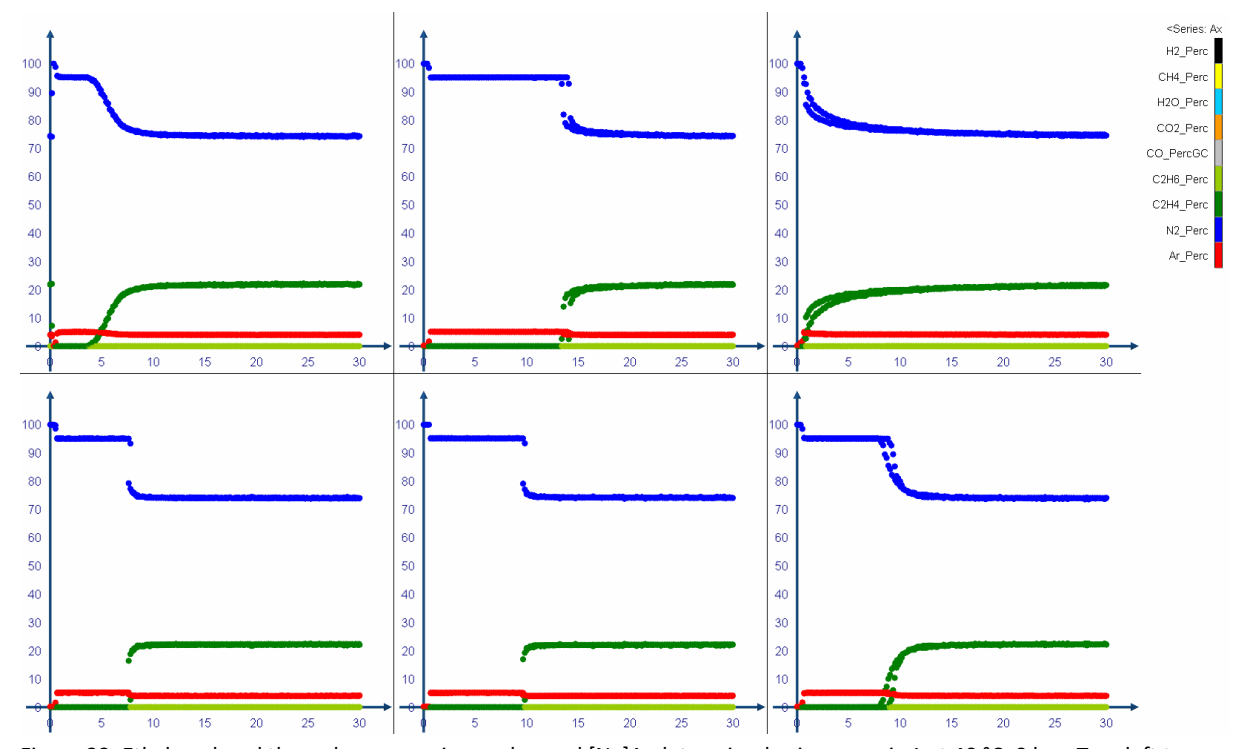


Figure 23. Ethylene breakthrough curve on ion exchanged [Na]A, determined using gas mix 1 at 40 °C, 0 bar. Top, left to right: untreated [Na]A, [Ag]A, [Li]A. Bottom, left to right: [Mg]A, [Mn]A, [Sr]A.

ECN-E--18-027 Page 35 of 79

<sup>&</sup>lt;sup>8</sup> Green Birds report (ECN-E—17-046), <a href="https://www.ecn.nl/publications/ECN-E--17-046">https://www.ecn.nl/publications/ECN-E--17-046</a>)

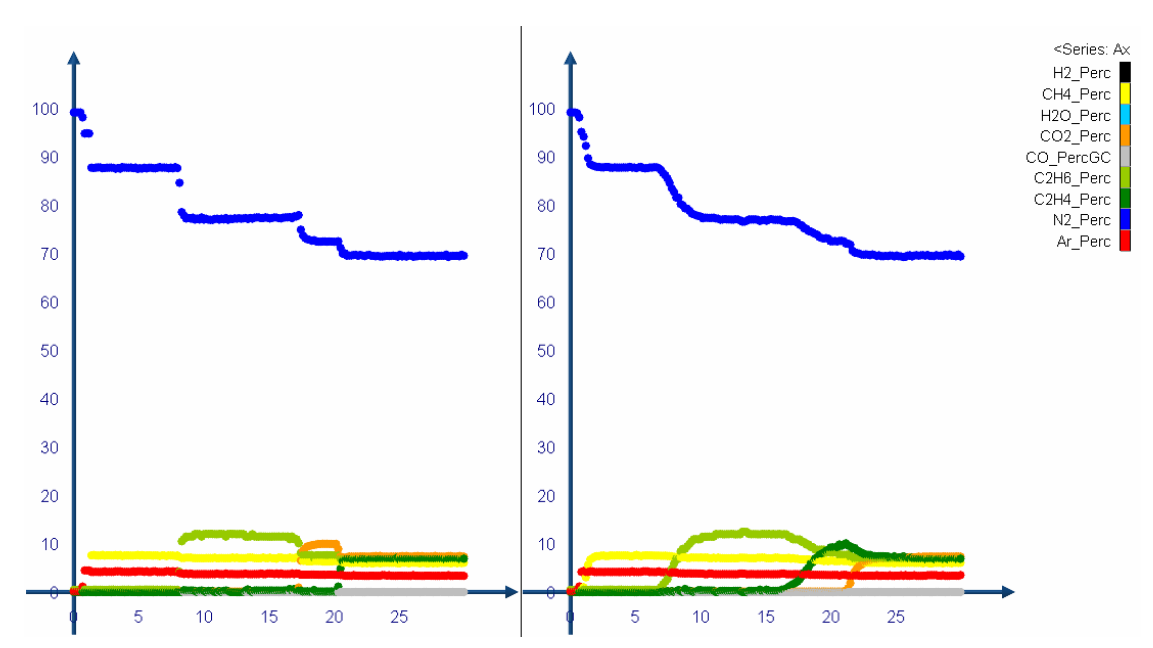


Figure 24. Selectivity of exchanged zeolite A: left [Mn]A, right [Sr]A. Determined using gas mixture 2 and CO<sub>2</sub> at 40 °C and 0 bar.

[Ca]A was functionalized with organic chains of different lengths ( $C_{12}$ ,  $C_{18}$  and  $C_{8}$ ) perfluoro (CF) surface groups. These functional groups were applied in concentrations ranging from 0.5-20 wt%. Applying organic functionalities on the surface decreased the ethylene sorption capacity and seemed to have a minor effect on the selectivity (figures not shown in this report). Another way of functionalizing the zeolite is partial exchange (25, 50%) of the  $Ca^{2+}$  with  $NH_4^+$  or  $N(CH_3)_4^+$ . Calcination of the ammonia functionalized zeolite gives its H-form. Exchanging 50% of the  $Ca^{2+}$  ion with  $Sr^{2+}$  or  $Mn^{2+}$  did not decrease the ethylene sorption capacity and did not significantly change the selectivity of the zeolite.

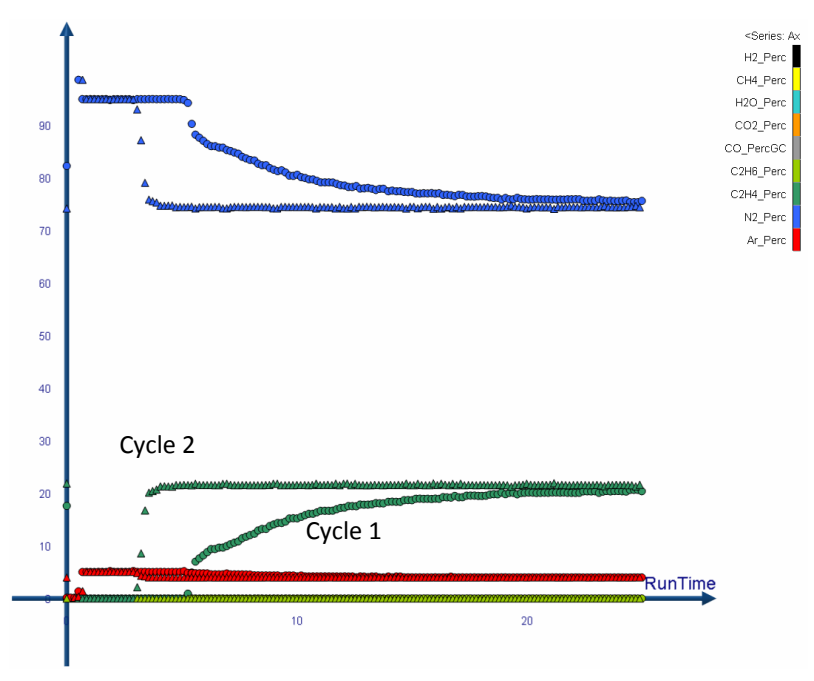


Figure 25. Change in of ethylene breakthrough curve on ZSM-5 at 40 °C and 0 bar using gas mixture 1. Cycle 1 is represented in circles. Cycle 2 is represented in triangles.

Page 36 of 79 ECN-E--18-027

ZSM-5 showed remarkable behaviour as the breakthrough curve was different in the second adsorption cycle at 40 °C and 0 bar reference pressure. In cycle 1 slow breakthrough is observed, indicating the presence of micropores with a diameter which is close to the kinetic diameter of ethylene. In the second cycle a sharp, steep breakthrough curve is observed that indicates adsorption without kinetic limitations. This can be explained by ethylene not being desorbed from the micropores or destruction of the micropores during the adsorption-desorption cycle (Figure 25). Further changes in the shape of the breakthrough curve were not observed during the following cycles. H-mordenite showed a similar behaviour but the decrease in microporosity seemed less strong.

Zeolite X and Y have same framework topology (or zeotype) Faujasite (FAU). Zeolite X shows good sorption capacity for ethylene, however selectivity for ethylene is low (Figure 26). An effect of ion exchange can be observed when comparing 13X ([Na]X) with [Li]X and [Ca]X, as the latter has the lowest affinity towards  $CO_2$  (Figure 26). There also a clear effect on the ethylene sorption capacity of zeolite X upon ion exchange with  $K^+$  (Figure 27). The effect of ion exchange of zeolite X is not as strong as for zeolite A. This can be explained by the pore size of zeolite X, which much larger than the kinetic diameter of ethylene (Table 2).

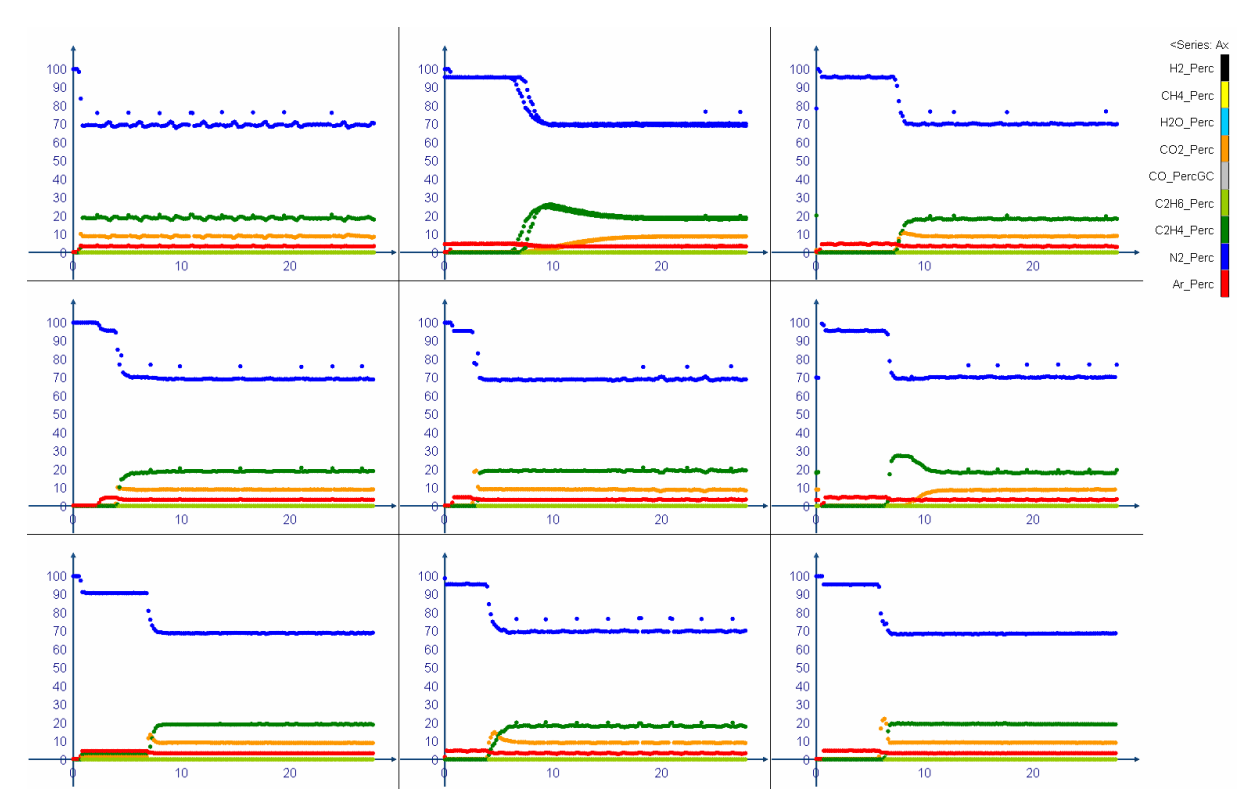


Figure 26. Ethylene and CO<sub>2</sub> sorption on zeolite Y and X (zeotype FAU), determined at 40 °C, 0 bar using gas mixture 1 with CO<sub>2</sub>. Double curves represent a repeated cycle. Top, left to right: H-SDUSY extrudates from Zeolyst, 13X beads from Aldrich, [Ca]X beads from Siliporite. Middle, left to right: H-SDUSY powder from Zeolyst, H-Y powder from Zeolyst, [Li]X beads from Siliporite. Bottom, left to right: [NH<sub>4</sub>]Y powder from Zeolyst, [Na]Y extrudates form Zeolyst, [Na]Y powder from Zeolyst.

 $[NH_4]$  and [Na] forms of zeolite Y adsorb ethylene but not selectively from  $CO_2$ . [H]Y shows a lower ethylene sorption capacity. The ethylene sorption of steam dealuminated Y (H-SDUSY) is very low due to the increased silica alumina ratio (SAR) of the material. For the breakthrough curves, it seems like the powder form of the zeolite adsorbs more ethylene than the extrudated form. This can be attributed to the use of binders such as clay to shape the zeolite, which means that effectively less zeolite is present in the reactor. However, shaping into strong, larger particles is essential to prevent a pressure drop over the sorbent bed when upscaling the sorption unit.

ECN-E--18-027 Page 37 of 79

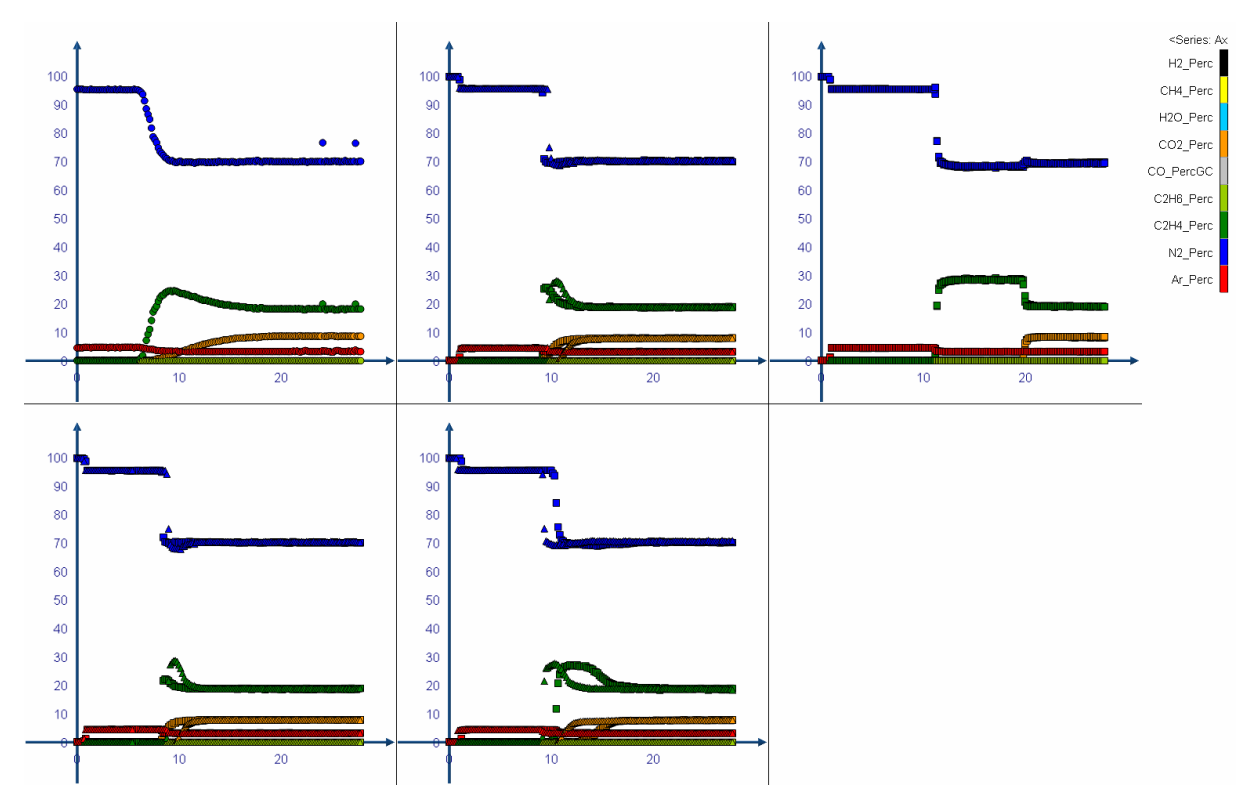


Figure 27. Ethylene and  $CO_2$  breakthrough curves on zeolite 13X determined at 40 °C, 0 bar using gas mixture 1 with  $CO_2$ . Double curves represent a second sorption cycle. Top, left to right: zeolite X, zeolite X exchanged with  $Ca^{2+}$  and  $K^{+}$  Bottom left to right: zeolite X exchanged with  $Mn^{+2}$  and  $Sr^{2+}$ 

Ethylene sorption on Ferrierite (Fer) depended strongly on cation on the material (figures not shown). As clearest example, the  $[NH_4]$ Fer did not adsorb at all. Fer extrudates showed good sorption performance, but sorption seemed kinetically limited. In all cases, ion exchange resulted in a better performance and sharper breakthrough curves. However, the extent of ion exchange did not a strong effect on the sorption capacity and selectivity, as ethane was observed to be co-adsorbed.

#### b) Active carbon

All active carbons were supplied by Norit/Cabot. These materials, except for and, CNR 115 adsorbed ethylene. Sorption capacity of C Gran was very low. The carbons have a higher affinity for ethylene than  $CO_2$  (Figure 28). In addition, large amounts of ethane were co-adsorbed by these materials.

**Page** 38 of 79

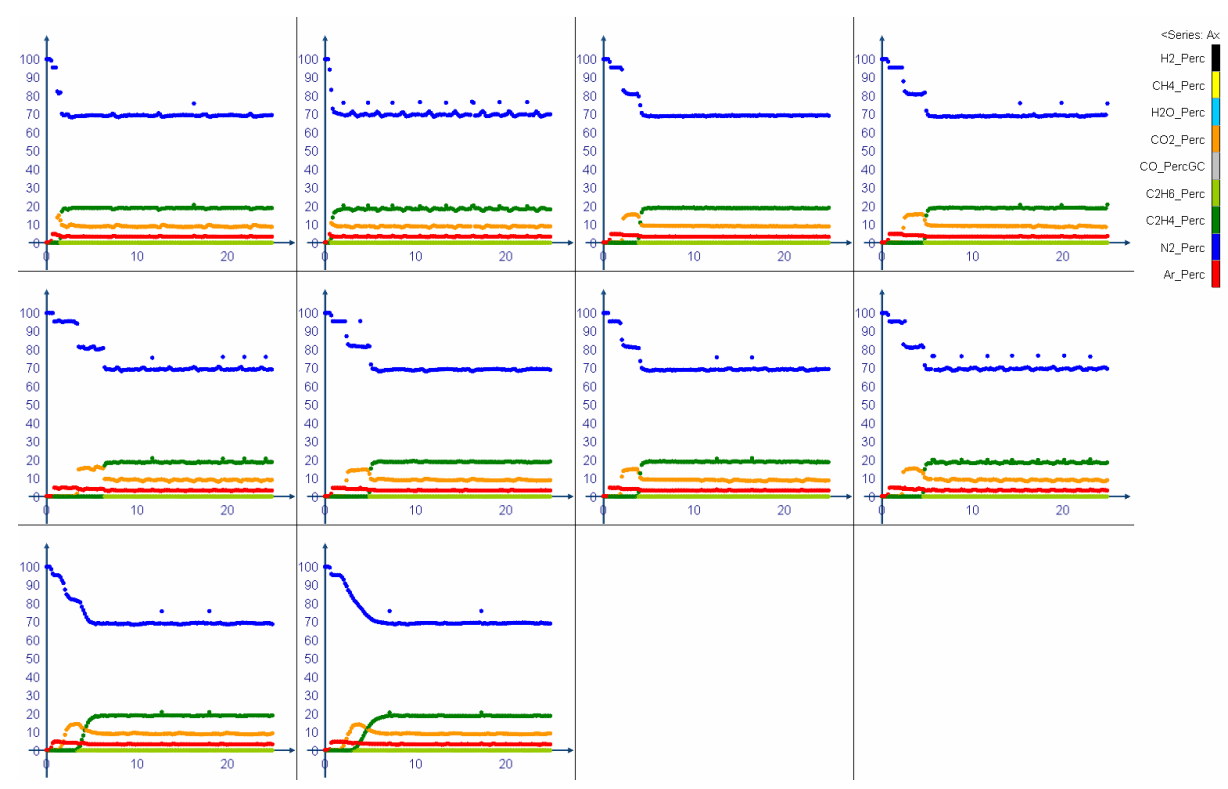


Figure 28. Ethylene and  $CO_2$  sorption on different active carbons, determined at 40 °C, 0 bar using gas mixture 1 with  $CO_2$ . Top, left to right: C GRAN, CNR 115, GAC 1240 EN, GAC 1240 Plus. Middle, left to right: GCN 3070, R1 Extra, ROW 0.8, ROX 0.8. Bottom, left to right: RX3 extra, RB3.

#### c) Metal oxides

Most tested metal oxides do not adsorb any ethylene at  $40^{\circ}$ C and 1 bar, which is related to their amorphous low-surface area character. Zirconia did only adsorb  $CO_2$  and remarkably this adsorption decreased with increasing silica content (Figure 29). Zirconia could thus be used as  $CO_2$  trap before the ethylene sorption bed. The absence of ethylene sorption on manganese oxide supports that Mn ions do not selectively bind to ethylene and that the selectivity of manganese exchanged zeolites is obtained by the pore size.

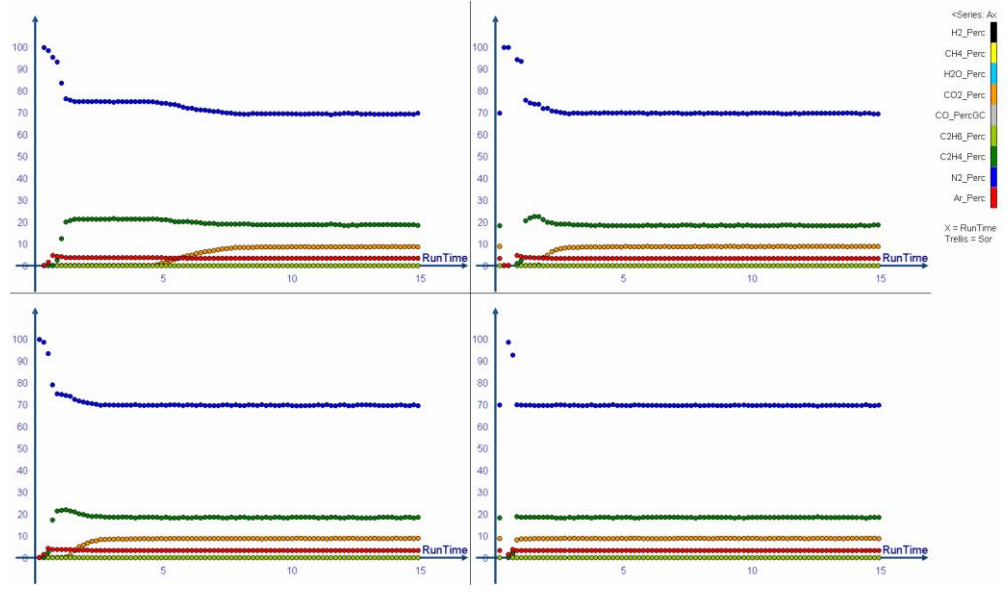


Figure 29. Breakthrough curves of ethylene and  $CO_2$  on Zirconia at 40 °C, 0 bar using gas mixture 1 with  $CO_2$ . Top, left to right: Zirconia-Silica 90-20. Bottom, left to right: Zirconia-Silica 90-10, Zirconia-Silica 40-60

ECN-E--18-027 Page 39 of 79

#### d) Metal Organic Frameworks (MOFs)

MOFs C300 and A100 have better ethylene sorption capacities than Z1200 and F300 (Figure 30, Figure 31, Figure 32 and Figure 33). However, the small particle size of the MOF crystals led to a pressure drop over the bed. A pressure difference of 5 bar noticed by the pressure indicator in the feed line. This was also observed as delay in Ar breakthrough, as it takes longer to fill up the reactor with the feed gas (Figure 30). The overcome this, the material was pressed into pellets under 3 tonnes pressure. The sorption capacity of the MOF decreased from 6.1 to 3.7 wt% upon pressing, which confirms that the material loses porosity under pressure. Of the tested MOFs, C300 and A100 have a good selectivity towards ethylene compared to CO<sub>2</sub>. Material A100 seemed to have a higher affinity toward ethane, while C300 has the highest affinity for ethylene.

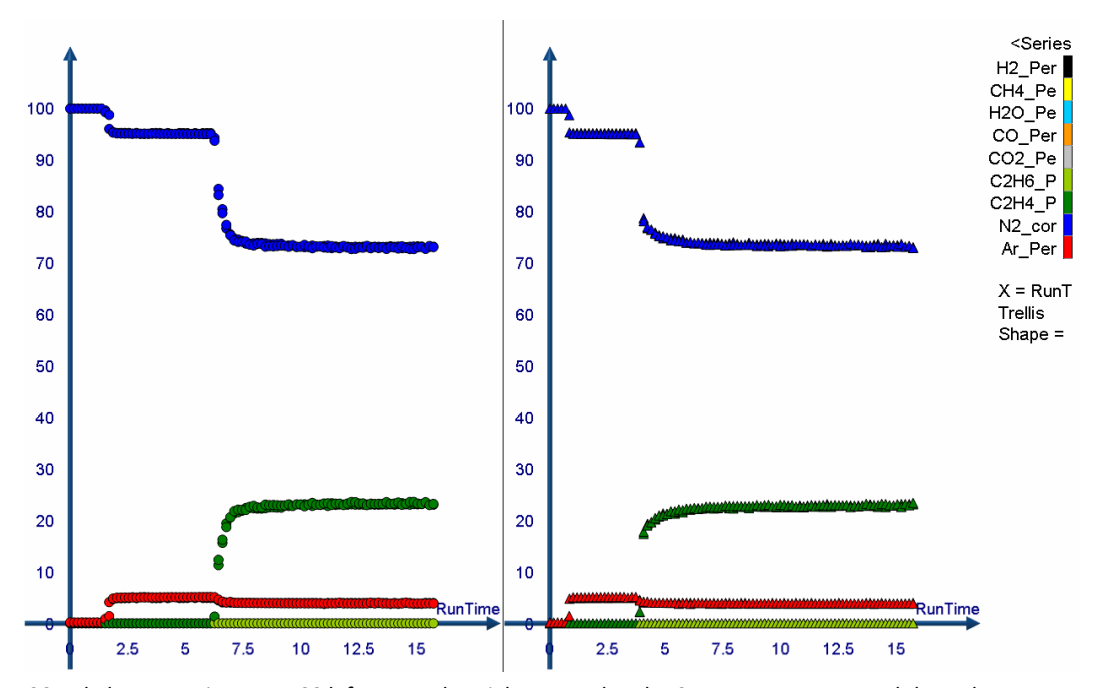


Figure 30. Ethylene sorption on A100 left as powder, right pressed under 3 tones pressure. Breakthrough curves are determined at 40 °C, 0 bar using gas mixture 1.

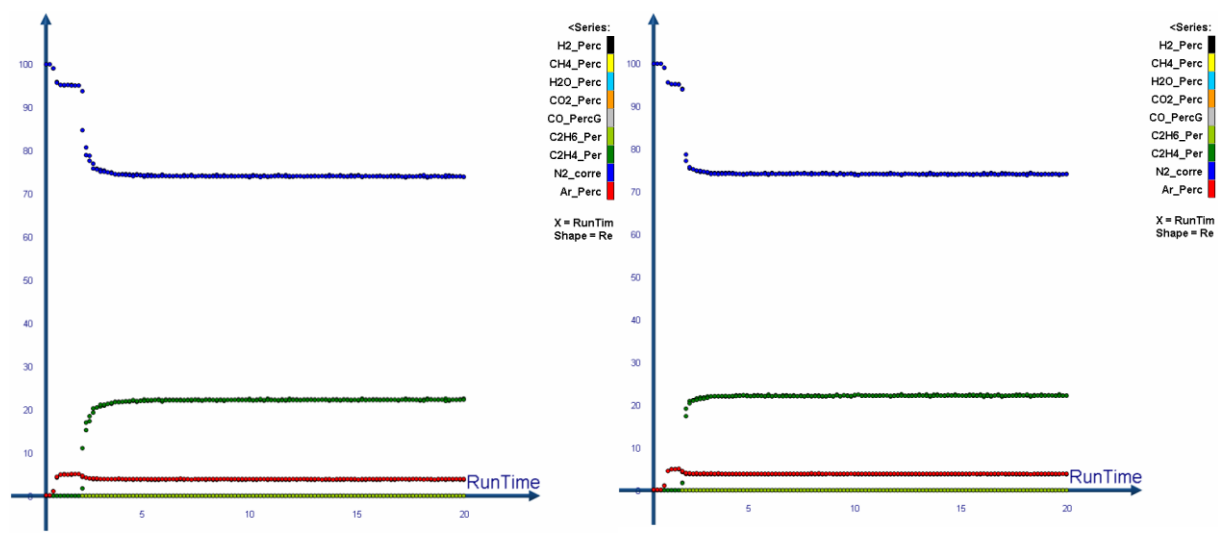


Figure 31. Ethylene sorption on F300 at 40  $^{\circ}$ C, 0 bar using gas mixture 1.

Figure 32. Ethylene sorption on Z1200 at 40 °C, 0 bar using gas mixture 1.

Page 40 of 79 ECN-E--18-027

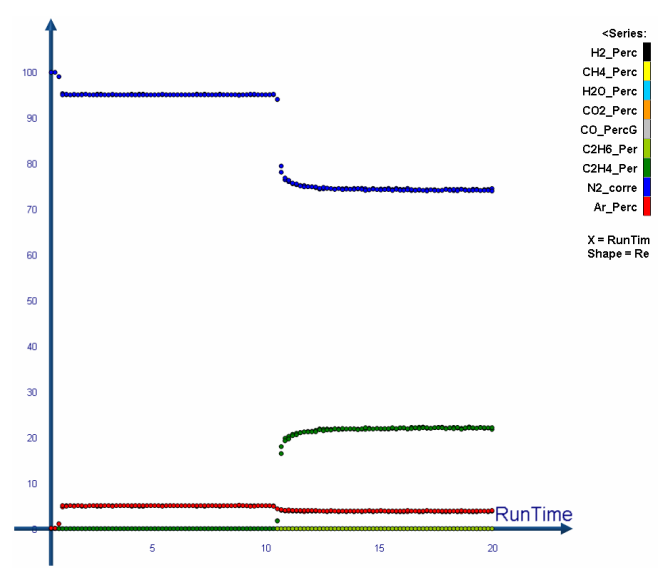


Figure 33. Ethylene sorption on C300 at 40 °C, 0 bar using gas mixture 1

#### 4.1.4 Long term testing

15 sorbents and a blank were loaded into the sorption unit and were measured over 15 subsequent adsorption-desorption cycles. Adsorption was measured at 40 °C and desorption at 200 °C. The gas mixture contained ethylene, ethane, methane, CO, CO<sub>2</sub>, H<sub>2</sub> to study the effect of reducing gases on ethylene sorption over multiple cycles. Most sorbents showed very stable performance (Table 4). MOF A100 showed a pressure drop over the sorbent bed of almost 5 bar, due to the small particle sizes as observed in earlier experiments. MOF C300 showed lower ethylene sorption in the first cycle than in the subsequent sorption cycles. A reason for this behaviour could not be found. TS-1 showed almost selective sorption of ethane, but in low quantities.

Table 4. Performance of samples over 15 adsorption desorption cycles

Sorbent	Stable operation 15 cycles	Front pressure (bar)
Blank	Yes	0.3
Carbon prepared in house	Yes	0.4
MOF A100	Yes	4.8
MOF C300	No	0.6
[Ca]A 25% H form	Yes	1.9
TS-1 silica titania	Yes	1.9
Zeolite Ca]A 40 wt% CF chains	Yes	1.1
Zeolite [Mn]A	Yes	0.8
Zirconia titania	Yes	10.2
Zeolite ZSM-5	No	1.9
Carbon Norit GAC 1240 plus	Yes	0.7
Zeolite [Na]Y	No	10.3
Zeolite ZSM-5	Yes	0.5
Zeolite [Ca]A 50% Sr <sup>2+</sup>	Yes	0.4
Zeolite Ferrierite	No	10.3
Zeolite [Ca]A 50% Mg <sup>2+</sup>	Yes	0.4

ECN-E--18-027 Page 41 of 79

Two different ZSM-5 samples were tested and both showed a decrease in ethylene sorption over repeated cycles. Zeolites [Na]Y and Fer showed an increasing ethylene sorption over time which is related to the pressure drop over the bed being equal to gas front pressure, which limited the gas feed flow. The cause of this pressure drop could not be explained in terms of particle size and might be related to technical issues. Other reactors might be affected as some fluctuation in the feed flow was observed.

#### 4.1.5 Conclusions

Amorphous metal oxides are not suitable as ethylene sorbents as they lack porosity. A range of zeolites was tested and it was shown that A and X have potential as ethylene sorbent. The effect of ion exchange and functionalization was tested; however their high affinity towards  $CO_2$  and water could not be overcome. Water can be removed from the producer gas by cooling and compression of the gas, but will increase CAPEX and OPEX of the process. In addition,  $CO_2$  will always be present in the producer gas. A combination of different zeolites could be considered to remove water and  $CO_2$  from the gas stream before sorption of ethylene.

Testing of the commercially available MOFs has shown that the materials have potential in gas adsorption and separation. However, MOFs are formed as small crystals, leading to a high pressure drop over the sorbent bed and should therefore be shaped into larger particles. It was shown that pressing the material into larger particles leads to a decrease in adsorption capacity.

Several active carbons show relatively low capacity, however a specific adsorption site for ethylene is not present. This could be improved by impregnation of the carbon with material with an ethylene specific interaction.

#### 4.2 Final tests of selected sorbents

#### 4.2.1 Experimental setup

Based on the screening study (see Section 4.1), Avantium delivered to ECN 2 selected sorbents for testing under real gasification conditions. The sorbents delivered were 2 types of zeolite (4A molecular sieve and Y-type) ion-exchanged with Mn. The complete set of results of the tests with the sorbents can be found in ECN reports ECN-BEE-2017-106 ([Mn]A) and ECN-BEE-2017-107 ([Mn]Y).

The experimental facility for the testing of the ethylene sorbent is schematically shown in Figure 34. The gasification gas was produced in the MILENA indirect gasifier. A gas slipstream of ~15 L/min was directed to the downstream equipment. The gas is cleaned from dust in a hot gas filter operating at 400°C. Then, the OLGA unit removes the tars contained in the gas. The producer gas is then cooled down to 5°C to condense out most of the water contained in the gas. Afterwards, the clean gas is compressed to ~ 6 bar and directed to units R11 (reactor which contains a ZnO sorbent for  $H_2S$  removal) and R12 (reactor filled with the Avantium sorbent). R11 was operated at 40°C (same temperature as R12) in order to avoid unwanted heating of R12, thus keeping the set temperature.

Page 42 of 79 ECN-E--18-027

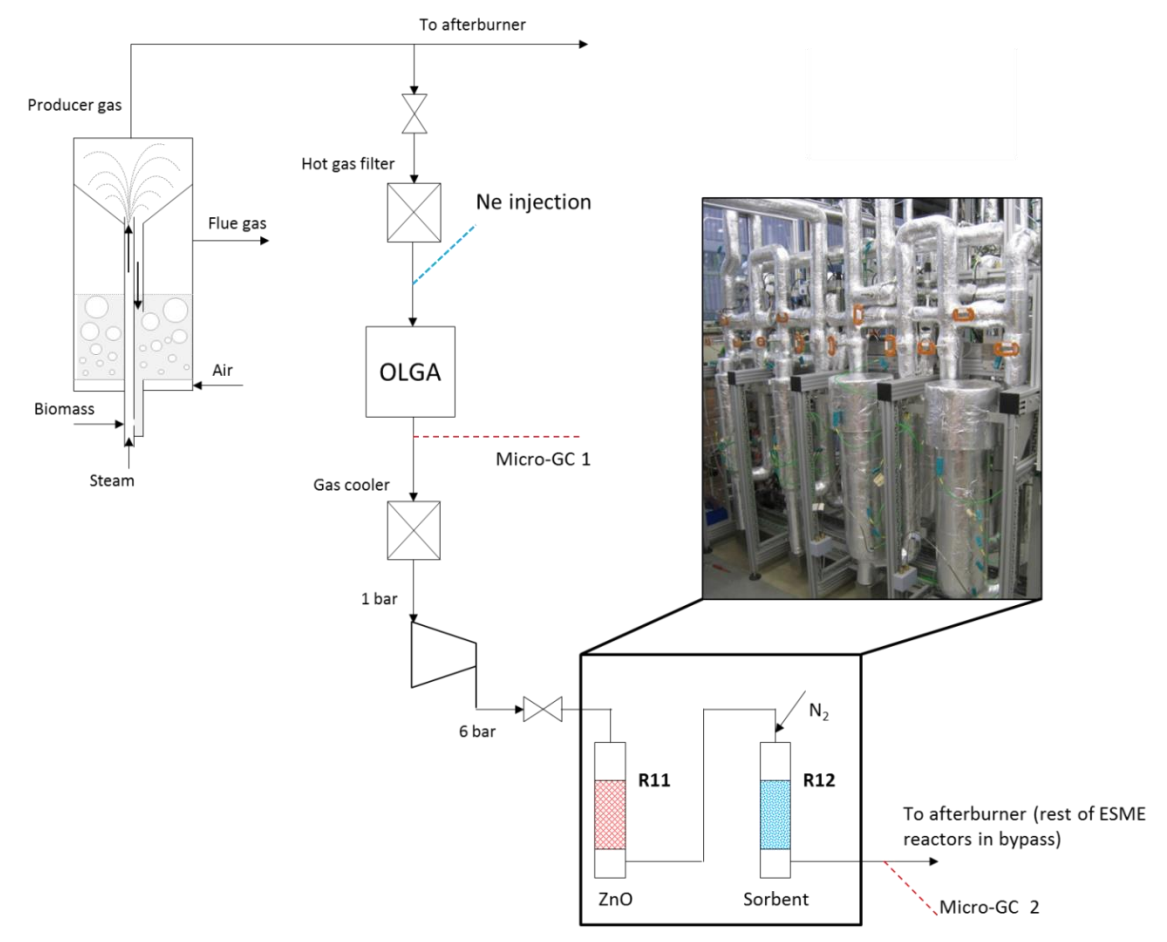


Figure 34. Schematic layout of experimental setup for the testing of Avantium sorbent for ethylene adsorption.

The MILENA gasifier was operated at standard conditions:  $^{\sim}$  5 kg/h beech wood, olivine as bed material,  $^{\sim}$  850°C riser temperature,  $^{\sim}$ 920°C combustor temperature. Both MILENA and OLGS kept stable operating conditions throughout the experiments, and their performance is out of the scope of this measurement report.

For the determination of the performance of the sorbent, online micro-GC analysis has been performed both at the inlet and outlet of the reactor. The micro-GC units can analyse the gas every 7 minutes. Neon (10 NmL/min) was moreover injected upstream the booster for the performance of balances around the reactor. Complementary, gas bags were sampled close to the start of the reactor operation and further analysed by GC-FPD and GC-FID for the determination of sulphur compounds and gaseous hydrocarbons, respectively.

The mass of sorbents and alumina placed in the bed, as well as the bed volume in each experimental set, are summarized below:

	[Mn]A zeolite	[Mn]Y zeolite
m sorbent (g)	400.5	243.1
m alumina (g)	1022.2	982
Bed height (mm)	210	~ 200
Reactor diameter (mm)	82	82
Bed volume (L)	1.11	1.06

ECN-E--18-027 Page 43 of 79

#### 4.2.2 Results of tests with [Mn]A sorbent

The experimental plan was composed of 4 cycle tests, each of them composed of 2 stages: adsorption and desorption (sorbent regeneration). Regeneration was performed in all tests by applying 10 NL/min  $N_2$  with the reactor heating up to 200°C. The tests were performed at ~ 6 bar operating pressure and 2 different GHSV values (~ 600 1/h and ~ 440 1/h) have been performed. The overview of the operating conditions in each of the cycle runs is summarized in Table 5. Test 1 consists of a cycle carried out at 40°C adsorption and 200°C regeneration and ~ 11 NL/min inlet gas. Test 2 is a replication of test 1. In test 3, a lower GHSV was applied by slightly decreasing the inlet gas flow to ca. 8 NL/min. Test 4 was finally performed using a lower adsorption temperature<sup>9</sup>.

Table 5. Overview of tests with Avantium [Mn]A sorbent for ethylene adsorption.

	Date	Inlet gas flow (NL/min)**	GHSV* (1/h)	T adsorption (TI12_04) (°C)	T regeneration (°C)
Test 1	28/06/17	11.0 ± 0.2	594.8	42.2	200
Test 2	29/06/17	11.2 ± 0.1	605.6	40.4	200
Test 3	30/06/17	8.2 ± 0.1	442.3	40.5	200
Test 4	03/07/17	8.0 ± 0.2	431.2	34.4	200

<sup>\*</sup> Calculated using the whole volume of bed (alumina + sorbent 50/50 vol.%).

In all tests, stable operating conditions were achieved. Figure 35 show as an example the results obtained during the first the sorbent reactor operated at  $^{\circ}$  5.7 bar throughout the test. The temperature indicated by TI12\_04, corresponding to the thermocouple located near the sorbent bed surface (Figure 35) showed a peak upon start of the adsorption stage. The temperature increased from 40°C to almost 70°C, and then gradually decreased to  $^{\circ}$  55°C during the adsorption stage. In any case, the use of the sorbent/inert in the bed has proved to be effective in avoiding sharp temperature peaks, such as the ones observed in the Green Birds tests in 2015. After the breakthrough of the adsorbed compounds was observed (which took place within the first 20 minutes operation), the inlet gas flow was stopped. The reactor was set to 200°C and 10 NL/min  $N_2$  was set for regeneration for 2 hours.

Page 44 of 79 ECN-E--18-027

<sup>\*\*</sup> Measured from neon balance (10 NmL/min neon as tracer gas).

<sup>&</sup>lt;sup>9</sup> In principle, R12 was set at 20°C for test 4. However, the actual temperature at the start of the test was ~ 34°C. Thus, test 4 was eventually performed under similar conditions as test 3 and can be thus considered a quasi-replication of Test 3.

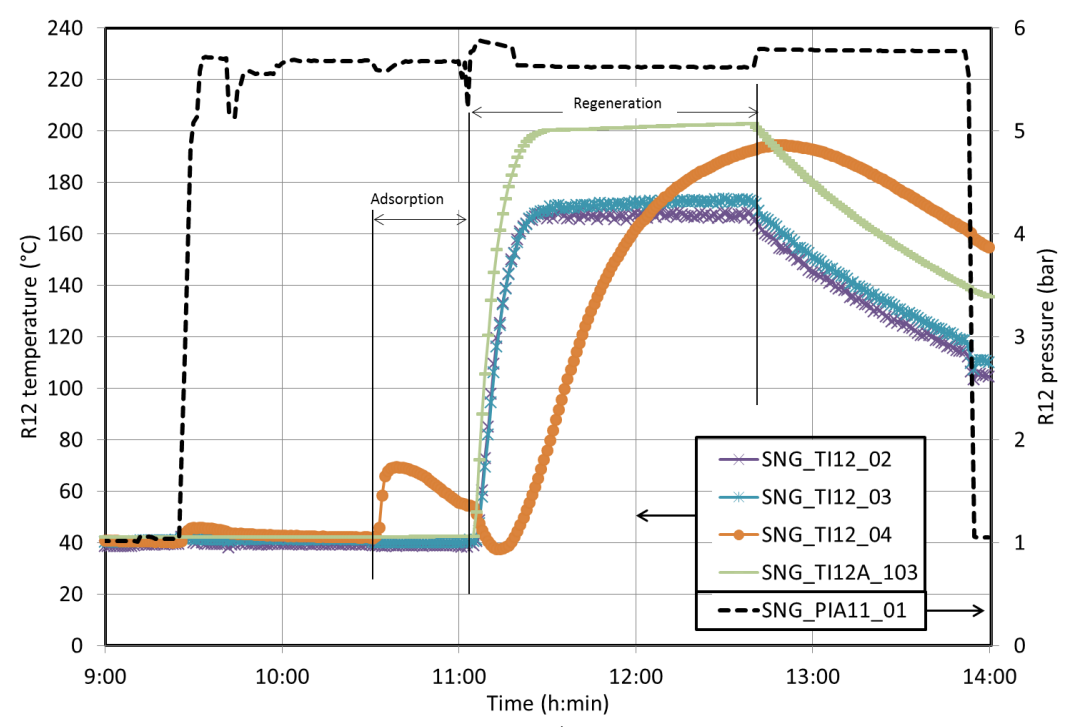


Figure 35. Reactor temperature and pressure during test 1, 28<sup>th</sup> June 2017.

Figure 36 and Figure 37 display the molar flows of the main gas compounds (calculated from balances performed around the reactor). Upon start of the feeding of producer gas in the sorbent reactor, adsorption of ethylene took place. The concentration of ethylene at the outlet of the reactor dropped to  $\sim 0.5$  vol.% dry (compared to the inlet concentration of 3.9 vol.%, dry basis). Thus,  $\sim 87\%$  of the ethylene was adsorbed in the material at the start of operation. However, also strong co-adsorption of  $CO_2$  took place. The  $CO_2$  concentration in the gas decreased from 21.2 vol.% to 3.85 vol.%. When translated into molar flows, it means that  $\sim 82\%$  of the inlet  $CO_2$  was adsorbed by the material within the first 6 minutes operation (first micro-GC analysis). Besides ethylene and  $CO_2$ , also  $C_2H_6$  and  $C_2H_2$  were captured by the sorbent (Figure 37). The results of GC-FID and GC-FPD analysis applied to gas bags sampled near the start of operation revealed that also C3-C5 gaseous hydrocarbons and sulphur compounds such as thiophene and mercaptans are partly adsorbed by the material. Simultaneously to the adsorption, a peak in the flows of CO and  $H_2$  (and to a minor extent, also of  $CH_4$ ) was observed. The adsorption process was accompanied by an increase in the bed temperature of approximately 30°C, up to  $\sim 70$ °C (Figure 35).

The adsorbed species exhibited different trends in terms of breakthrough behaviour. After  $^{\sim}$  14 minutes operation, the concentration of  $CO_2$  at the outlet of the reactor is already similar to the inlet  $CO_2$  concentration (breakthrough). Ethane follows a similar trend to  $CO_2$ , that is, rapid breakthrough taking place. In the case of ethylene, the inlet and outlet concentrations become similar after  $^{\sim}$  28 minutes operation, the outlet concentration being gradually increased after 14 minutes. Lastly, acetylene is almost completely adsorbed for more than 20 minutes.

ECN-E--18-027 Page 45 of 79

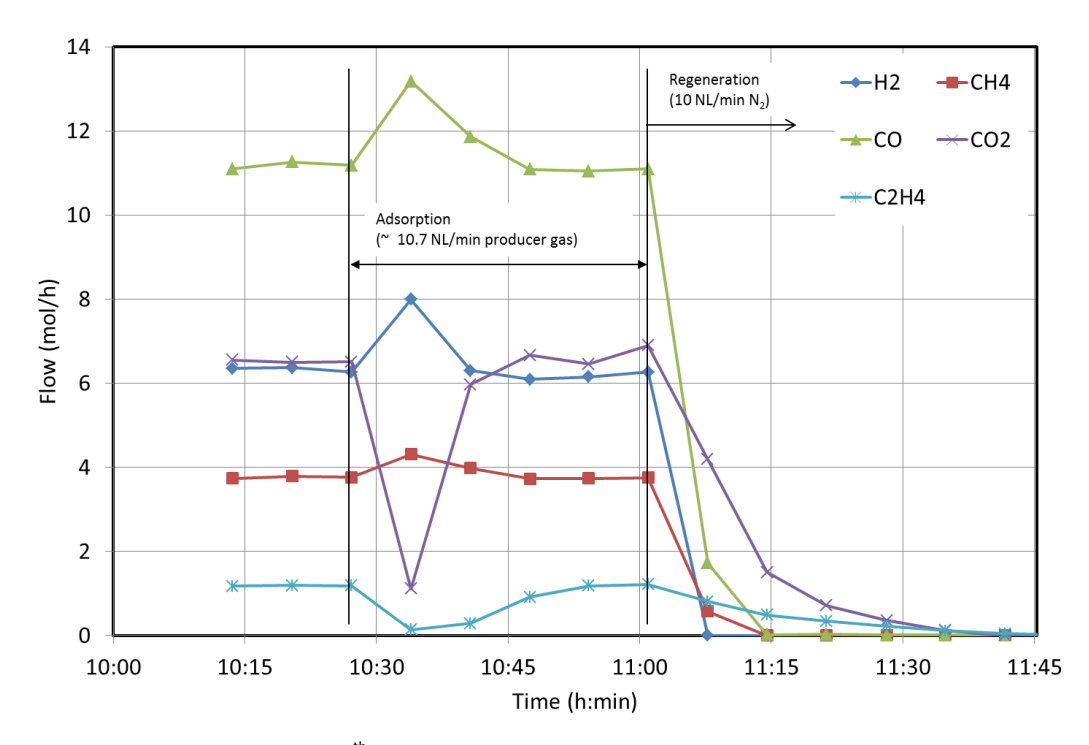


Figure 36. Molar flows during test 1, 28<sup>th</sup> June 2017: H<sub>2</sub>, CO, CO<sub>2</sub>, CH<sub>4</sub> and C<sub>2</sub>H<sub>4</sub> (measured by micro-GC, neon applied as tracer gas).

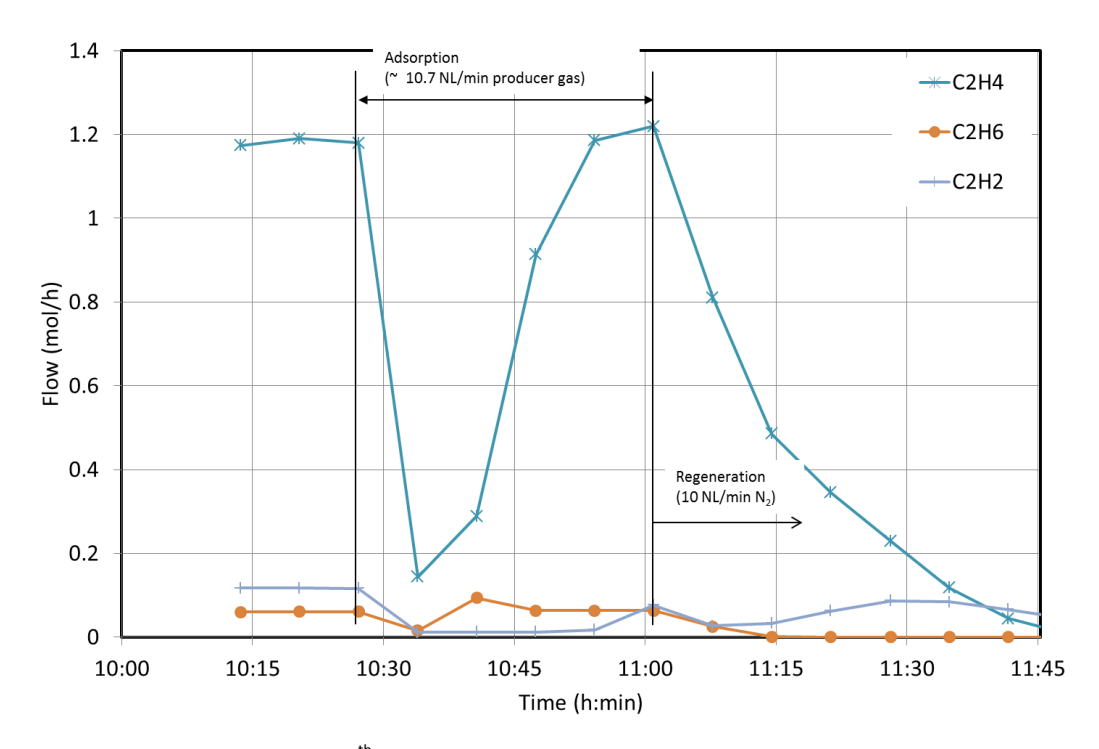


Figure 37. Molar flows during test 1, 28<sup>th</sup> June 2017: C<sub>2</sub> hydrocarbons (measured by micro-GC, neon applied as tracer gas).

After the breakthrough of all compounds was observed, the gasification gas flow was stopped, and  $10 \text{ NL/min N}_2$  was applied for the desorption stage. It must be noted that desorption took place during the heating up of the reactor to  $200^{\circ}\text{C}$ , that is during the ramp-up of temperature and not at the final set temperature. Despite the reactor heating, a clear decrease in bed temperature was observed upon start of the desorption stage, from  $55^{\circ}\text{C}$  to below  $40^{\circ}\text{C}$  (Figure 35). During regeneration, a gradual release of the adsorbed compounds was observed. In the case of ethylene

Page 46 of 79 ECN-E--18-027

and CO<sub>2</sub>, the desorption processes stretched on for approximately 40 minutes. Interestingly enough, acetylene started to be released somewhat later than ethylene and CO<sub>2</sub>. It might be possible that higher temperatures are needed for the desorption of acetylene.

Table 6 and Table 7 summarize the performance of the sorbent during the 4 cycle tests performed. As observed in Table 6, during the peak of maximum adsorption (upon the start of the test), between 88% and 93% of the ethylene contained in the inlet gas is captured by the sorbent. However, 83-89%  $CO_2$ , 57-80%  $C_2H_6$  and 90-94%  $C_2H_2$  are also co-adsorbed in the material. In this sense, the results obtained in this report are quite similar to those obtained in the first Green Birds test with a [Ca]zeolite sorbent. On the other hand, the performance of the sorbent in terms of % adsorption remains approximately constant when decreasing the GHSV.

Table 6. Summary of adsorbed ethylene and CO<sub>2</sub> in each test (outlet molar flows and % adsorbed compounds referring to the start peak of the adsorption stage).

	C <sub>2</sub> H <sub>4</sub> adsorbed (%)	CO <sub>2</sub> adsorbed (%)	C <sub>2</sub> H <sub>6</sub> adsorbed (%)	C <sub>2</sub> H <sub>2</sub> adsorbed (%)
Test 1	87.82	82.90	73.65	90.59
Test 2	90.96	87.33	76.90	93.00
Test 3	92.59	89.43	57.23	94.18
Test 4	91.63	88.54	79.99	93.71

Table 7 summarizes the total (cumulative) adsorbed ethylene and  $CO_2$  per test. Taking into account that 400.4 g sorbent was placed in the reactor, the ethylene adsorption capacity has been determined as 66-87 g/kg. As a reference, the [Ca]A sorbent tested within the Green Birds project exhibited values of  $^{\sim}$  60 g ethylene/kg sorbent. The [Mn]A sorbent tested in this experimental plan shows a reduction of the ethylene sorption capacity when decreasing GHSV: in tests 3-4, the sorption capacity for ethylene has reduced by  $^{\sim}$  21% with respect to tests 1-2. It is however not clear whether this is an effect of the different GHSV or a certain deactivation over time of the sorbent itself. Upon regeneration of the sorbent, 85-97% of the adsorbed ethylene and 65-87% of the adsorbed  $CO_2$  are released in the flush gas.

Table 7. Summary of total adsorbed ethylene and CO<sub>2</sub> by [Mn]A sorbent.

	Total adsorbed C <sub>2</sub> H <sub>4</sub> (mol)	Total adsorbed CO <sub>2</sub> (mol)	Total adsorbed C <sub>2</sub> H <sub>4</sub> (g)	Total adsorbed CO <sub>2</sub> (g)	C <sub>2</sub> H <sub>4</sub> adsorption capacity (g/kg)
Test 1	1.18	5.48	33.1	241.2	82.6
Test 2	1.23	5.59	34.5	246.0	86.1
Test 3	0.96	5.26	26.8	231.4	66.9
Test 4	0.95	4.12	26.6	181.4	66.4

#### 4.2.3 Results of tests with [Mn]Y zeolite sorbent

The experimental plan was composed of 3 cycle tests, each of them composed of 2 stages: adsorption and desorption (sorbent regeneration). Regeneration was performed in all tests by applying 10 NL/min  $N_2$  with the reactor heating up to 200°C. Test 2 was intended as a repetition of test 1 (reproducibility). Test 3 was carried out at lower pressure. A final blank test was carried out using a mixture of fresh alumina and alumina beads used in the previous tests mixed with

ECN-E--18-027 Page 47 of 79

sorbents. The overview of the operating conditions in each of the cycle runs is summarized in Table 8.

	able 8. Overview of tests with Avantium [Mn]Y sorbent for ethylene adsorption	(+ final blank test with alumina
--	---	----------------------------------

	Date	Inlet gas flow (NL/min)**	p (bar)	GHSV* (1/h)	T adsorption (°C)	T regeneration (°C)
Test 1	17/07/17	7.8 ± 0.10	5.7	443.1	40	200
Test 2	18/07/17	7.95 ± 0.13	5.7	450.0	40	200
Test 3	19/07/17	7.43 ± 0.04	1.6	420.6	40	200
Test 4 (blank)	20/07/17	n.m.	5.7	-	40	200

<sup>\*</sup> Calculated using the whole volume of bed (alumina + sorbent 50/50 vol.%).

<sup>\*\*</sup> Measured from neon balance (10 NmL/min neon as tracer gas).

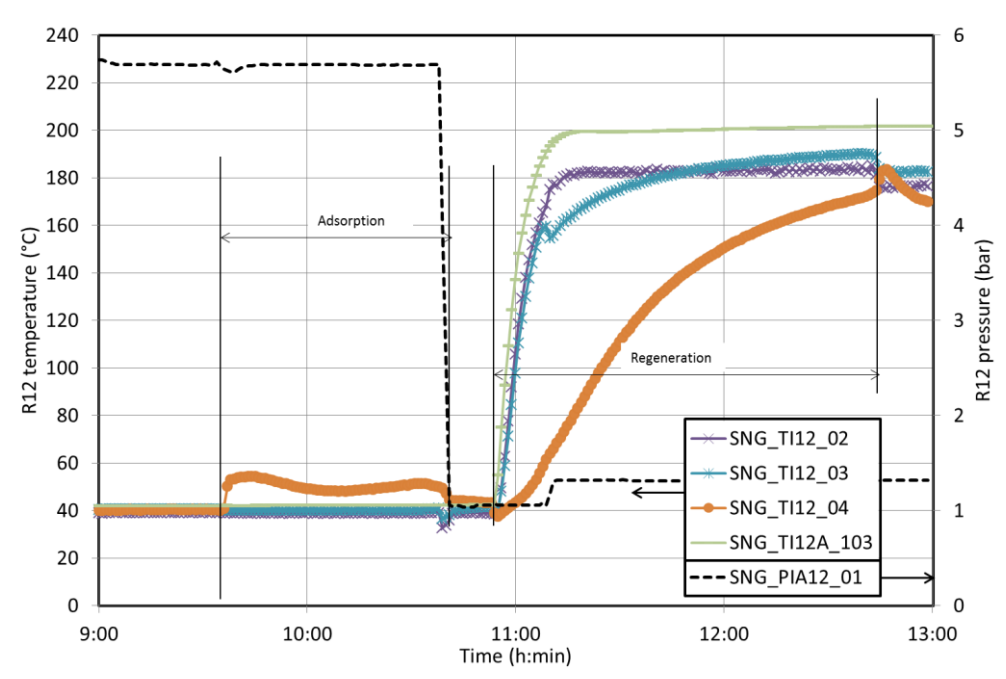


Figure 38. Reactor temperature and pressure during test 1 with [Mn]Y sorbent.

Figure 38, Figure 39, and Figure 40 plot as an example the results obtained during the first cycle test (the rest of results can be found in the measurement report ECN-BEE-2017-107). Adsorption was performed at 40°C and 5.7 bar, whereas regeneration was applied at 1.4 bar and heating up the reactor to 200°C. Upon start of adsorption, the reactor temperature increased from 40°C to almost 60°C. When comparing the performance of sorbents, [Mn]Y exhibits a less significant temperature increase than the [Mn]A sorbent (first measurement report,  $\Delta T^25-27$ °C). Moreover, the temperature profile also differs significantly: whereas the [Mn]A sorbent showed an initial peak of temperature and then returned to the set temperature , the [Mn]Y material exhibits a plateau of temperature between 50-60°C throughout the adsorption stage. On the other hand, it is worth observing that the temperature drop during regeneration of the [Mn]Y sorbent is lower than that observed with the [Mn]A sorbent (~ 10°C). In consistency with previous results using the [Mn]A sorbent, the [Mn]Y material is able to capture ~90% of the ethylene contained in the gas, but it also captures a large fraction of  $CO_2$ , as well as other hydrocarbons such as  $C_2H_6$ ,  $C_2H_2$  and benzene. The breakthrough in  $CO_2$  and ethylene takes place less than 10 minutes after the start of the experiment.

**Page** 48 of 79

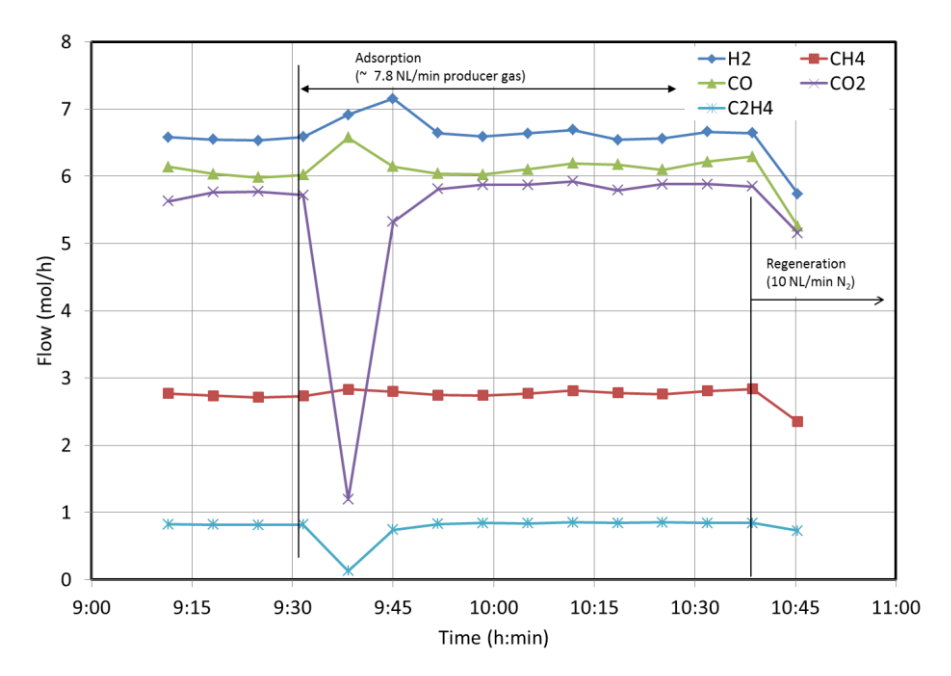


Figure 39. Molar flows during test 1 with [Mn]Y sorbent: H<sub>2</sub>, CO, CO<sub>2</sub>, CH<sub>4</sub> and C<sub>2</sub>H<sub>4</sub> (measured by micro-GC, neon applied as tracer gas).

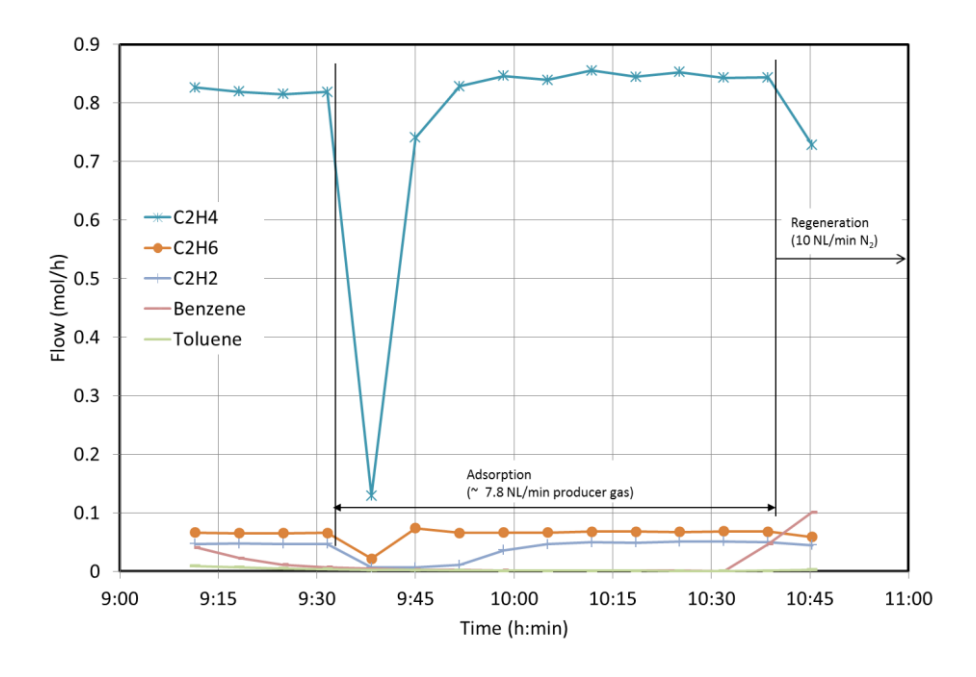


Figure 40. Molar flows during test 1 with [Mn]Y sorbent: C<sub>2</sub> hydrocarbons (measured by micro-GC, neon applied as tracer gas).

Table 9 summarizes the adsorbed ethylene and  $CO_2$  during the experiments performed, and the ethylene adsorption capacity of the [Mn]Y sorbent, respectively. The [Mn]Y material can adsorb approximately 76.6 g ethylene/kg sorbent. Thus, the ethylene sorption capacity (as well as the  $CO_2$  adsorption capacity) is slightly higher for the [Mn]Y sorbent than those of the [Mn]A sorbent.

ECN-E--18-027 Page 49 of 79

Table 9. Summary of C<sub>2</sub>H<sub>4</sub> and CO<sub>2</sub> adsorbed by [Mn]Y sorbent.

	Inlet flow (NL/min)	C <sub>2</sub> H <sub>4</sub> cumulative (mol)	CO <sub>2</sub> cumulative (mol)
Test 1, 17/07/2017	$7.8 \pm 0.10$	0.65	4.30
Test 2, 18/07/2017	7.95 ± 0.13	0.68	4.42
Test 3, 19/07/2017	7.43 ± 0.04	0.52	-0.23

#### 4.2.4 Conclusions of sorbent testing

In line with the results obtained by Avantium, both the [Mn]A and [Mn]Y sorbents are able to capture a large fraction of ethylene, but also can co-adsorb CO<sub>2</sub>, ethane and acetylene. In both sorbents, rapid breakthrough of CO<sub>2</sub> takes place before 10 minutes after start of operation.

Although the ethylene capture is reduced from  $\sim 90\%$  to 72% when decreasing the operating pressure from 5.7 bar to 1.6 bar ([Mn]Y tests), the adsorption selectivity gets considerably improved, since  $C_2H_6$  and  $CO_2$  are not adsorbed by the [Mn]Y material anymore. Still, the sorbent still co-adsorbs ethylene and acetylene. It has been estimated that the [Mn]Y material can adsorb  $\sim 76.6$  g ethylene/kg sorbent, whereas the capacity of the [Mn]A sorbent is in the range 66-87 g/kg.

Based on the results obtained, it seems that operation at low pressures and high gas flows, together with the use of materials with improved sorption capacity such as the [Mn]Y sorbent, could lead to a good trade-off between capture efficiency and sorption selectivity. However, it would be recommended to further explore in future tests a broader range of GHSV values to get a window of suitable operating conditions of the sorbent. It would also be interesting to explore new strategies of regeneration.

**Page** 50 of 79

# 5. Catalytic aromatization of ethylene

Within WP4 of the Blue Bird project, partner ECN in collaboration with partner Catalok, have explored an alternative route for the recovery of valuable compounds from gasification product gas, namely the catalytic conversion of ethylene to bio-BTX. This chapter summarizes the most relevant findings obtained during the project<sup>10</sup>.

#### 5.1 Why reactive separation?

Ethylene accounts for ~ 3.5 mol % of product gas from biomass gasification. In terms of energy, ethylene accounts for a significant fraction (~16%) of the gas. Ethylene has a harmful effect in synthesis processes as coking precursor of downstream catalysts (e.g. nickel catalysts for methanation or reforming processes). Ethylene has a higher economic value than the methane product itself (~17 Euro/GJ the former with respect to ~6 Euro/GJ the latter). However, separation of ethylene from product gas is technically challenging. Light olefins and paraffins are commonly separated by high-pressure cryogenic separation. Nevertheless, ethylene and ethane have similar boiling points, and therefore the separation of ethane/ethylene is difficult and expensive fractionation steps are needed. Therefore, low-temperature separation of olefins from gases requires high capital investment and high energy costs. Alternative processes for the separation of olefins and paraffins, such as extractive distillation, adsorption, absorption, membrane separation and hybrid processes thereof, face technical challenges such as contamination/poisoning, need for water content control, chemical and thermal stability, and fouling. A smart alternative approach consists of the implementation of reactive separation processes to convert ethylene into other high-value compounds such as aromatics, which can be more easily harvested from the gas via e.g. scrubbing. Moreover, compared with other routes for ethylene separation, the conversion of ethylene (gas) into aromatics (liquid product) is more advantageous from the logistics point of view, since expensive infrastructure for the transport of the ethylene gas stream is avoided.

The Blue Bird project has studied the catalytic conversion of ethylene to aromatic hydrocarbons using bifunctional Ga-zeolite catalysts as an alternative approach for the implementation of

ECN-E--18-027 Page 51 of 79

.

 $<sup>^{10}</sup>$  Further details about the experimental work performed in this project can be found in:

Y-T. Kuo, G. Aranda Almansa. ECN-BEE-2016-123

<sup>•</sup> G. Aranda Almansa. ECN-BEE-2016-151

Y.T. Kuo, G. Aranda Almansa, B.J. Vreugdenhil. Catalytic aromatization of ethylene in syngas from biomass to enhance economic sustainability of gas production.

co-production schemes in gasification processes. The ultimate goal is the integration of reactive separation steps into a bio-SNG process in order to enhance the business case of the process by the co-production of high-value green chemicals.

#### 5.2 State-of-the-art of ethylene aromatization

Partner Catalok performed an extensive review on the status of aromatization of alkanes and olefins, which covered research work, existing commercial technologies and patents<sup>11</sup>. This literature study was used as complementary background for the experimental work developed in the project (see Section 5.3). In this section, the main ideas of the literature and patent review are briefly outlined.

For both lower alkane and ethylene aromatization, the preferred catalysts are promoted ZSM-5 catalysts that synergistically combine a dehydrogenation (Mo, Ga or Zn) and an acidic function (H $^+$ ). In the case of ethylene aromatization, Ga/ZSM-5 and Zn/ZSM-5 are effective catalysts. The best Ga/ZSM-5 catalyst in conversion of 5% ethylene in N $_2$  showed > 90% ethylene conversion with 80% aromatics selectivity at 400°C. In general, factors which dictate the performance of the catalyst include the Ga content and the Si/Al ratio. With increasing aromatics formation, benzene increases, especially at higher temperatures while the formation of toluene passes through a maximum at 500°C and C8-aromatics decline.

A variety of zeolites of different structures have been claimed in patent literature, but ZSM-5 remains the preferred zeolite because of its greater stability. Additional promoters in combination with Ga have been claimed extensively. Ga/ZSM-5 as aromatization catalyst has been widely patented at least since 1988 and thus the first patents have expired and the general principle of using Ga/ZSM-5 as a catalyst should be free to operate. A number of companies and institutes are active in patenting the aromatization of alkanes, olefins or biomass, among others Anellotech, Sabic, ExxonMobil, BP, UOP, Süd-Chemie, ENI, Shanxi Coal Chemistry Institute, Daqing Petroleum College, Oklahoma State University, University Notre Dame du Lac, University of Tulsa, University of Louisiana, and the Institute Français Du Petrole.

The production of aromatics from lower alkanes (C3-C6) is technically feasible and several commercial processes (>8) have been proposed using bi-functional ZSM-5 zeolites promoted with Ga, Zn or Pt. These processes are based on natural gas or refinery streams. Regeneration of the catalyst is mostly performed by switching reactors. In Anellotech's single-reactor Catalytic Fast Pyrolysis (CFP) process for converting pinewood sawdust and other biomass, the addition of Ga to ZSM-5 in a bubbling fluidized-bed reactor at 550°C increased the aromatics yield from 15 to 23% based on biomass input (overall carbon yield). Reaction temperatures between 450°C and 600°C gave the best BTX yields.

#### 5.3 Experiments for ethylene aromatization

Within WP4 of Blue Birds, an extensive study of the effect of the main operating conditions on the catalytic conversion of ethylene contained in gasification product gas to aromatics using bifunctional Ga-ZSM-5 catalysts has been performed.

A number of Ga-ZSM-5 catalysts were synthesized. Most of the catalysts were prepared by slurry wet impregnation to achieve different loadings of Ga, although ion exchange was also used to

Page 52 of 79 ECN-E--18-027

<sup>&</sup>lt;sup>11</sup> For further details refer to M. Lok 'Aromatization of Ethylene and Lower Alkanes - A Literature Review' and 'Aromatization of Alkanes and Olefins, a Patent Search'

study the effect of catalyst preparation. All the catalysts were pelletized and sieved to 40/70 mesh before testing<sup>12</sup>.

The Ga-ZSM-5 catalysts were tested in terms of activity and stability under relevant gasification conditions. The schematic layout of the experimental setup is presented in Figure 41. The experiments were carried out in an oven fixed-bed reactor placed downstream the 25 kWth MILENA gasifier, the OLGA tar removal system and the gas cooler. A slipstream of  $^{\sim}$  1 Nm³/h dry gas from MILENA was directed to the system downstream. Then, most of the water contained in the gas is removed in a gas cooler operating at 5°C. Although  $^{\sim}$  90% of the ammonia contained in the gas is removed in the condensed water, the remaining traces of ammonia in the feed gas were further removed in a flask containing a 1 M nitric acid solution.

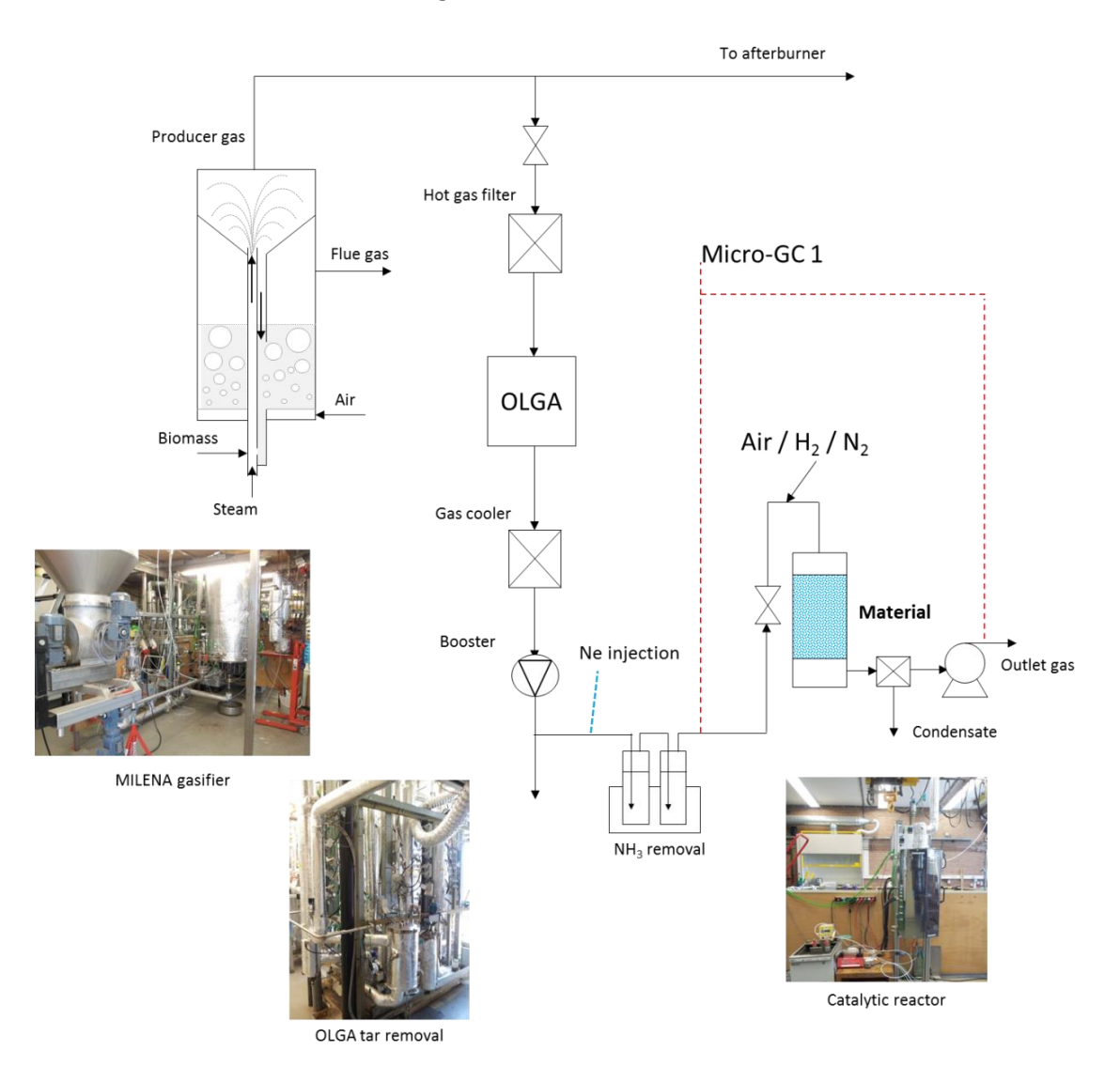


Figure 41.Schematic layout of experimental setup for the testing of ethylene aromatization catalysts.

The MILENA gasifier was operated under the following operating conditions: ~ 5 kg/h beech wood as biomass fuel, olivine as bed material, ~ 850°C gasification temperature, 1000 g/h steam fluidization, and 10 NmL/min neon injected as tracer gas in the settling chamber.

ECN-E--18-027 Page 53 of 79

 $<sup>^{12}</sup>$  Further details about the synthesis procedure can be found in the note ECN-BEE-2017-123

From the molar balances performed over the reactor, several parameters have been calculated in order to assess the performance of the catalysts:

Ethylene conversion (%) = 
$$\frac{X_{C_2H_4,in}-X_{C_2H_4,out}}{X_{C_2H_4,in}} \times 100$$
 (Eq. 1)

where X is the molar flow in mol/h. The inlet value of gas composition has been taken in all cases as the last micro-GC analysis before switching to the outlet gas composition.

Carbon selectivity to product 
$$C_x H_y$$
 (%) = 
$$\frac{x(\hat{\mathbf{n}}_{C_x H_y, out} - X_{C_x H_y, in})}{2(X_{C_2 H_4, in} - X_{C_2 H_4, out}) + 2(X_{C_2 H_2, in} - X_{C_2 H_2, out})} \times 100$$
 (Eq. 2)

where  $\dot{n}i$  represents the molar flow of compound i in the gas (in mol/h), and x is the number of moles of carbon contained in the generic compound with formula  $C_xH_y$ . (Eq. 2) considers all the carbon converted from  $C_2H_4$  and  $C_2H_2$ .

Before the test, the catalyst was activated by heating up to  $500^{\circ}$ C at a heating at a rate of  $2^{\circ}$ C/min under 0.5 L/min of a gas mixture composed of 60 vol.%  $H_2$  in  $N_2$ . The  $H_2/N_2$  activation gas was applied overnight. After intermediate  $N_2$  flushing, 0.5 L/min air was applied for 0.5 hours. After flushing again the reactor with  $N_2$ , clean gas from the MILENA gasifier and the OLGA tar removal system was started to be fed to the reactor.

The experimental plan included the effect of the main operating conditions, namely reaction temperature (300-500°C), Ga loading (0-2.5 wt.%), gas hourly space velocity (700-2100 1/h), zeolite acidity and catalyst preparation. In this report we will include some of the main results. Further details can be found elsewhere<sup>13</sup>.

#### 5.4 Results

#### 5.4.1 Effect of reaction temperature

The catalyst containing 2.5 wt% Ga was investigated in the range  $300-500^{\circ}$ C. Complete conversion of acetylene was achieved regardless of the reaction temperature. This is consistent with its highest reactivity among  $C_2H_x$  compounds. Moreover, lower temperatures lead to higher conversion of ethylene, but to lower ethane production (not shown here). Therefore, the conversion of ethylene is inversely proportional to the formation of ethane. Ethane and methane are by-produced as a consequence of the hydrogen-transfer mechanisms in which the formation of diene, cyclic diolefins and aromatics is balanced by the formation of paraffins. In Figure 42 it can be observed that benzene and toluene production show different trends. On the one hand, benzene production is favored at higher temperatures. On the other hand, the decrease of toluene concentration is only evident when decreasing the temperature from  $400^{\circ}$ C to  $300^{\circ}$ C. Although lower temperatures lead to lower benzene and toluene production, higher ethylene conversion was also observed. Thus, there is a trade-off between conversion and selectivity to aromatics. These results indicate that the reactions mechanisms and active sites of toluene and benzene are different. In other words, the formation mechanism of toluene does not need benzene as an intermediate, which suggests that their active sites are not at the same location.

Page 54 of 79 ECN-E--18-027

<sup>&</sup>lt;sup>13</sup> Please refer to ECN-BEE-2016-151

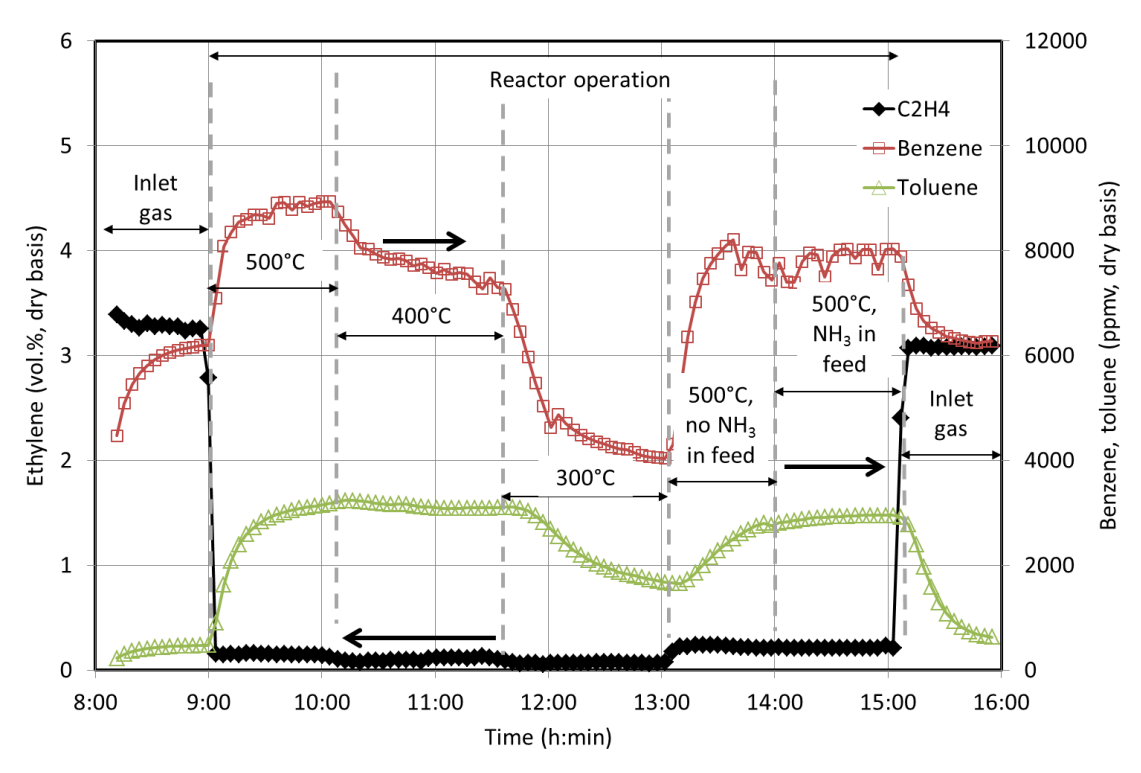


Figure 42. Effect of temperature on the inlet and outlet concentrations of ethylene, benzene and toluene.

Figure 43 summarizes the effect of the reactor temperature on the conversion and carbon selectivity performance of the 2.5 wt.% Ga-ZSM-5 catalyst. Although decreasing the temperature from 500°C to 300°C leads to a slight increase of the ethylene conversion from 95% to 97%, it also leads to lower carbon selectivity to aromatics. The carbon selectivity to benzene decreases from ~30% to even negative values when decreasing temperature from 500°C to 300°C, whereas the effect of temperature on selectivity to toluene starts to be visible when decreasing temperature from 400°C to 300°C, values halving from >30% to ~15%.

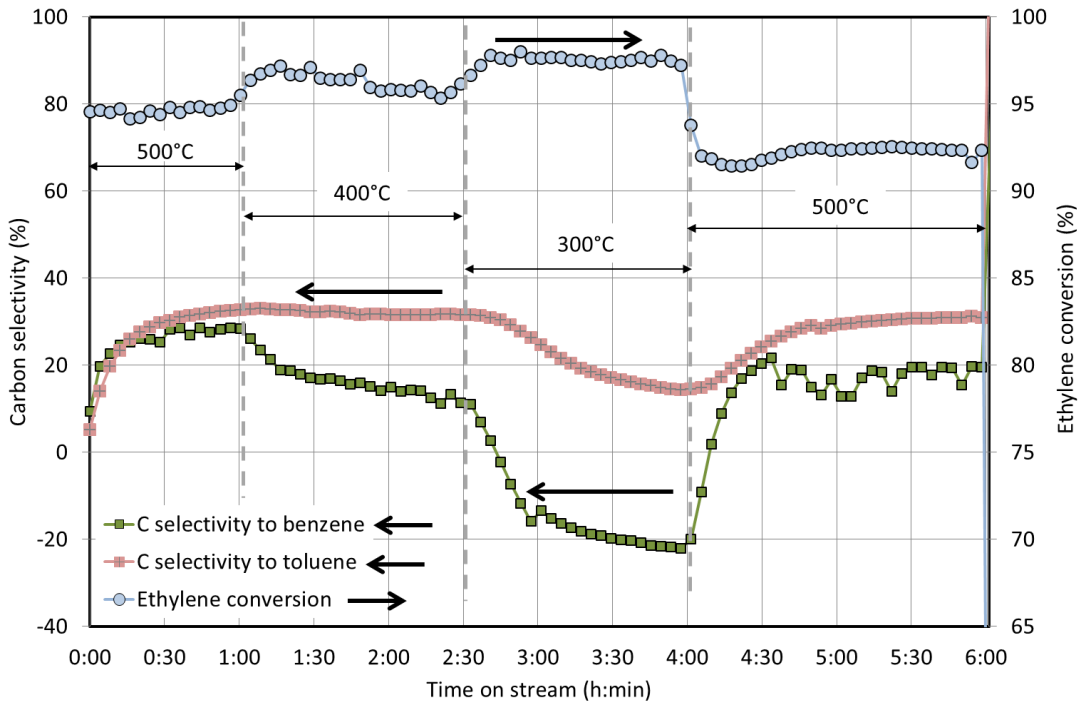


Figure 43.Effect of temperature on ethylene conversion and carbon selectivity to benzene and toluene.

ECN-E--18-027 Page 55 of 79

Complementary Solid Phase Adsorption (SPA) analyses were also carried out at the inlet and outlet gases under stable conditions for the determination of the content and composition of other aromatic compounds besides benzene and toluene which cannot be measured online by micro-GC. The results (not shown in this report) revealed that the catalytic aromatization reaction produces besides benzene and toluene other aromatic compounds such as ethylbenzene, xylenes, indene, naphthalene and methyl naphthalene. The reaction temperature influences dramatically on the distribution of the aromatic products. Whereas lower temperatures favor the production of ethylbenzene and xylenes, higher temperatures promote the production of naphthalene and naphthalene derivatives.

Figure 44 shows as an example the trends obtained during the test with a 2.5 wt.% Ga in ZSM-5 and 500°C (similar stable conditions were achieved with the rest of catalysts tested). The ethylene concentration dropped initially from 3.5 vol.% dry to < 0.1 vol.% dry (thus, approximately 97% conversion). Ethylene conversion slightly decreased over time to over 0.1 vol.%, but in general, the behavior of the catalyst material was very stable. It might be possible that the feed producer gas composition leads to milder reducing conditions than e.g. pure hydrocarbon feeds. Benzene increased from  $\sim$  7000 ppmv to above 10000 ppmv, whereas toluene values increased from  $\sim$  500 ppmv to 4000 ppmv (all values in dry basis). Although not shown in this paper, the temperature near the catalyst bed surface increased by  $\sim$  13°C upon start of the operation.

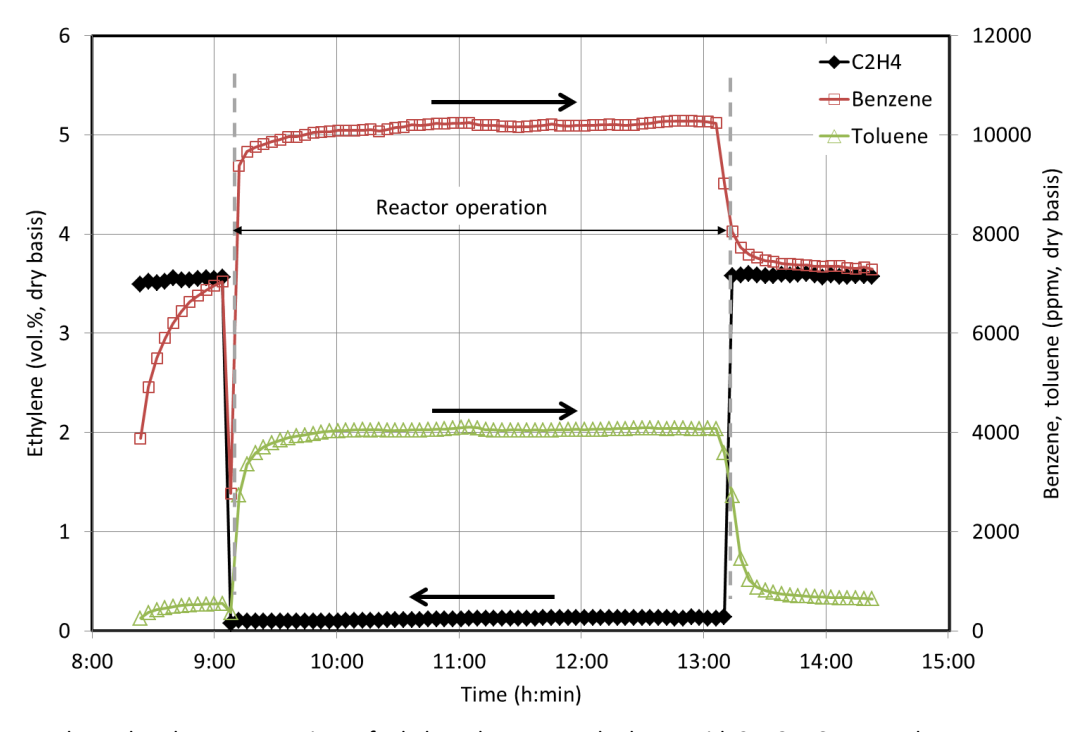


Figure 44. Inlet and outlet concentrations of ethylene, benzene and toluene with 2.5 Ga ZSM-5 catalyst.

Complete conversion of acetylene, as well as a dramatic increase of ethane concentration from  $^{\circ}0.25$  vol.% dry to over 1 vol.% was observed during the tests (not shown in this report). Both methane and ethane are by-products of aromatization. The reciprocal trends of  $C_2H_6$  and  $CH_4$  over time might be attributed to the progressive hydrogenation of ethane to methane. In any case, the by-production of methane and ethane is a feature that makes ethylene aromatization an attractive option for integration in bio-SNG processes, since the aromatization by-products are added up to the bio-SNG product itself.

**Page** 56 of 79 ECN-E--18-027

#### 5.4.2 Effect of Ga loading

Figure 45 shows that higher Ga loadings favor the conversion of ethylene. The reference Ga-free zeolite leads to ethylene conversion values of  $^{\sim}$  80%. At a Ga loading of 0.5 wt.%, the ethylene conversion still can keep as high as 85-90%. The conversion values with the 2.5 wt.% Ga catalyst were highest, around 96-97%.

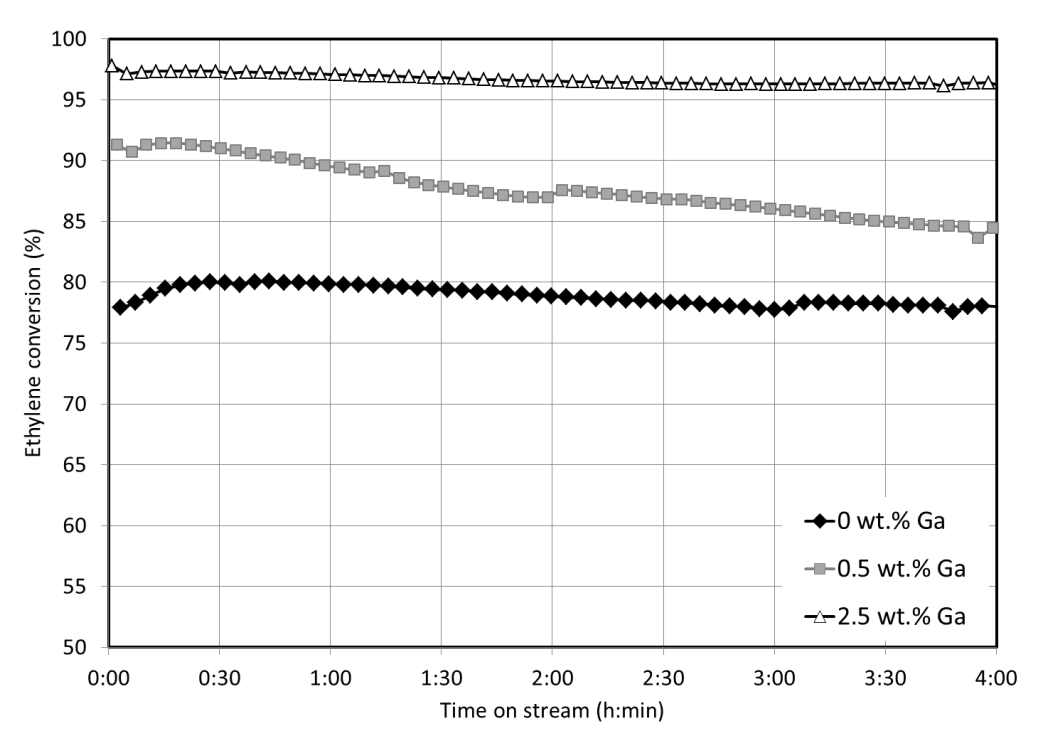


Figure 45. Effect of Ga loading on ethylene conversion.

The carbon selectivity to benzene, displayed in Figure 46, dramatically increases from 8% (Ga-free zeolite) to 32% (0.5 wt.% Ga). In all cases, the activity of the catalyst remained fairly stable over time. The 0.5 wt.% Ga-catalyst reaches the maximum selectivity to benzene. The blank ZSM-5 sample exhibits the lowest carbon selectivity to benzene (~8%), but the highest carbon selectivity to toluene (~45%). Moreover, it can be observed that the unloaded zeolite requires a longer time (about 1.5 hours) to reach a stable equilibrium state than the Ga-zeolites. Both the 0.5 wt.% Ga and the 2.5 wt.% Ga catalysts display have similar carbon selectivity to toluene (~30%). The results support the reaction mechanism proposed when studying the effect of temperature, which suggests that the active sites for toluene and benzene production are different. Toluene formation does not need Ga<sup>+</sup> active sites. The addition of Ga reduces the number or density of Brønsted-Lowry acid actives sites, thereby reducing the conversion of ethylene to toluene. The 0.5 wt.% Gazeolite catalyst leads to a maximum in the overall carbon selectivity to aromatics of over 60%.

ECN-E--18-027 Page 57 of 79

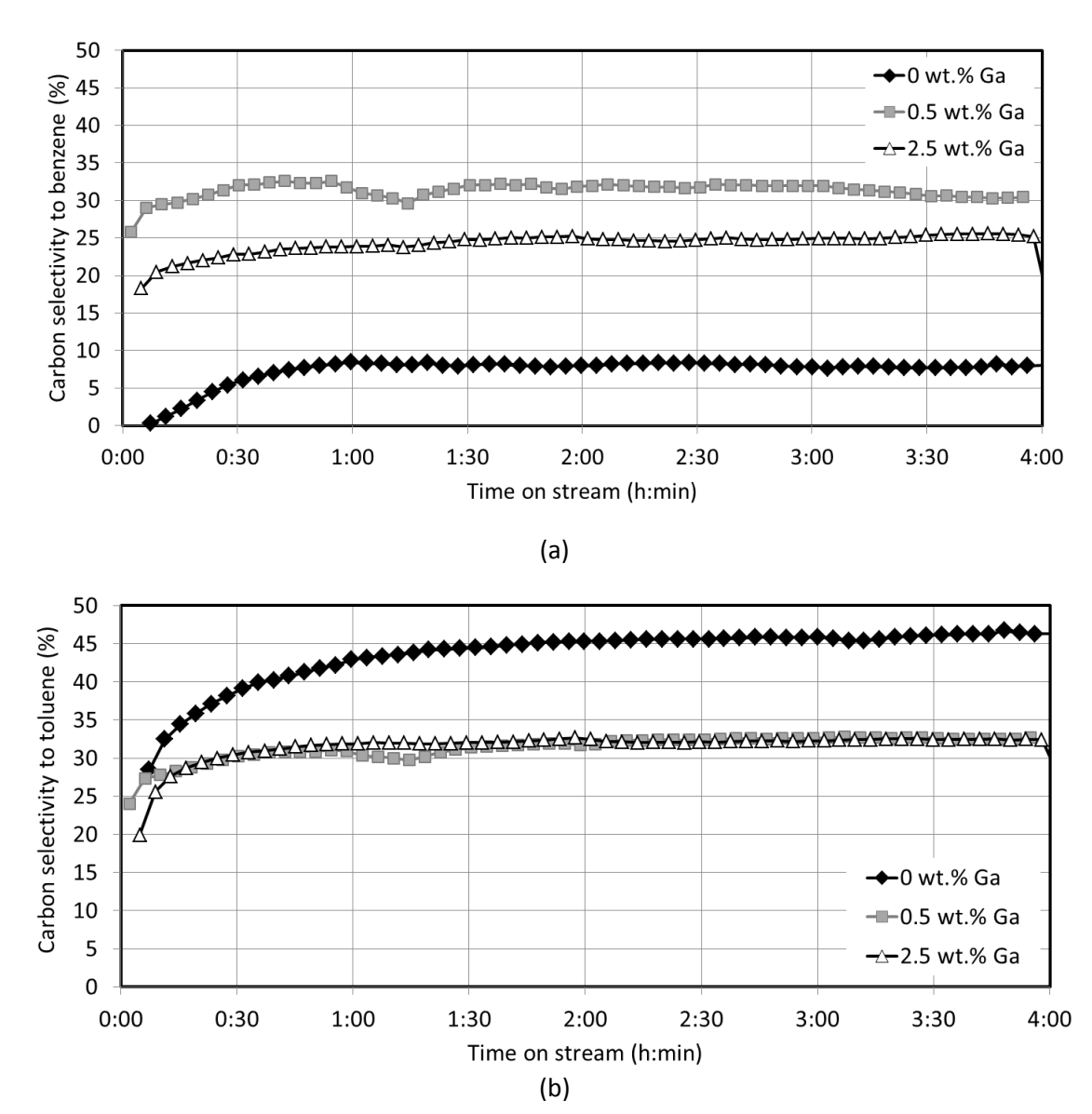


Figure 46. Effect of Ga loading on carbon selectivity to benzene (a) and toluene (b).

Ethane formation is favored at higher Ga contents in the catalyst (figure not shown in this report). This trend is consistent with the benzene formation mechanism, which presumes that the reaction is produced at the Ga<sup>+</sup> active sites. Moreover, there are 2 main reactions required in the formation mechanism of benzene: dehydrogenation and proton transfer. The Ga<sup>+</sup> active sites display both functionalities. Indeed, it also means that the two reactions are in competition with each other. After ethylene adsorbs on the active site of Ga<sup>+</sup> and forms the intermediate (dissolved complex), the reaction can either continue to oligomerization to aromatics, or be hydrogenated to ethane. Therefore, simultaneously to the reaction of ethylene to benzene, the alkylation of ethylene to ethane takes place as well.

Complementary SPA analyses (not shown) revealed that the addition of Ga to the ZSM-5 zeolite favors the yield of naphthalene and naphthalene derivatives. Taking into account the production of high-molecular weight aromatic hydrocarbons, a maximum in the overall carbon selectivity to aromatic hydrocarbons of about 73% has been determined for the 0.5 wt.% Ga-zeolite, as reported in the summary Table 10. The aromatic products can afterwards be separated in the BTX scrubbing unit (see Section 3 of this report), thus leading to an increase of the value chain by co-producing fuels and chemicals.

**Page** 58 of 79

Table 10. Summary of effect of Ga loading on ZSM-5 zeolite on the catalyst performance.

		Carbon selectivity (%)					
Test	C <sub>2</sub> H <sub>4</sub> conv (%)*	Benz*	Tol*	XyI †	EB †	C10 †	Total
		Deliz					aromatics
0 Ga-ZSM-5-I	78.9± 0.8	7.5±1.4	43.9±3.2	8.7	1.3	5.6	66.9
0.5 Ga-ZSM-5-I	87.6 ±2.2	31.4±0.8	31.5±1.3	4.1	0.7	5.5	73.2
2.5 Ga-ZSM-5-I	96.7±0.4	24.4± 1.1	31.8±1.3	3.6	0.2	7.0	67.1

<sup>\*</sup>From average values measured by online micro-GC analysis.

No severe carbon deposition occurred on any of the catalysts tested after 4 hours operation, as determined during post-inspection, although some carbon was present (greyish material after test compared to white material before test).

#### 5.4.3 Proposed reaction mechanism

Based on the results discussed in this section, a reaction mechanism (based on models presented in literature<sup>14,15</sup>) is proposed and summarized in Figure 47. The trends of carbon selectivity towards the different products lead us to the conclusion that the formation of benzene and toluene takes place in different active sites. We suggest that the addition of Ga favors dehydrogenation, and dehydrocyclization of intermediate compounds formed from the oligomerization of ethylene. This leads to the increase of ethylene conversion observed with the increase of Ga loading. The hydrogen produced in the dehydrogenation and dehydrocyclization reactions becomes available for further hydrodealkylation reactions. Moreover, the trends of benzene and toluene carbon selectivity seem to indicate that toluene is mainly formed on the external surface of the zeolite and does not require Ga. The addition of Ga produces a partial replacement of the zeolite acid sites with Ga species sites within the pore channels of the zeolite which eventually modifies the extent of the aromatics interconversion reactions. Whereas the unloaded zeolite seems to promote mainly the hydrodealkylation of xylenes to toluene (which leads to the side production of methane), the creation of Ga sites leads to the enhancement of hydrodealkylation of xylenes to benzene. Thus, the selectivity towards benzene increases at the cost of the (competing) production of toluene at the zeolite acid sites. Ethane is co-produced in the benzene formation reactions, which explains the parallel trends observed between ethane and benzene. It might be possible that when increasing the Ga loading beyond ~ 0.5 wt.%, the bond strength of ethylene and Ga+ complex becomes too weak, so that reverse hydrogen transfer reactions forming alkanes such as ethane and methane are more likely to happen than further dehydrocyclization to produce aromatics. This would explain the observed decrease in selectivity to benzene, and the increase of carbon selectivity to methane and ethane.

ECN-E--18-027 Page 59 of 79

\_

<sup>†</sup> From SPA analysis taken under stable conditions (after ~ 2 hours on stream). Xyl: o- + m- + p-xylene; EB: ethylbenzene, C10: naphthalene + 1-methyl-naphthalene + 2-methylnaphthalene

<sup>&</sup>lt;sup>14</sup> V.R. Choudhary, P. Devadas, S. Banerjee, A.K. Kinage. Aromatization of dilute ethylene over Ga-modified ZSM-5 type zeolite catalysts. Microporous and Mesoporous Materials 47 (2001) 253-267

<sup>&</sup>lt;sup>15</sup> D.B. Lukyanov, N. Suor Gnep, M.R. Guisnet. Kinetic modeling of ethane and propene aromatization over HZSM-5 and GaHZSM-5. Ind. Eng. Chem. Res. 33 (1994) 223-234

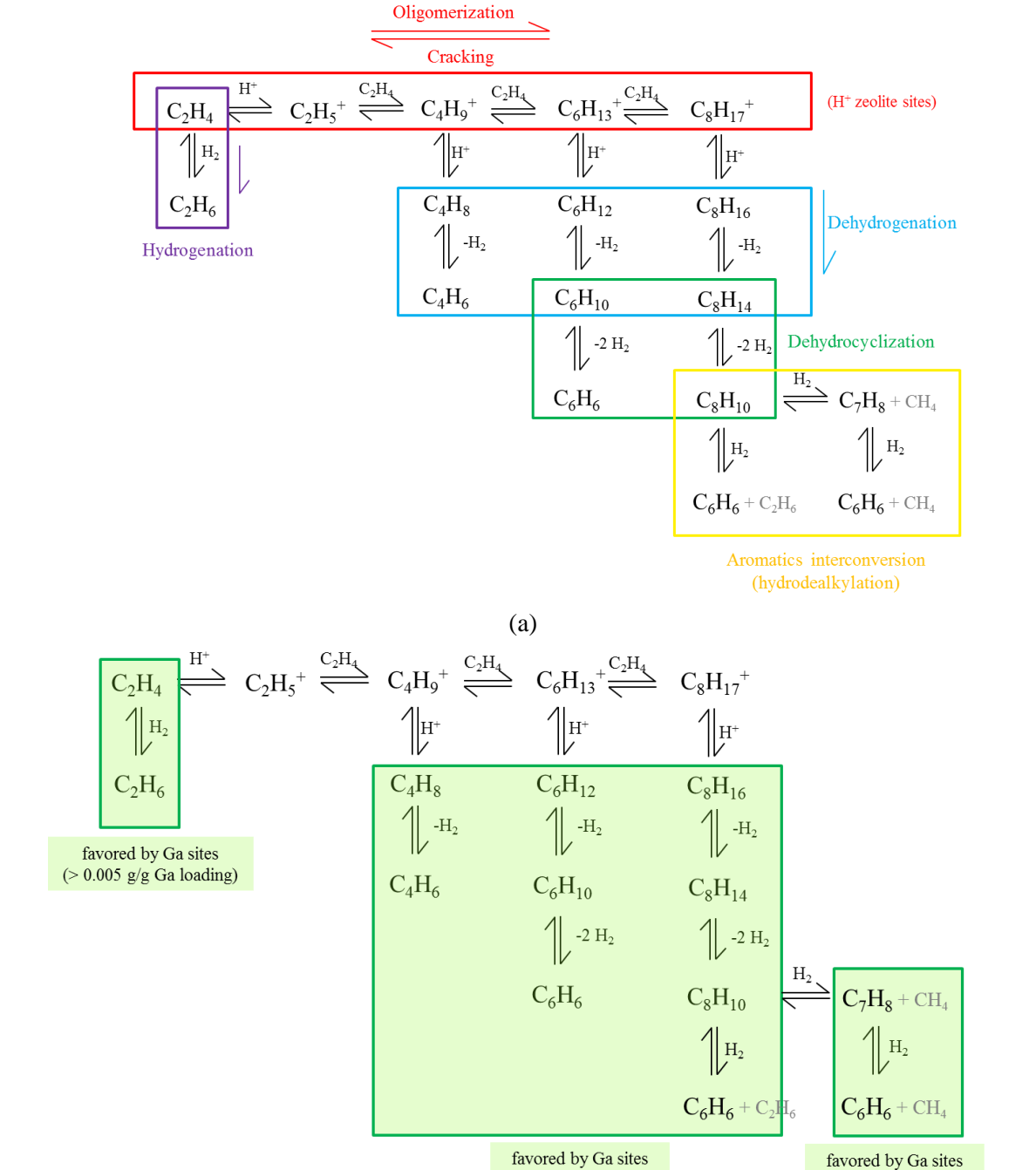


Figure 47.Mechanism of ethylene aromatization proposed: (a) Reaction stages; (b) stages favoured by the addition of Ga to the ZSM-5 zeolite.

(b)

#### 5.4.4 Effect of catalyst preparation – impregnation vs. ion-exchange

The 2.5 wt.% Ga catalyst was selected due to its high ethylene conversion, high stability and good carbon selectivity to benzene for the study of the effect of the incorporation of Ga into the zeolite support. With this purpose, 2 different catalyst preparation procedures were examined - a slurry impregnation method or ion exchange.

The results show that even though ethylene conversion is slightly decreased from 96-97% to 93-95% when using an ion-exchange catalyst compared to the slurry impregnation catalyst (not shown), the carbon selectivity to benzene is considerably increased from ~20% to 25% (Figure 48 (a)), although the carbon selectivity to toluene is slightly lower (from 32% to 30%). The combined

Page 60 of 79 ECN-E--18-027

effect results in an overall increase of the combined carbon selectivity to benzene + toluene from 55% to 60%, as plotted in Figure 48 (b). The selectivity towards  $CH_4 + C_2H_6$  of the catalyst prepared by slurry impregnation is much higher than ion exchange prepared catalyst (not shown in this report).

In order to explain the enhancement of carbon selectivity to benzene of the ion-exchange catalyst, 2 reasons can be proposed: (1) Ga<sup>+</sup> active sites are more uniformly dispersed and into the pore channel of the zeolite; and (2) part of the Ga replaces aluminum and enters into the zeolite framework. The inference is mainly attributed to that Ga<sup>+</sup> active sites are efficiently introduced into the pore channel. When Ga replaces Al in the framework of the zeolite, it does not only change the pore structure of the zeolite but also changes the acid strength distribution of the zeolite and affects the bonding of ethylene to the active sites. Moreover, if the pore channels are considered as the active sites for aromatization of ethylene to benzene, the characters of high steric effects can be provided as a hint. The temperature dependence of the benzene yield, and the fact that Ga needs to be diffused into the pore channel indicate that the active sites of benzene might be in the pore channel of the zeolite. On the contrary, the yield of toluene is not temperature-dependent and does not require the addition of Ga to the zeolite. Therefore, the active sites for benzene and toluene production are located at different places on the zeolite.

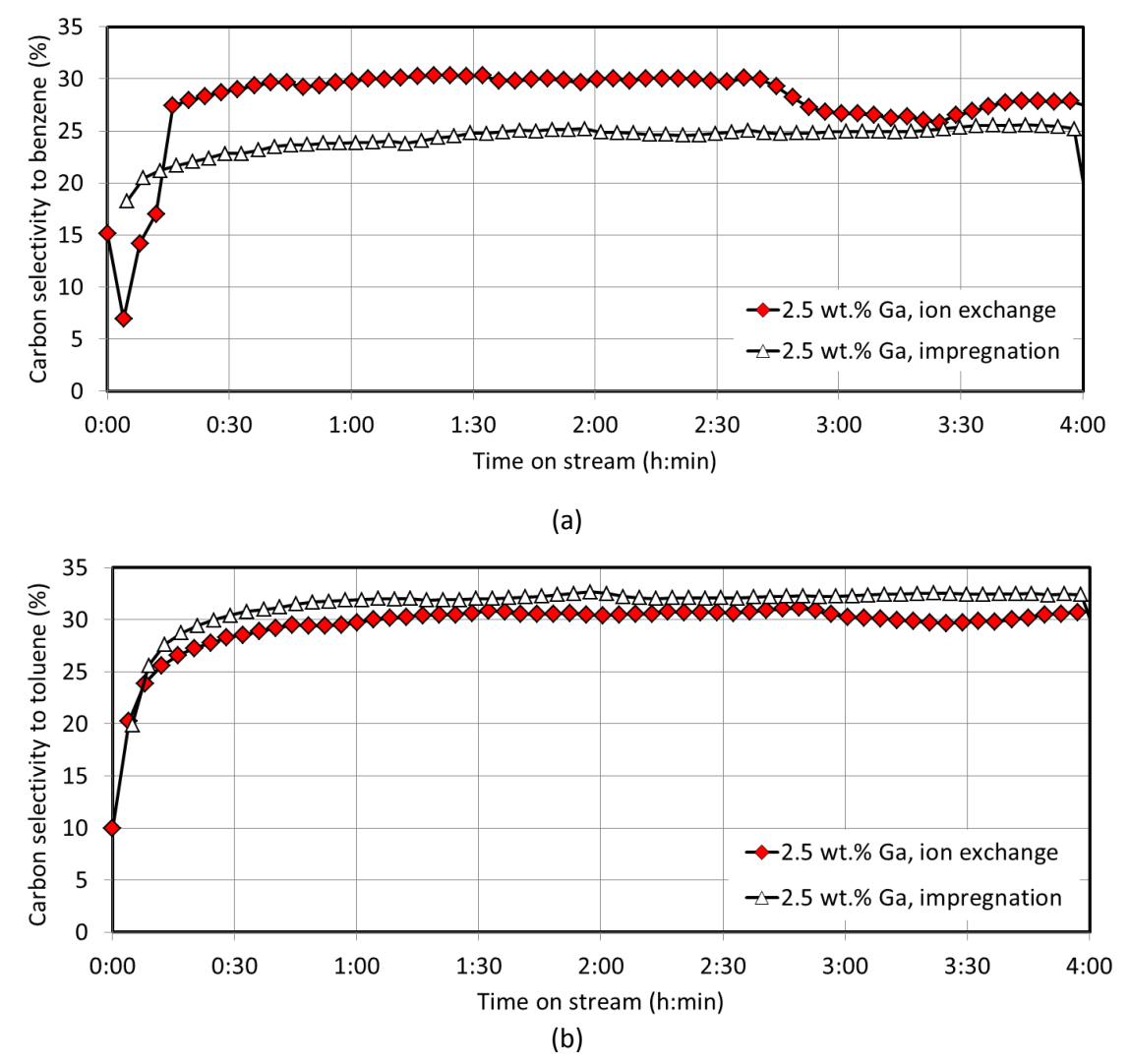


Figure 48.Effect of Ga loading method on carbon selectivity to (a) benzene (b) toluene.

ECN-E--18-027 Page 61 of 79

## 6. Market analysis of bio-BTX and bio-ethylene

Within WP5 of the project, partner Kodok has performed a market study for the target compounds addressed in Blue Bird, namely bio-BTX and bio-ethylene. In this report, the main findings of the study are summarized.

#### 6.1 Existing processes for bio-BTX and bio-ethylene production

There are several processes available for the production of bio-BTX and bio-ethylene. In this document a brief overview is given of alternative production routes. A number of processes use biomass or components from biomass as feedstock, whereas other processes are developed for waste treatment (e.g. mixed plastics).

#### 6.1.1 Bio-BTX production

#### Processes based on pyrolysis

An alternative route for the production of bio-benzene is via pyrolysis of biomass with (f.i. Gadoped ZSM-5)<sup>16,17</sup> and without the use of catalysts. Technically this seems possible. However, the number of operating biomass pyrolysis installations is limited and mainly aimed at producing pyrolysis-oil. More initiatives are being set-up, which have added separation techniques in order to produce individual chemical components from the pyrolysis-oil. In general, a complex set of separation techniques are needed to produce chemicals with sufficiently high purity.

In an overview report of technologies for the production of bio-aromatics<sup>18</sup>, a large number of initiatives are presented. Only a limited number of these is in pilot-, demo-, or commercial phase and are shown in Table 11. The majority of the processes are still in the R&D phase.

Page 62 of 79 ECN-E--18-027

<sup>&</sup>lt;sup>16</sup> Aromatics from biomass pyrolysis vapour using a bifunctional mesoporous catalyst; S.Kelkar, C.M. Saffron, Z. Li, S-S. Kim, T. J. Pinnavaia, D. J. Miller and R. Kriegel Green Chem., 2014,16, 803-812

<sup>&</sup>lt;sup>17</sup> http://www.rug.nl/research/portal/files/14412062/EES-2013-165M AnneMeuwese.pdf; The sustainability of producing BTX from biomass

<sup>&</sup>lt;sup>18</sup> APC, Overzicht initiatieven rond bio-aromaten (update mei 2014), Platform Papier-Agro-Chemie, G.J. Gruter (Avantium) en E. Engelen (APC)

Table 11. Overview of processes for production of bio-BTX and bio-ethylene.

Company	feedstock	Technology	Product(s)	Status	Website
BioBTX	Biowaste, glycerine, biomass	Pyrolysis + catalysis, CFB	BioBTX	Lab scale/pilot	https://www.biobtx.nl/
Annellotech	Biowaste	HT pyrolysis + catalysis	Mix of aromatics	Pilot	http://anellotech.com/
ChEnergy	Plastic waste, tyres	Batch pyrolysis	Fuel oil	Pilot in NL	https://www.chenergy.nl/
Patpert Teknow Systems	Plastic waste, tyres	Pyrolysis	Fuel oil	Commercial Pilot in NL	http://patpert.in/
Nettenergy	Woody biomass, grass	Flash pyrolysis	Mix of aromatics Wood vinegar, biochar	Pilot (mobile)	http://www.nettenergy.com/inde x.php/en/
VTT	Wood	Gasification + FT + aromatization	втх	Lab scale	http://www.vttresearch.com/
ECN	Biowaste/wood	Gasification	Syngas + BTX	Gasifier pilot; BTX lab scale	
GEVO	Carbohydrates	Fermentation to isobutanol + Dehydration + Dimerization + dehydrogenation	p-xylene	Commercial (isobutanol) Pilot for p- xylene in preparation	http://www.gevo.com/
Virent	Carbohydrates	Aqueous phase + Reforming + Catalysis	BioBTX alkanes	Pilot	http://www.virent.com/
Braskem	Ethanol (from sugar cane) dehydration		ethylene	Commercial scale	https://www.braskem.com.br/ho me-en
SABIC	Waste animal and vegetable oil	Hydrocracking	ethylene	Commercial scale	https://www.sabic.com/en

#### BioBTX<sup>19</sup>

The BioBTX process is based on catalytic pyrolysis with specific process conditions and catalysts. The catalyst (zeolite) is not in direct contact with the biomass, thereby preventing deactivating of the catalyst by the minerals in the biomass. The present status is that a pilot-scale installation is being construction as follow up of a lab-scale set-up. The pilot-installation is based on circulating fluidized bed technology. No detailed information on mass balances or foreseen production costs are available.

The objective of the consortium (BioBTX, KNN Advies, Syncom, DuFor Resins and Cumapol Emmen) is to develop a "green" PET bottle completely based on bio-based chemicals from the BioBTX process.

ECN-E--18-027 Page 63 of 79

 $<sup>^{19}\,</sup>http://www.asqasubsidies.nl/uploads/pagetree/files/Artikel\_Noord\_ASQA\_Subsidies.pdf$ 

#### Anellotech<sup>20,21</sup>

Biomass (wood, sawdust, corn stover, sugar cane bagasse and other non-food materials) is dried and ground. The biomass is rapidly heated, and the resulting gases are immediately converted into hydrocarbons by a proprietary, reusable, sand-like zeolite catalyst. The resulting mixture of benzene, toluene and xylenes can be further purified and separated by using known commercial technologies.

Bio-TCat™ (United States Patent Application 20160145496)<sup>22</sup> performs all process reactions in one fluid bed reactor, where biomass is thermally broken down and then catalytically converted into BTX. This single step process uses a cost effective catalyst being jointly developed with Johnson Matthey, to produce bio-BTX in commercially attractive yields. By going directly from biomass to BTX in one step, this process does not make highly oxygenated bio-oil intermediate products and so avoids the need to add significant amounts of hydrogen. In fact, a process by-product stream that is planned to burn to generate electricity could alternatively be converted to a renewable source of hydrogen via a water-gas shift reactor.

The Bio-TCat process starts with biomass and generates the required process energy from the feedstock itself. No detailed information on the mass balance or foreseen production costs was found. In 2016 commissioning of a pilot plant started in Pearl River (USA). There is public protest against the erection of the demonstration plant predominantly aimed at the risk of BTX emissions from this plant. The present status of this plant is not clear A (second) pilot plant has been built in Texas and the first test results have been reported.

#### ChEnergy<sup>23</sup>

Another example of a pyrolysis based production process is the CSTDRP (Closed System Thermally Depolymerisation Refining Process) process from ChEnergy, which converts plastic and organic waste into gas and (fractionated) oil. The pyrolysis process is operated as a batch process. The aimed end-product is applied as petrol, diesel or kerosene replacement.

In the process, the waste is heated and converted into gas. Subsequently the gas is treated by a catalyst. This "treated" gas is cooled in a condenser to condensed gas (oil) and non-condensable gas (a mixture of natural gas and LPG). Because of the heat, the substances that cannot be converted into gas are transformed into carbon, which exhibits the most similarities in terms of composition with coal. The waste residue is also processed (metal, glass, stone, etc.). After the cracking process, these materials remain behind in the reactor, together with the carbon. After emptying the reactor, these residues can be easily separated from the carbon and are offered for further reuse as well as the carbon itself. When the plastic waste is processed in the CSTDRP installation, the following mass balance is obtained: 1000 kg of plastic waste is roughly equivalent to 127 kg of gas, 190 kg of carbon and 683 kg of oil. This oil has a specific gravity of about 0.78 kg/L, thus allowing producing about 880 litters of oil per 1000 kg of waste. The released gas is used as a source of energy to the continued operation of the plant. This makes the entire system self-supporting. The oil is sold on the commodity market to oil companies and power plants. ChEnergy has a pilot plant in operation in Groningen (EnTranCe location)<sup>24</sup>.

**Page** 64 of 79

<sup>&</sup>lt;sup>20</sup> http://anellotech.com/sites/default/files/HydroCarbonProcessingMagazine\_2016.03.01.pdf

<sup>&</sup>lt;sup>21</sup> https://www.youtube.com/watch?v=MdDgNYyS1h0

<sup>&</sup>lt;sup>22</sup> http://www.freepatentsonline.com/20160145496.pdf

<sup>&</sup>lt;sup>23</sup> http://www.chenergy.nl/recycling/het-recycling-proces/

<sup>&</sup>lt;sup>24</sup> http://www.chenergy.nl/en/news/

#### **Patpert Teknow Systems**

The pyrolysis process is used to convert end-of-life plastic waste and car tyres into diesel oil. No details on the used technology are available. Patpert, an India based company, claims to have sold several commercial installations.

#### Nettenergy

Nettenergy has developed a mobile pilot pyrolysis installation for biomass (wood, grass, agricultural waste) for the production of a combination of oil, wood vinegar, biochar and gas. The energy necessary for the process is supplied by the gas.

#### Processes based on gasification

VTT Technical Research Centre of Finland Ltd has developed a method of manufacturing BTX chemicals by combining the gasification of lignocellulosic biomass, the Fischer-Tropsch synthesis and aromatisation<sup>25</sup>. Over 85% of the separated benzene exceeded 90% purity and around 50% of the separated toluene was over 70% purity. The process can be applied to the production of biobased chemicals. Since the compound's synthetic route requires pure source materials, VTT's research proves the high quality of aromatics produced through gasification. VTT has calculated that the estimated price of pure BTX fractions is EUR 1.40 per litre. This price is higher than the current price of raw material derived from crude oil, but significantly more competitive than the price of other bio-based routes.

**ECN** is developing a scrubbing technology for the capture of BTX from product gas. This is part of the scope of Blue Bird. More details about the technology can be found in Section 3 of this report and elsewhere.

#### Processes based on conversion in aquatic systems

**Virent**<sup>26</sup> is replacing crude oil by creating the chemicals and fuels the world demands through utilization of a wide variety of naturally occurring, renewable resources. The patented BioForming technology features catalytic chemistry, which converts plant-based sugars into a full range of hydrocarbon products identical to those made from petroleum, including gasoline, diesel, jet fuel, and chemicals for plastics and fibres. The process can accommodate a broad range of compounds derived from biomass, including C5/C6 sugars, polysaccharides, organic acids, furfurals and other degradation products generated from the decomposition of biomass.

The soluble carbohydrate streams can consist of a wide range of molecules and are processed through the aqueous phase reforming step. The aqueous phase reforming step utilizes heterogeneous catalysts at moderate temperatures and pressures to reduce the oxygen content of the carbohydrate feedstock. Some of the reactions in the APR step include: (1) reforming to generate hydrogen; (2) dehydrogenation of alcohols/hydrogenation of carbonyls; (3) deoxygenation reactions; (4) hydrogenolysis; and (5) cyclization. A key advantage to the BioForming process is the ability to produce hydrogen in-situ from the carbohydrate feedstock or utilize other sources of hydrogen such as natural gas for higher yields and lower costs.

The product from the APR step is a mixture of chemical intermediates including alcohols, ketones, acids, furans, paraffins and other oxygenated hydrocarbons. Once these intermediate compounds are formed they can undergo further catalytic processing to generate a cost-effective mixture of non-oxygenated hydrocarbons.

ECN-E--18-027 Page 65 of 79

\_

 $<sup>^{25}\</sup> http://www.vttresearch.com/media/news/pure-industrial-chemicals-by-gasifying-lignocellulosic-biomass$ 

<sup>&</sup>lt;sup>26</sup> http://www.virent.com/

The chemical intermediates from the APR step can react over a Virent modified ZSM-5 catalyst to produce a high-octane gasoline blendstock that has a high aromatic content similar to a petroleum-derived reformate stream. Virent has trademarked this product BioFormate™. Using its demonstration plant in Madison, Wisconsin (USA), Virent has demonstrated the production of biobased aromatic chemicals, including p-xylene, mixed xylenes, toluene and benzene. The Virent process claims to produce its hydrocarbon chemicals and fuels from plant sugars in a few hours.

#### 6.1.2 Bio-ethylene production

**Braskem**'s green ethylene plant was commissioned in September 2010. This marked the beginning of "I'm greenTM Polyethylene" production on a commercial scale, securing the company's global leadership position in bioplastics. The plant has received an investment of \$290 million and has annual production capacity of 200,000 tons of "I'm greenTM Polyethylene"<sup>27</sup>. Feedstock is sugarcane ethanol; the ethanol is dehydrated to form ethylene. The transformation of the green ethylene into "I'm greenTM Polyethylene" is performed in the same polymerization plants that produce polyethylene from fossil source.

**SABIC** produces bio-poly-ethylene from "bio-naphtha" produced by a hydrocracking process of waste animal and vegetable oil.

#### 6.2 Summary

Many different processes (summarized in Table 12) have been developed for the production of chemicals from biomass or waste. Most of these processes are based on pyrolysis and still in the pilot phase, but progress is being made towards commercialization. Bottlenecks for the pyrolysis processes are still the upgrading of the primary product (mostly a pyrolysis oil comprising of a large number of components) into separate saleable products. In some cases the oil is sold as it is and used as fuel oil.

Table 12. Summary of processes for the production of bio-BTX and bio-ethylene from biomass/waste.

Name	Type of process	Products	Status	Production costs	Mass balance
BioBTX	Catalytic pyrolysis	BTX	Lab scale	n.i. <sup>1</sup>	n.i.
Anellotech	Catalytic pyrolysis	втх	Pilot scale in operation	n.i.	n.i.
ChEnergy	Pyrolysis of waste with catalytic upgrading – batch process  Fuel oil		Pilot-scale in n.i.		0,68 kg oil per kg waste
Patpert	Pyrolysis	Fuel oil	Pilot/ commercial	n.i.	n.i
Nettenergy	Flash pyrolysis	Mix of aromatics, wood vinegar, char	Pilot	n.i.	n.i.
VTT	Gasification with FT and aromatization	BTX	Lab scale	€ 1,40/kg	n.i.
GEVO	Fermentation, dehydration, dimerization, dehydrogenation	p-xylene	pilot	n.i.	n.i.
Virent	Aquatic catalytic process with catalytic upgrading	втх	Demo scale	n.i.	n.i.
Braskem	Ethanol (from sugar cane) dehydration	ethylene	Commercial scale	n.i.	n.i.
SABIC	Hydrocracking waste animal and vegetable oils	PE	Commercial scale	n.i.	n.i.

<sup>&</sup>lt;sup>1</sup> n.i. = no information available

Page 66 of 79 ECN-E--18-027

\_\_\_

<sup>&</sup>lt;sup>27</sup> http://www.braskem.com/site.aspx/Im-greenTM-Polyethylene

## 7. LCA analysis of coproduction schemes

Within WP5 of the project, the environmental impact of bio-SNG production from residual biomass (waste wood) was assessed. Furthermore, the consequence of replacing natural gas (Case 1), and the effect on the environmental impact of the implementation of co-production schemes for the combined production of bio-BTX and bio-SNG (Case 2) were also evaluated. The reference scenario was the production and use of Groningen natural gas. The LCA identifies the major environmental impact and suggests the optimised use of fossil energy and chemicals during the bio-SNG production phase.

#### 7.1 Selected pathways and preliminary economic evaluation of coproduction

Based on the experimental results obtained in the tests of catalytic aromatization of ethylene (see Section 4) and derived from ASPEN Plus calculations, ECN performed a preliminary economic evaluation of a selected number of routes, schematically depicted in Figure 49, Figure 50 and Figure 51. The 4 MWth thermal input AMBIGO bio-SNG plant (Figure 49) is the reference case for the evaluation of the implementation of co-production. The addition of a BTX scrubber (case 1, Figure 50) and of an ethylene aromatization unit + BTX scrubber (case 2, Figure 51) for the co-production of aromatics and bio-SNG has been considered.

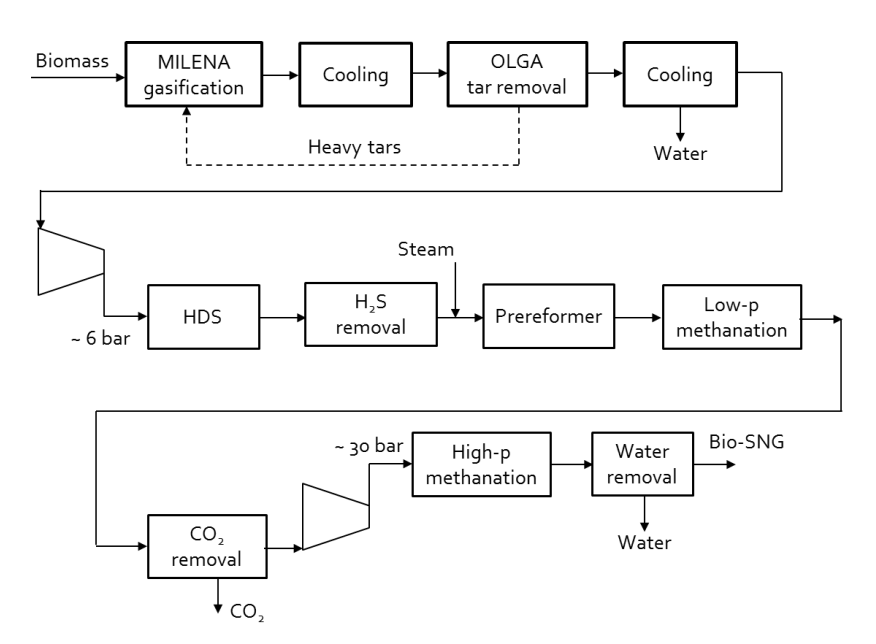


Figure 49. Schematic flow diagram of bio-SNG process (base case).

ECN-E--18-027 Page 67 of 79

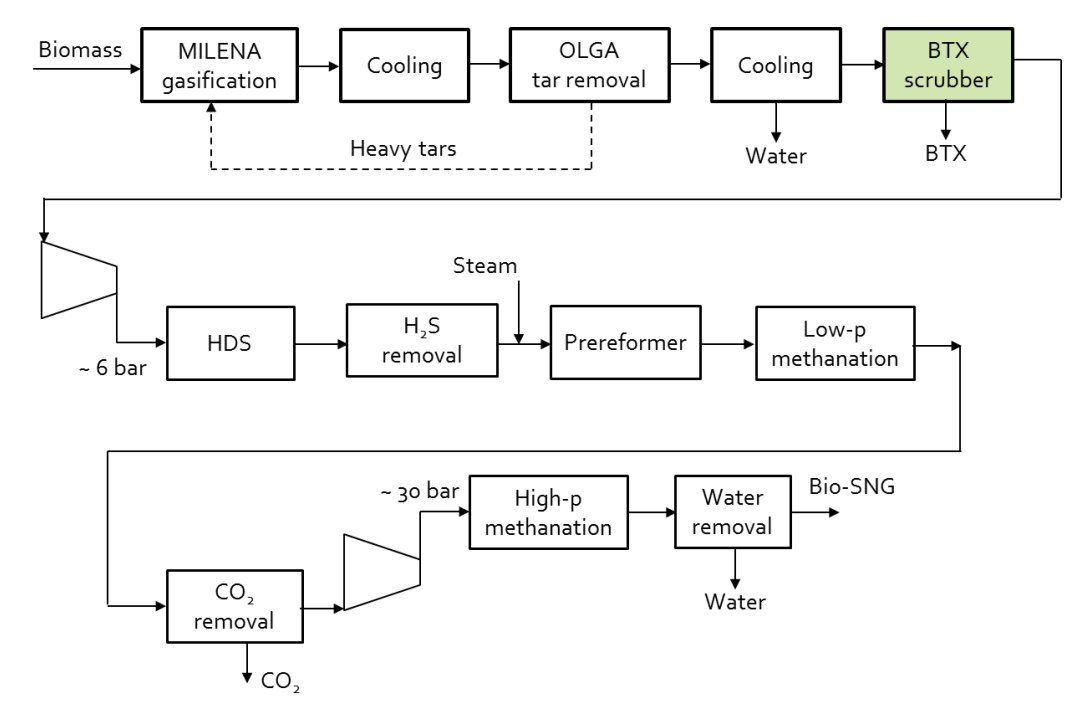


Figure 50. Schematic flow diagram of bio-SNG + bio-BTX co-production (case 1).

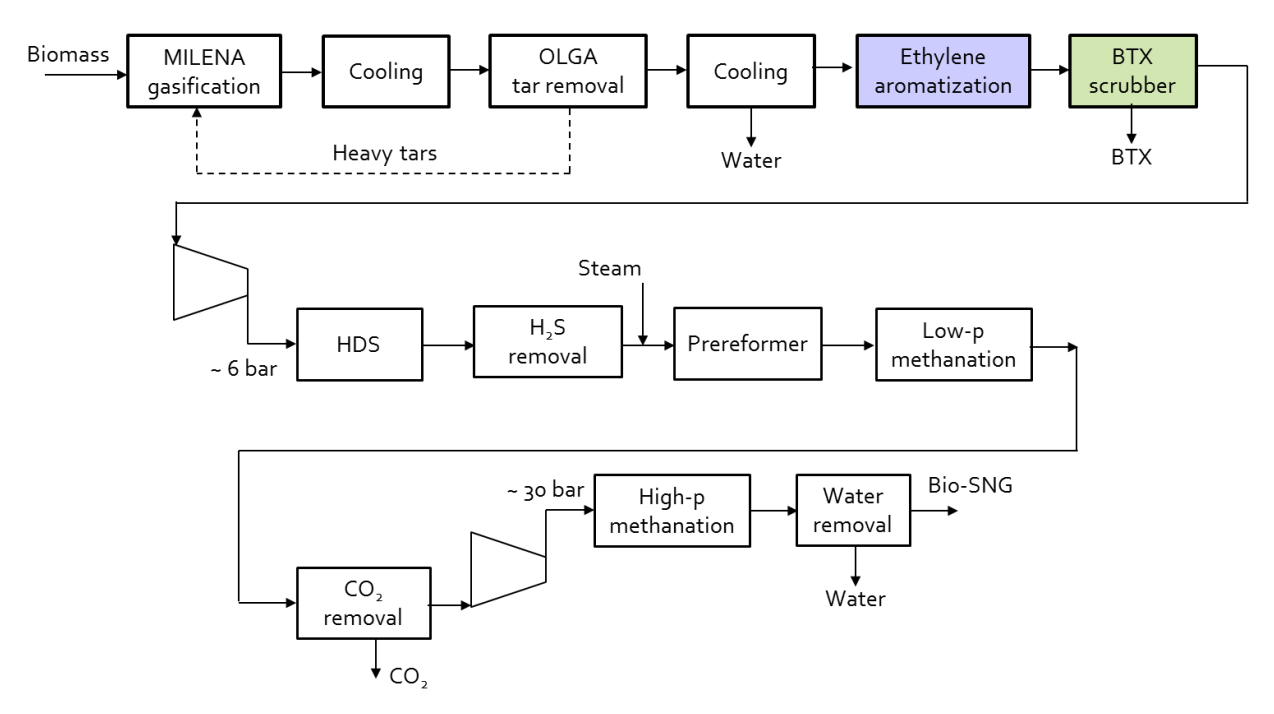


Figure 51. Schematic flow diagram of bio-SNG + bio-BTX co-production with catalytic ethylene aromatization (case 2).

The 3 selected routes were modelled in ASPEN for mass and energy balances, in order to calculate the effect of co-production on the plant revenues. For this, market prices for SNG and BTX (thus, no subsidy prices) were assumed. The results of the calculations are presented in Table 13. As can be seen, the harvesting of a bio-BTX product reduces the volume of bio-SNG product by 25%, but in return, the yearly plant revenues can increase by 28% by adding just the bio-BTX scrubber and by  $\sim$  59% by adding the ethylene aromatization and BTX scrubber to the ESME system. The overall energy efficiency (calculated as the ratio between the energy contained in the products and the energy contained in the inlet biomass) is also slightly increased from 65.8% to 66.8%.

**Page** 68 of 79

Table 13. Summary of results of ASPEN calculations – effect of implementation of (ethylene aromatization +) BTX scrubbing in the ESME system (all cases based on 4 MWth thermal input).

		Reference case, bio-SNG	Case 1 - Bio-SNG + bio- BTX, addition of BTX scrubber	Case 2 - Bio-SNG + bio-BTX, addition of ethylene aromatization + BTX scrubber
Bio-SNG product	Nm³/h	299.10	265.54	222.84
CH₄ content in bio-SNG	vol.%	88.5	88.6	88.6
Bio-BTX product	kg/h	0	29.31	63.41
Energy bio-SNG	MW	2.63	2.34	1.96
Energy bio-BTX	MW	0	0.33	0.71
Total energy products	MW	2.63	2.67	2.67
Energy efficiency 28	%	65.8	66.6	66.9
Revenues bio-SNG <sup>29</sup>	Euro/y	306 220.47	272 048.33	228 283.06
Revenues bio-BTX <sup>30</sup>	Euro/y	0.00	119 920.48	259 395.40
Total revenues	Euro/y	306 220.47	391 968.81	487 678.46

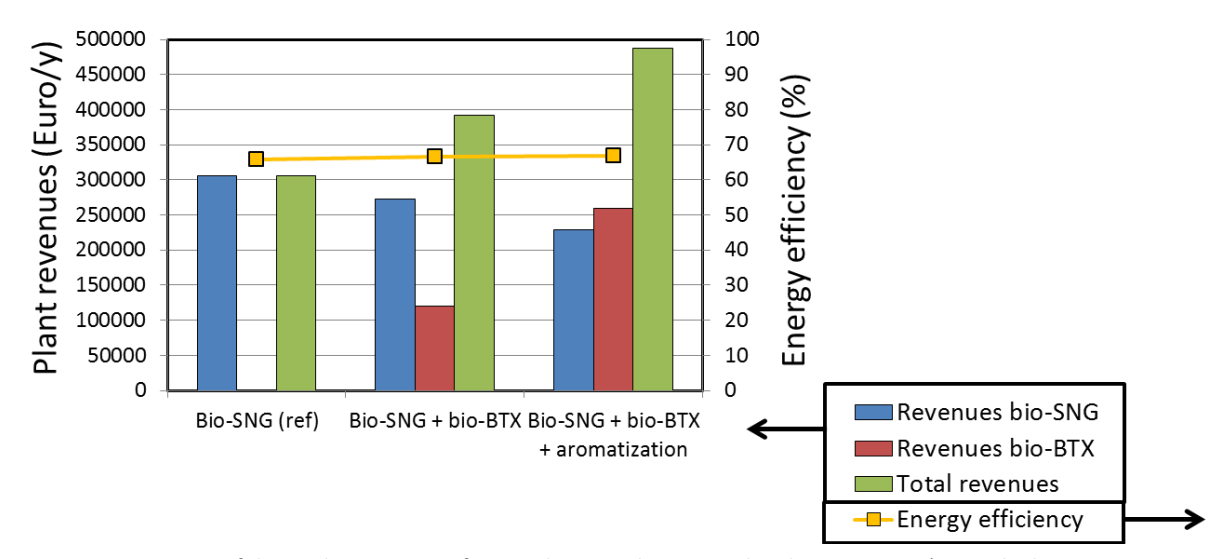


Figure 52. Comparison of the implementation of co-production schemes on the plant revenues (4 MWth plant as reference) and the energy efficiency (LHV basis).

#### 7.2 Life Cycle Analysis (LCA) of co-production schemes

This section summarizes the results of the environmental impact assessment of bio-SNG and bio-BTX co-production and application in comparison with the current reference fossil natural gas and BTX production and application. Moreover, the environmental impact of the implementation of co-production of bio-BTX and bio-SNG to replace NG and fossil BTX has been quantified, and finally the impact of replacing fossil heat and combined heat and power (CHP) was assessed. The study identifies the major environmental impact sources and suggests the optimised use of fossil energy and chemicals during the bio-SNG production and use phase.

ECN-E--18-027 Page 69 of 79

<sup>&</sup>lt;sup>28</sup> Inlet: 4 MWth biomass (size of AMBIGO plant in Alkmaar, www.ambigo.nl).

<sup>&</sup>lt;sup>29</sup> Assuming 5 \$/MMBtu (Europe price of natural gas 2017, <a href="https://www.statista.com/statistics/444286/natural-gas-price-forecast-by-region/">https://www.statista.com/statistics/444286/natural-gas-price-forecast-by-region/</a>) = 4.3 Euro/GJ price of SNG (no subsidy considered).

<sup>&</sup>lt;sup>30</sup> Assuming 600 \$/ton BTX (source: Platts <a href="https://www.platts.com/news-feature/2016/petrochemicals/global-aromatics-pricing-analysis/index">https://www.platts.com/news-feature/2016/petrochemicals/global-aromatics-pricing-analysis/index</a>), exchange rate: 1 Euro = 1.1 \$

The system boundaries are set by a 2-stage approach, namely cradle-to-gate (Stage 1), which is the production of bio-SNG and bio-BTX, and gate-to-grave (stage 2), which is the use of the bio-SNG for heat and/or or CHP (combined heat and power). An overview of the various studied cases is shown in Table 14. The system boundary considers the combination of the gasifier and the subsequent gas cleaning and methanation process as one unit, while the feedstock, chemicals and energy form the input and the produced SNG (or SNG and bio-BTX) is the output. The system boundary with the input and output streams are shown in Figure 53.

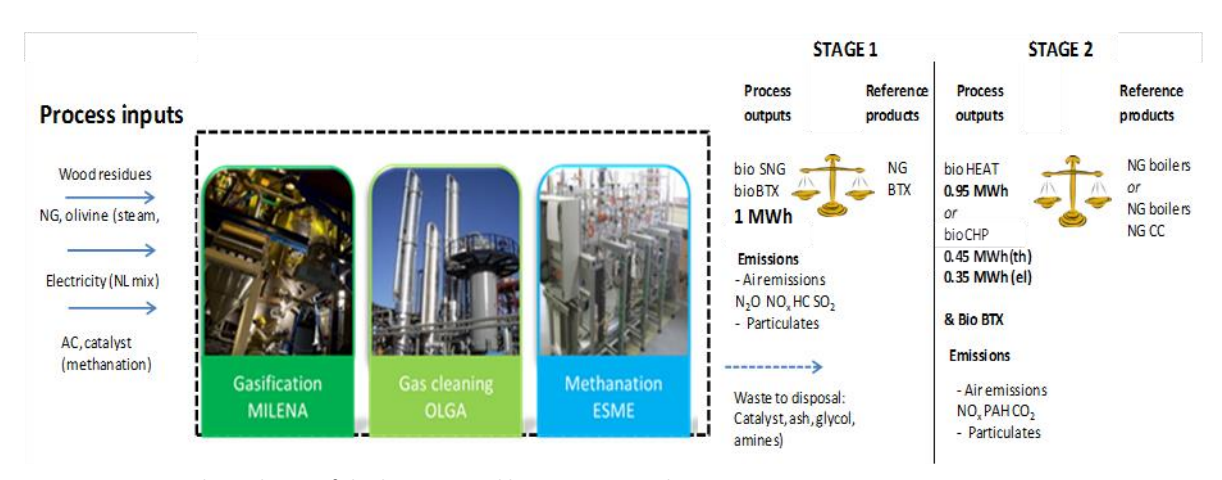


Figure 53. System boundaries of the bio-SNG and bio BTX LCA study.

Table 14. Cases studied in the LCA study.

Stage	Biomass source	Main product valorisation	Replaces (reference system)	
1a	Waste wood	Bio-SNG (grid injection)	Natural gas (grid injection)	
1b	Waste wood	Bio-SNG & bio-BTX	Natural gas & fossil BTX	
2a	Waste wood	Heat from bio-SNG	Natural gas heat	
2b	Waste wood	CHP from bio-SNG	Natural gas CHP	

Changes to the reference system due to bio-SNG plus bio-BTX as well as bio-CHP production were quantified using LCA methodology. The software Simapro v.8.4 was used for the analysis. The Functional Unit of the study is 1 MWh of SNG energy content delivered at the 'factory gate'. The biomass is demolition wood (residual wood from industrial activities) with data taken from Ecoinvent v.3.3. The product gas is upgraded to SNG substituting natural gas. The bio-SNG quality is compatible with Groningen gas quality, and is fed in the natural gas network.

Figure 54 compares the impact of bio-SNG for natural gas replacement (Case 1a, Stage 1) vs. bio-SNG plus bio-BTX for natural gas and fossil BTX replacement (Case 1b, Stage 1). Figure 55 compares cases 2a and 2b - replacement of fossil-based heat and application of bio-SNG for CHP production. The negative bars represent benefits from the application of the novel system compared to the reference case. System impacts are not negative in absolute terms but relative to the reference system. From Figure 55 it can be seen that the co-production of bio-SNG + bio-BTX performs better than the base case. This is due to the greater avoided impact of fossil BTX compared with the impact of avoided natural gas per energy unit. Due to avoiding any fossil base auxiliary heat and power consumption, the combined bio-SNG and bio-BTX leads to an overall avoided impact even at the production stage (Stage 1). Therefore, the results from the LCA analysis reveal that co-production of bio-SNG and BTX is not only a promising option to improve the business case of bio-SNG production, but also environmentally performs better.

**Page** 70 of 79

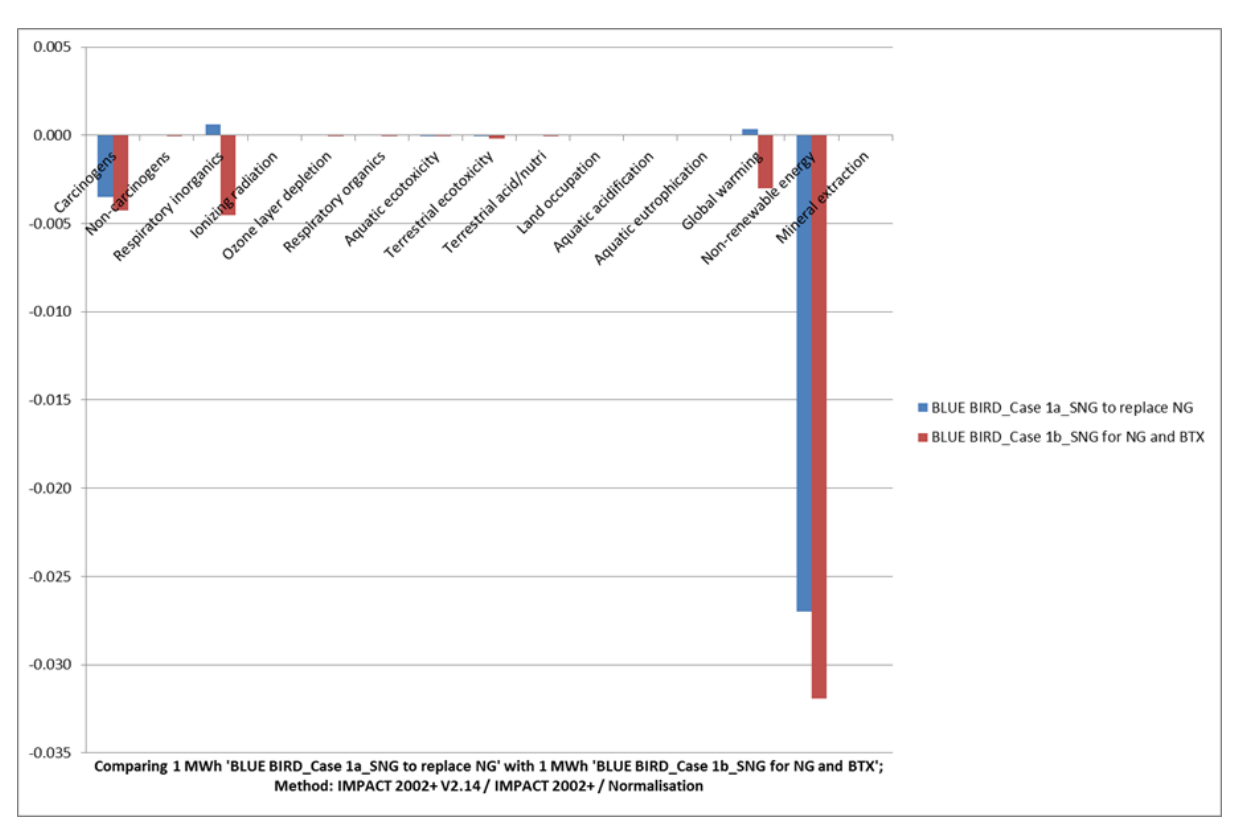


Figure 54. Comparative results of impact assessment of bio-SNG production (blue bars) and bio-BTX + bio-SNG co-production (red bars).

From Figure 55 it can be seen that the avoided impact from replacing heat only production based on natural gas is smaller than the avoided impact (that is, the obtained benefit) when avoiding natural gas-based CHP. This conclusion is based on the high efficiency with which current gas boilers are operating, rendering their replacement by bio-SNG driven heat and power slightly less beneficial (by comparison) than the replacement of CHP units based on natural gas. The conclusion from this observation is that priority should be given to replacing natural gas-driven heat and power with bio-SNG driven heat and power in a first place, rather than high-efficiency gas boilers.

Based on the fact that replacing fossil BTX through bio-BTX leads to greater avoided impact than only replacing natural gas, a suggestion for future work is to further promote bio-SNG production for replacing current fossil transportation fuels due to their high environmental impact. In the light of increasing renewable energy sources (solar, wind) biomass-based SNG can play a more important role as transportation fuel, rather than supplying energy (heat and electricity) in competition with carbon free renewable energy sources.

ECN-E--18-027 Page 71 of 79

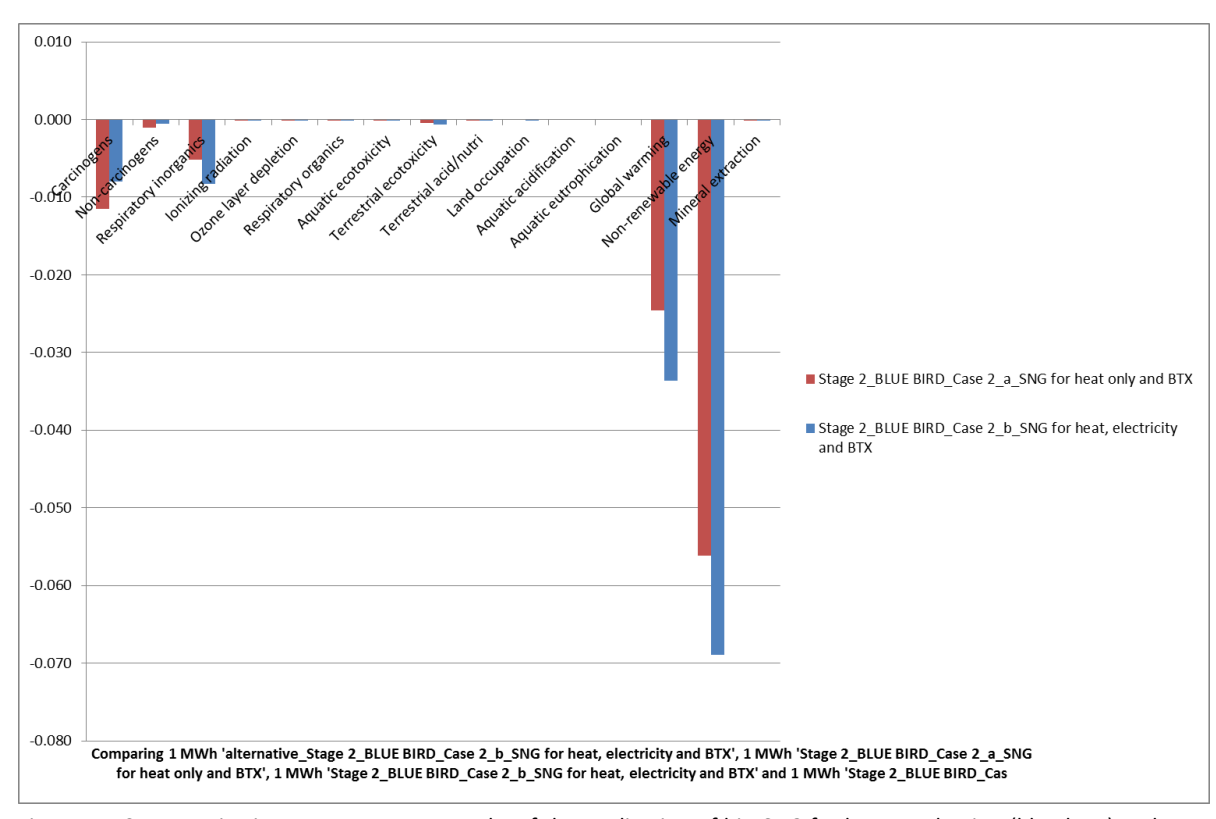


Figure 55. Comparative impact assessment results of the application of bio-SNG for heat production (blue bars) and use of bio-SNG for CHP (red bars).

**Page** 72 of 79

### 8. Conclusions and outlook

Within the Blue Bird project, a number of technologies have been developed for the recovery of valuable compounds (BTX, ethylene) from gasification product gas in co-production schemes. The implementation of co-production allows the reduction of the production cost of bio-SNG (or other biofuels). Moreover, the SNG production cost can be further reduced if low-cost biomass residues are used as feedstock. Within Blue Bird, thermochemical valorization of humins (a by-product from Avantium's YXY biorefinery process for sugar conversion into chemicals) via fluidized-bed gasification and combustion has been evaluated. The co-production technologies studied in the project include liquid absorption for bio-BTX capture, solid adsorption for the separation of bio-ethylene, and catalytic conversion of ethylene to aromatics (reactive separation).

In 2016, Avantium completed the production of 1000 kg humins from the XYX process at the Geleen pilot plant. Humins from different sugar sources and containing different concentrations of 5-hydroxymethyl furfural were produced. Part of this batch of humins was delivered to ECN for gasification/combustion tests. Preliminary spraying tests confirmed that the tested humins presented reasonable properties to be mixed with water and then to be fed by spraying. The tested humins showed to be a very challenging material for thermochemical conversion. Due to its low reactivity, accumulation of humins-char in the bed is expected to create operational problems under gasification conditions. Combustion seems to be more appropriate for humins valorization under the fluidized-bed conditions tested due to higher conversion rates. Stable combustion operating conditions were achieved with complete fuel conversion and no emissions. However, bed temperatures higher than 950°C should be used, which is not compatible with most FB existing systems. Humins in-bed injection proved to be a good option for the feeding of this problematic fuel, but a more efficient probe cooling system must be considered to avoid pyrolysis of the humins before injection (which will clog the feeding line). The sample of humins tested in this project did not show any operational problem regarding bed agglomeration, slagging and fouling issues. Thus, the optimization of the Avantium's process increases the chances of the valorization of the resulting humins.

Within WP3 of the project, ECN has worked on the improvement of the BTX scrubbing unit for the harvesting of bio-BTX from biomass gasification gas. In particular, ECN has designed, constructed and tested a unit for the automated separation of water and aromatics. The new AWOS unit (Aromaat-Water Opvang en Scheiding) enables continuous, automated operation of BTX harvesting from gasification product gas. Along the design process, a number of experiments were performed to test some of the critical phenomena: the formation of turbulences in the condensing unit, the conductivity of the water and aromatics entering the AWOS unit, and spillover of washing

ECN-E--18-027 Page 73 of 79

liquid. All these issues were properly handled before the final commissioning test. The whole BTX scrubbing unit including the new AWOS unit was successfully tested for almost 12 hours with product gas coming from the MILENA gasifier and the OLGA tar removal. The main goal was to test whether the level sensors and the water pump operated within specifications, switching between the sensors (essential for continuous operation). It was demonstrated that the automation of the condensing unit worked very well, and proper separation of water and aromatics was achieved. The benzene removal efficiency of the BTX scrubber was approximately 98.6%, whereas 100% toluene removal was achieved.

Reactive separation of ethylene from producer gas via catalytic conversion to aromatics has successfully been proven as a promising and feasible option for the implementation of coproduction schemes. An extensive experimental plan using bifunctional Ga-loaded ZSM-5 zeolites as catalyst was carried out at ECN. The results showed that 80-97% ethylene can be converted depending on the operating conditions (Ga loading and operating temperature). In all cases, acetylene conversion was complete. The carbon contained in ethylene and acetylene is mainly converted to benzene, toluene, ethane and methane (the two latter being by-products of the reaction). Ethane and methane by-products end up in turn as part of the bio-SNG product, which is favorable in view of the application in bio-SNG processes. The addition of Ga to the zeolite significantly improved both the ethylene conversion (90-97%) and the carbon selectivity to benzene. On the contrary, the unloaded zeolite exhibited the highest values of carbon selectivity to toluene (~ 45%). The 0.5 wt.% Ga catalyst achieved the highest total carbon selectivity to aromatics (73%). The reaction temperature dramatically influences the distribution of carbon selectivity towards aromatics. Lower temperatures favor the production of ethylbenzene and xylenes, whereas benzene, naphthalene and naphthalene derivatives are promoted at higher temperatures. Based on the results, it is proposed that the formation of benzene and toluene need different active sites to promote their reaction.

Avantium has worked on the development of solid sorbents for the selective removal of ethylene from gasification product gas. Within Blue Bird, the library of sorbents was extended to find stable and selective sorption materials for ethylene. The selected materials include amorphous metal oxides, clay, active carbon, and metal organic frameworks (MOFs). The results of the tests showed that amorphous metal oxides are not suitable as ethylene sorbents as they lack porosity. Among the zeolites tested, types A and X have potential as ethylene sorbent. Among the zeolites tested, [Mn]A exhibited the highest selectivity towards ethylene with a reasonable sorption capacity. Despite applying ion exchange and functionalization, high affinity towards CO2 and water could not be overcome. A combination of different zeolites could be considered to remove water and CO2 from the gas stream before sorption of ethylene. MOFs have potential in gas adsorption and separation, but being formed as small crystals, they lead to a high pressure drop over the sorbent bed and should therefore be shaped into larger particles. However, the sorption capacity of MOF decreased from 6.1 to 3.7 wt% upon pressing, which confirms that the material loses porosity under pressure. Several active carbons show relatively low capacity, however a specific adsorption site for ethylene is not present. This could be obtained by impregnation of the carbon with material with an ethylene specific interaction.

The 2 best Avantium candidates from the screening tests ([Mn]A and [Mn]Y zeolite) were delivered to ECN for testing under relevant gasification conditions. Both sorbents were tested in a number of adsorption/desorption cycles. For both sorbents a temperature increase was observed upon start of adsorption, whereas the desorption process resulted in a drop in the temperature bed. The [Mn]Y sorbent exhibits a less significant temperature increase as well as a different temperature profile compared to the [Mn]A sorbent. Both sorbents were shown to be able to capture a large fraction of ethylene from the gas, but they also co-adsorb CO<sub>2</sub>, ethane and

Page 74 of 79 ECN-E--18-027

acetylene (as well as of other C3-C5 hydrocarbons and organic sulphur compounds). In both sorbents, rapid breakthrough of  $CO_2$  took place within 10 minutes after start of operation. The ethylene adsorption capacity of the [Mn]A sorbent was determined as 66-87 g ethylene/kg sorbent, whereas the [Mn]Y sorbent has a capacity of ~76.6 g ethylene/kg sorbent. During the tests with [Mn]Y sorbent, it was observed that although the ethylene capture is reduced from ~90% to 72% when decreasing the operating pressure from 5.7 bar to 1.6 bar, the adsorption selectivity gets considerably improved, since  $C_2H_6$  and  $CO_2$  are not adsorbed by the [Mn]Y material anymore. Still, the sorbent still co-adsorbs ethylene and acetylene. Based on the results, it seems that operation at low pressures and high gas flows, together with the use of materials with improved sorption capacity such as the [Mn]Y sorbent, could lead to a good trade-off between capture efficiency and sorption selectivity. However, further work is required to get a window of suitable operating conditions of the sorbent and to explore new strategies of regeneration.

In parallel to the technology development work, Blue Bird has included a market analysis of bio-BTX and bio-ethylene, and a cradle to grave environmental impact assessment of the production and use of bio-SNG from gasification of residual wood and the effect of the implementation of co-production schemes for the combined production and use of bio-SNG + bio-BTX. The market analysis has shown that the production of bio-BTX via gasification and/or pyrolysis in the short term can contribute to the overall production of BTX to a limited extent (in the order of a few %) due to the very large production volumes of these aromatics. Different processes for BTX production predominantly based on pyrolysis and gasification are being developed. Most of these processes are in lab- or pilot scale phase. At first it is recommended to focus on niche applications of BTX in order to be competitive. A number of BTX producing and consuming companies have also been identified in the study. On the other hand, the results of the LCA analysis have revealed that substituting natural with bio-SNG is environmentally beneficial concerning global warming and fossil fuel depletion. Co-production of bio-SNG + bio-BTX performs environmentally better than the base case of production of only bio-SNG. This is due to the greater avoided impact of fossil BTX compared with the impact of avoided natural gas per energy unit. Due to avoiding any fossil base auxiliary heat and power consumption, the combined bio-SNG and bio-BTX leads to an overall avoided impact even at production stage. Moreover, the avoided impact from replacing heat-only production based on natural gas is smaller than the obtained benefit when avoiding natural gas-based CHP. This result indicates that priority should be given to replacing natural gas-driven CHP with bio-SNG in a first place. Therefore, the LCA results reveal that co-production of bio- SNG and BTX is not only a promising option to improve the business case of bio-SNG production, but also environmentally performs better.

All in all, the extensive work performed within the Blue Bird project has resulted in a number of successful results which contribute to the development and demonstration of co-production technologies, the implementation of which will lead to lower production cost of bio-SNG and biofuels. The next step of the development phase, the upscaling of the demonstrated technologies, will be tackled in the follow-up Black Birds project (TEBE117010).

ECN-E--18-027 Page 75 of 79

# 9. Dissemination, exploitation and project deliverables

The activities of the Blue Bird project have been released in a number of publications and conference contributions:

#### Scientific publications

I. van Zandvoort, G.P.M. van Klink, E. de Jong, C.C. van der Waal. Selectivity and stability of zeolites [Ca]A and [Ag]A towards ethylene adsorption and desorption from complex gas mixtures. Microporous and Mesoporous Materials. In press, <a href="https://doi.org/10.1016/j.micromeso.2017.12.004">https://doi.org/10.1016/j.micromeso.2017.12.004</a>

Y.T. Kuo, G. Aranda Almansa, B.J. Vreugdenhil. Catalytic aromatization of ethylene in syngas from biomass to enhance economic sustainability of gas production. Applied Energy 215 (1) 2018), 21-30

https://www.sciencedirect.com/science/article/pii/S0306261918300965

#### Contributions to conferences and workshops

B.J. Vreugdenhil, Y.T. Kuo, G. Aranda Almansa, C.M. Lok. Catalytic conversion of ethylene into BTX. IEA Task 33 meeting. Luzerne (Switzerland), 25<sup>th</sup> October 2016

A. Bos, L.P.L.M. Rabou, B.J. Vreugdenhil, J.C. van der Waal, I. van Zandvoort. Recovery of valuable hydrocarbons from biomass/waste gasification producer gas. 24<sup>th</sup> European Biomass Conference and Exhibition. Amsterdam, 6-9 June 2016 [poster awarded at the conference], ECN-M--16-055 <a href="https://www.ecn.nl/publications/ECN-M--16-055">https://www.ecn.nl/publications/ECN-M--16-055</a>

- B.J. Vreugdenhil, Y.T. Kuo, G. Aranda Almansa, C.M. Lok. Catalytic conversion of ethylene from gasification producer gas into bio-aromatics. 25<sup>th</sup> European Biomass Conference and Exhibition. Stockholm (Sweden), 12-15 June 2017 <a href="https://www.ecn.nl/publications/PdfFetch.aspx?nr=ECN-M--17-022">https://www.ecn.nl/publications/PdfFetch.aspx?nr=ECN-M--17-022</a>
- F. Hoonte. Renewable Chemistry onderzoek, van CO2 en biomassa naar nuttige componenten, hoe analyseer je "alles"? LabAnalyse event, Rotterdam, 19th September 2017 http://labanalyse.nl/programma-2017/
- I. van Zandvoort J.C van der Waal. Presentation for MCEC PhD students (2017).

Page 76 of 79 ECN-E--18-027

G. Aranda, A. Bos, J. Groen, B.J. Vreugdenhil, J.H.A. Kiel, J.C. van der Waal, I. van Zandvoort, G. van Klink, J. van Doorn, C.M. Lok. Blue Bird project. RVO TKI overleg. Geertruidenberg, 19th October 2017

Blue Bird banner at Biorizon meeting. Antwerp (Belgium), 29-30<sup>th</sup> November 2017

#### Patent applications

B.J. Vreugdenhil, A. Bos, G. Aranda Almansa. Production and isolation of monocyclic aromatic compounds from a gasification gas. P6066420NL (submitted, under review).

#### Internal/confidential project deliverables

- C. Martin Lok. Aromatization of ethylene and lower alkanes. A Literature Review (2017)
- C. Martin Lok. Aromatization of alkanes and olefins, a Patent Search (2017)
- A. Bos. OLGA and BTX 2; dubbel stoomstrippen & gecombineerde product condensatie, resultaat. ECN-BEE-2016-077 (2016)
- A. Bos. Uitgangspunten/randvoorwaarden ontwerp OLGA & BTX (dubbel) stoomstrip & gecombineerde product condensatie SKID unit. ECN-BEE-2016-081
- Bos. Initial testing of the automated AWOS unit in the BioBTX SKID-mounted system, 2017.
   ECN-BEE-2018-004
- I. van Zandvoort, J.K. van der Waal, G. van Klink, E. de Jong. Selective adsorption of ethylene (2017).
- Y-T. Kuo, G. Aranda Almansa. Blue Bird Project catalytic conversion of ethylene: first experimental plan. ECN-BEE-2016-123 (2016)
- G. Aranda Almansa. Blue Bird project Catalytic conversion of ethylene into aromatics: Effect of the operating conditions. ECN-BEE-2016-151 (2016)
- Y.T. Kuo, G. Aranda Almansa, B.J. Vreugdenhil. Catalytic aromatization of ethylene in syngas from biomass to enhance economic sustainability of gas production. Submitted to Applied Energy, accepted manuscript.
- P.M.R. Abelha. Project 5.4111 Blue Birds: Feeding and thermo-conversion strategy (Humins). ECN-BEE-2018-005 (2016).
- J. van Doorn. Alternative processes for bio-BTX and bio-ethylene (2017).
- J. van Doorn. Global market volumes of bio-BTX and bio-ethylene (2017).
- L.E. Fryda. Cradle to gate Life Cycle Analysis of co-production of bio-BTX and bio-SNG (2017).
- Update of <u>www.biobtx.com</u> site (in progress)

ECN-E--18-027 Page 77 of 79

#### Internal communication

Date	Venue	Type of meeting	Participants
04-02-2016	Avantium, Amsterdam	Project kick off	All partners
07-04-2016	-	Phone conference	All partners
07-07-2016	-	Phone conference	All partners
14-10-2016	-	Phone conference	All partners
16-01-2017	ECN, Petten	Update with RVO	ECN, RVO
20-01-2017	Avantium, Amsterdam	Project 1-year meeting	All partners
23-02-2017	Catalok, Den Haag	Update aromatization activities	Catalok, ECN
17-07-2017	ECN, Petten	Project update	Avantium, ECN, Kodok (Catalok excused)
29-11-2017	Biorizon event, Antwerp	Project update	Avantium, ECN, Kodok (Catalok excused)

**Page** 78 of 79 ECN-E--18-027

